

The molecular gas in Luminous Infrared Galaxies II: extreme physical conditions, and their effects on the X_{CO} factor

Padelis P. Papadopoulos

Max Planck Institute for Radioastronomy, Auf dem Hügel 69, D-53121 Bonn, Germany

padelis@mpifr-bonn.mpg.de

Paul van der Werf

Leiden Observatory, Leiden University, P.O. Box 9513, NL-2300 RA Leiden, The Netherlands

pvdwerf@strw.leidenuniv.nl

E. Xilouris

Institute of Astronomy and Astrophysics, National Observatory of Athens, I.Metaxa & Vas.Pavlou str., GR-15236, Athens, Greece

xilouris@astro.noa.gr

Kate G. Isaak

Research and Scientific Support Department, European Space Agency, ESTEC, Keplerlaan 1, NL-2201, The Netherlands

kisaak@rssd.esa.int

and

Yu Gao

Purple Mountain Observatory, Chinese Academy of Sciences, Nanjing, Jiangsu 210008, China

pmogao@gmail.com

ABSTRACT

In this work we conclude the analysis of our CO line survey of Luminous Infrared Galaxies (LIRGs: $L_{\text{IR}} \gtrsim 10^{11} L_{\odot}$) in the local Universe (Paper I), by focusing

on the influence of their average ISM properties on the total molecular gas mass estimates via the so-called $X_{\text{co}}=M(\text{H}_2)/L_{\text{co},1-0}$ factor. One-phase radiative transfer models of the global CO Spectral Line Energy Distributions (SLEDs) yield an X_{co} distribution with: $\langle X_{\text{co}} \rangle \sim (0.6 \pm 0.2) M_{\odot} (\text{K km s}^{-1} \text{ pc}^2)^{-1}$ over a significant range of average gas densities, temperatures and dynamical states. The latter emerges as the most important parameter in determining X_{co} , with unbound states yielding low values and self-gravitating states the highest ones. Nevertheless in many (U)LIRGs where available higher-J CO lines (J=3–2, 4–3, and/or J=6–5) or HCN line data from the literature allow a separate assesment of the gas mass at high densities ($\geq 10^4 \text{ cm}^{-3}$) rather than a simple one-phase analysis we find that *near-Galactic* $X_{\text{co}} \sim (3-6) M_{\odot} (\text{K km s}^{-1} \text{ pc}^2)^{-1}$ values become possible. We further show that in the highly turbulent molecular gas in ULIRGs a high-density component will be common and can be massive enough for its high X_{co} to dominate the average value for the entire galaxy. Using solely low-J CO lines to constrain X_{co} in such environments (as it has been the practice up to now) may have thus resulted to *systematic underestimates of molecular gas mass in ULIRGs* as such lines are dominated by a warm, diffuse and unbound gas phase with low X_{co} but very little mass. Only well-sampled high-J CO SLEDs (J=3–2 and higher) and/or multi-J observations of heavy rotor molecules (e.g. HCN) can circumvent such a bias, and the latter type of observations may have actually provided early evidence of it in local ULIRGs. The only way that the global X_{co} of such systems could be significantly lower than Galactic is if the average dynamic state of the dense gas is strongly gravitationally unbound. This is an unlikely possibility that must be nevertheless examined, with lines of rare isotopologues of high gas density tracers (e.g. H^{13}CN , high-J ^{13}CO lines) being very valuable in yielding (along with the lines of the main isotopes) such constraints. For less IR luminous, disk-dominated systems, we find that the galaxy-averaged X_{co} deduced by one-phase models of global SLEDs can also underestimate the total molecular gas mass when much of it lies in a SF-quiescent phase extending beyond a central star-forming region. This is because such a phase (and its large X_{co}) remain inconspicuous in global CO SLEDs. Finally detailed studies of a subsample of galaxies finds ULIRGs with large amounts ($\sim 10^9 M_{\odot}$) of very warm ($\geq 100 \text{ K}$) and dense gas ($\gtrsim 10^5 \text{ cm}^{-3}$) that could represent a serious challenge to photon-dominated regions as the main energy portals in the molecular ISM of such systems.

Subject headings: galaxies: ISM — galaxies: starburst — galaxies: AGN — galaxies: IRAS — ISM: molecules — ISM: CO

1. Introduction

Soon after the discovery of the luminous infrared galaxies (LIRGs), whose bolometric luminosities are dominated by the infrared part of their Spectral Energy Distributions (SEDs) ($L_{\text{IR}} \geq 10^{11} L_{\odot}$) (e.g. Soifer et al. 1987), single dish and interferometric CO J=1–0, 2–1 line observations were used to determine their total molecular gas mass and its distribution (Sanders et al. 1988a; Tinney et al. 1990; Wang et al. 1991; Sanders et al. 1991; Solomon et al. 1997; Downes & Solomon 1998; Bryant & Scoville 1996, 1999). These efforts were paralleled by several investigations of the so-called $X_{\text{co}} = M(\text{H}_2)/L_{\text{CO}}(1-0)$ factor and its dependance on the average ISM conditions both theoretical (Dickman et al. 1988; Maloney & Black 1988; Wolfire et al. 1993; Sakamoto 1996; Bryant & Scoville 1996; Wall 2007) and observational (e.g. Israel 1988, 1993, 1997; Solomon et al. 1997; Downes & Solomon 1998; Yao et al. 2003). The average molecular gas conditions in LIRGs used in such studies have been typically constrained using CO(2–1)/(1–0) and CO/ ^{13}CO J=1–0, 2–1 line ratios (e.g. Braine & Combes 1992; Horellou et al 1995; Aalto et al. 1995; Papadopoulos & Seaquist 1998). Higher-J transitions (J=3–2 and higher) were used only sporadically and mostly for star-forming galactic nuclei (e.g. Devereux et al. 1994; White et al. 1994; Güsten et al. 1996; Nieten et al. 1999; Mauersberger et al. 1999; Dumke et al. 2001; Yao et al. 2003). This was a result of the larger difficulties such observations pose in terms of available submm receivers, their sensitivity, and the dry weather conditions needed (especially for $\nu \gtrsim 460$ GHz, CO J=4–3). Receiver sensitivity limitations also hindered large multi-J line surveys of the much fainter lines from heavy rotor molecules such as HCN that probe higher density gas ($>10^4 \text{ cm}^{-3}$) except in nearby galactic nuclei (Jackson et al. 1995; Paglione et al. 1997) and a few luminous ULIRGs (e.g. Gracia-Carpio et al. 2008).

Such limitations will soon be overcome after the ongoing commissioning of the Atacama Large Millimeter Array (ALMA) is completed. Then routine multi-J observations of CO and heavy rotor molecules will yield unhindered view over the entire range of physical conditions in molecular clouds, from their quiescent and low-density phase ($n(\text{H}_2) \sim (10^2 - 10^3) \text{ cm}^{-3}$, $T_{\text{kin}} \sim (10-15) \text{ K}$) to the dense and warm gas intimately associated with star formation ($n(\text{H}_2) \sim (10^4 - 10^7) \text{ cm}^{-3}$, $T_{\text{kin}} \sim (30-150) \text{ K}$). The power of interferometric multi-J line imaging in revealing the mass distribution of dense warm SF gas in LIRGs has already been demonstrated by pioneering SMA observations (Sakamoto et al. 2008; Wilson et al. 2009; Iono et al. 2007, 2009), while in the grand spiral M51 CO line ratio imaging at high resolution revealed AGN-excited gas in its nucleus (Iono et al. 2004). The influence of the high-excitation conditions found in SF regions gas on the X_{co} in galaxies may not necessarily be strong since dense and warm SF gas amounts to only $\sim (0.5-3)\%$ of typical Giant Molecular Clouds (GMCs) mass. Even smaller fractions of the total molecular gas in spirals disks resides in their centers ($\sim (0.1-1)\%$) where strong tidal fields, high cosmic ray energy densities

and/or AGN can drive a high molecular line excitation. Nevertheless this may no longer be true for the merger-driven starbursts in ULIRGs where a dense SF gas phase can contain the bulk of their total molecular gas mass (e.g. Solomon et al. 1992; Gao & Solomon 2004). Moreover, cases of AGN-driven mechanical and radiative feedback affecting the bulk of the molecular gas of the host galaxy and the corresponding CO SLEDs have now been identified (Papadopoulos et al. 2008; van der Werf et al. 2010). These systems along with ULIRGs, yield a nearby glimpse of ISM conditions that could be prevailing in the distant Universe.

In the present work we examine the influence of the average molecular gas conditions found in LIRGs (Papadopoulos et al 2011, hereafter Paper I) on the X_{co} factor. We do so by using the largest combined database of LIRGs/CO transitions for which such a study has been conducted, while discussing also the limitations and potential biases of past theoretical and observational studies. We then outline methods that could be employed in the upcoming era of ALMA, and the special role the Herschel Space Observatory (HSO) can play, towards improved total molecular gas mass estimates, especially for ULIRGs ($L_{\text{IR}} > 10^{12} L_{\odot}$). Several such galaxies whose CO line ratios indicate extreme ISM conditions (see Paper I) are now studied individually, their impact on the X_{co} values examined in detail. Throughout this paper we adopt a flat Λ -dominated cosmology with $H_0 = 71 \text{ km s}^{-1} \text{ Mpc}^{-1}$ and $\Omega_m = 0.27$.

2. Molecular gas physical conditions and mass estimates in LIRGs

The formal dependence of the X_{co} factor on the average density, temperature, and kinematic state of large molecular cloud ensembles (where the statistical notion of X_{co} remains applicable) is explored in several papers (e.g. Dickman et al. 1986; Young & Scoville 1991; Bryant & Scoville 1996; Solomon et al. 1997; Papadopoulos & Seaquist 1999; Downes & Solomon 1998; Yao et al. 2003). CO and ^{13}CO lines can yield constraints on these ISM properties, and thus on the corresponding X_{co} , via radiative transfer models (e.g. Mao et al. 2000; Weiss et al. 2001). In this regard low-J CO SLEDs (up to J=3–2) with $n_{\text{crit}} \sim (400 \text{ cm}^{-3} - 10^4) \text{ cm}^{-3}$ and $E_J/K_B \sim (5.5 - 33) \text{ K}$ are adequate for determining the average state of the molecular gas and thus the appropriate X_{co} , provided that most of its mass is distributed in ordinary GMCs. The low-J CO SLED segment and its modeling can then in principle yield the mass normalization for the entire CO or of any other molecular line SLED (e.g. of HCN) typically emanating from much smaller mass fractions. For several ULIRGs in our sample whose CO SLEDs will be extended up to J=13–12 using the HSO this normalization is especially important as it allows determining the mass of the highly-excited molecular gas emitting the very high-J lines, and setting important constraints on the energy source responsible for its excitation (van der Werf et al. 2010; Rangwala et al. 2011).

2.1. Prior work and some methodological limitations

There are currently only three major observational studies of X_{CO} using CO lines for substantial LIRG samples (Solomon et al. 1997; Downes & Solomon 1998; Yao et al. 2003). For the highly turbulent molecular gas in (U)LIRGs these typically find $X_{\text{CO}}=(1/10-1/3)X_{\text{CO,Gal}}$, with the low values attributed mostly to non self-gravitating gas distributions. For SF spiral disks a $X_{\text{CO,Gal}}\sim(4-5)X_1^1$ remains applicable as most of their molecular gas is found in cool, low-density, self-gravitating GMCs as those in the Milky Way, pockmarked by SF “spots” of warm and dense gas with also nearly Galactic X_{CO} (e.g. Young & Scoville 1991). In isolated spirals low $X_{\text{CO}}\sim(1/20-1/5)X_{\text{CO,Gal}}$ values can be found only in their nuclei ($2r\lesssim 100-200$ pc) (Regan 2000), but involve only small fractions of the total molecular gas reservoirs. Thus for the metal-rich environments of LIRGs current observational work points to a bimodal X_{CO} distribution, with near-Galactic values for all isolated spiral disks, and $\langle X_{\text{CO}}\rangle\sim(1/4-1/5)\times X_{\text{CO,Gal}}$ in the merger-driven starbursts of ULIRGs. This view has even been widely adopted even for high- z star-forming LIRGs where only sparse sampling of their CO SLEDs exists (e.g. Greve et al. 2005; Tacconi et al. 2006; Dannerbauer et al. 2009). It is worth noting that the claimed bimodality of the Schmidt-Kennicutt star formation relations (linking SFR and molecular gas supply) between disks and mergers (Daddi et al. 2010a; Genzel et al. 2010) is nearly equivalent to such an X_{CO} bimodality (Narayanan et al. 2010 and references therein).

Nevertheless much of the aforementioned observational work contains some serious methodological limitations borne out from the limited molecular line data available per object and specific assumptions made about the radiative transfer models. These are:

- Setting $T_{\text{kin}}=T_{\text{dust}}$ in the CO line radiative transfer models used to constrain X_{CO} even though photoelectric, turbulent, or cosmic-ray heating can easily induce $T_{\text{kin}}\gg T_{\text{dust}}$.
- Using a constant dV/dR (usually $1\text{ km s}^{-1}\text{ pc}^{-1}$) in the Large Velocity Gradient (LVG) radiative transfer models that interpret CO line ratios even if: a) virial gas motions alone correspond to $\sim 8-10$ times higher values for the dense gas ($n\gtrsim 10^5\text{ cm}^{-3}$) that may be dominant in ULIRGs, and b) stellar mass concomitant with molecular gas and/or tidally-induced velocity fields can easily yield much larger dV/dR values.
- The use of empirical relations and object-specific assumptions for obtaining X_{CO} expressions that can account for the potentially significant stellar mass concomitant with the molecular gas, an issue that arises especially in ULIRGs.

¹ $X_1=M_{\odot}(\text{K km s}^{-1}\text{ pc}^2)^{-1}$

- The molecular lines used in such studies (low-J CO lines) are insensitive to the properties of the gas with densities $n(\text{H}_2) > 10^3 \text{ cm}^{-3}$.

The last two set the most serious methodological limitations on the very influential study of X_{CO} in ULIRGs by Downes & Solomon 1998 (hereafter DS98), whose results are widely used for presumably similar systems at high redshifts. In that study models of the CO J=1–0, 2–1 interferometric images of 5 ULIRGs were used to deduce $X_{\text{CO}} \sim (1/5-1/6)X_{\text{CO,Gal}}$, attributing these low values to a continuous molecular gas distribution encompassing large fractions of stellar mass and thus velocity fields determined by the total (gas)+(stellar) mass (see also Downes et al. 1993; Solomon et al. 1997). The use of empirical relations (e.g. $L_{\text{IR}}/L'_{\text{CO}} = 200 L_{\odot} (\text{K km s}^{-1} \text{ pc}^2)^{-1}$), and setting a $r_{\text{m},*} = M_{\text{new},*}/M_{\text{bulge},*} \sim 0.5$ mass ratio of newly formed stars ($M_{\text{new},*}$) to those in an old stellar bulge ($M_{\text{bulge},*}$) in the pre-merger spirals make the computed X_{CO} *specific to the few ULIRGs studied* and certainly not automatically applicable to other ULIRGs in the local or the distant Universe. Moreover “freezing” dV/dR to $1 \text{ km s}^{-1} \text{ pc}^{-1}$ renders such models incapable of constraining the average dynamical state of the gas and thus exploring its effect on X_{CO} in a straightforward way (see section 2.2).

Furthermore, while the DS98 formalism can be generalized to arbitrary $r_{\text{m},*}$ values, it remains impractical for the dusty gas-rich systems at high redshifts where stellar populations are heavily dust-enshrouded. Finally an X_{CO} factor deduced solely from CO J=1–0, 2–1 line emission models may be inapplicable for a much denser gas phase ($n(\text{H}_2) \gtrsim 10^4 \text{ cm}^{-3}$). This will yield a small error when such a phase represents only a few% of the total mass per typical GMC (as is the case in spiral disks), but to a potentially much larger error if the dense gas dominates the molecular gas mass budget. These difficulties are compounded by setting $dV/dR = 1 \text{ km s}^{-1} \text{ pc}^{-1}$, which while justified by the sole CO(2-1)/(1-0) line ratio available in the DS98 study, may be partly responsible for the contradictory results obtained for the average gas density and CO line excitation. Indeed while HCN and high-J CO observations indicate much of the gas in some ULIRGs to be very dense ($n(\text{H}_2) > 10^4 \text{ cm}^{-3}$), radiative transfer models of CO J=1–0 and J=2–1 interferometric images of some of the same ULIRGs (e.g. Arp 220) become incompatible with these images already for $n \gtrsim 10^3 \text{ cm}^{-3}$ (DS98). Velocity gradients of $dV/dR \gg 1 \text{ km s}^{-1} \text{ pc}^{-1}$ (expected for the highly turbulent gas disks of ULIRGs) and high temperatures for the dense gas can much reduce line optical depths and the emergent CO line emission possibly alleviating these discrepancies.

In summary all current observational studies of X_{CO} in LIRGs, leave its range and dependence on the average density, temperature and kinematic state of the molecular gas still largely unexplored. The small LIRG/CO line datasets used in such studies, and the aforementioned limitations of the analysis methods, limits their applicability to other such systems in the local or the distant Universe.

2.2. The average state of the molecular gas and X_{co}

Our dataset of total CO lines luminosities for a substantial sample of LIRGs provides a good opportunity for exploring the X_{co} dependance on the average ISM state in vigorously star-forming systems. The average dV/dR for the gas is now a free parameter to be constrained by LVG radiative transfer models along with the density and temperature. This provides an extinction-free and straightforward method for determining the effects of stellar mass concomitant with molecular gas and/or tidal disruption of molecular clouds on X_{co} .

To place our discussion regarding molecular gas mass estimates in LIRGs in an autonomous context we reproduce the X_{co} factor (see Appendix) as

$$X_{\text{CO}} = \frac{M(\text{H}_2)}{L'_{\text{CO}(1-0)}} = \frac{3.25}{\sqrt{\alpha}} \frac{\sqrt{n(\text{H}_2)}}{T_{\text{b},1-0}} K_{\text{vir}}^{-1} \left(\frac{M_{\odot}}{\text{K km s}^{-1} \text{ pc}^2} \right), \quad (1)$$

where $\alpha=0.55-2.4$ depending on the assumed cloud density profile (see Bryant & Scoville 1996, Eqs A 11, A 17), and $n(\text{H}_2)$, $T_{\text{b},1-0}$ are the average gas density and CO J=1–0 brightness temperature of the molecular cloud ensemble. The parameter K_{vir} is given by

$$K_{\text{vir}} = \frac{(dV/dR)}{(dV/dR)_{\text{virial}}} \sim 1.54 \frac{[\text{CO}/\text{H}_2]}{\sqrt{\alpha} \Lambda_{\text{co}}} \left(\frac{n(\text{H}_2)}{10^3 \text{ cm}^{-3}} \right)^{-1/2}, \quad (2)$$

(with $\Lambda_{\text{co}} = [\text{CO}/\text{H}_2]/(dV/dR)$ being one of the outputs of a typical LVG model), and determines the average dynamic state of the molecular gas, with $K_{\text{vir}} \sim 1-3$ for the (mostly) self-gravitating GMCs in the Galactic disk (and $K_{\text{vir}} \ll 1$ corresponding to dynamically unattainable gas motions). For a typical value of $\alpha=1.5$ Equation 1 becomes

$$X_{\text{CO}} = 2.65 \frac{\sqrt{n(\text{H}_2)}}{T_{\text{b},1-0}} K_{\text{vir}}^{-1} \left(\frac{M_{\odot}}{\text{K km s}^{-1} \text{ pc}^2} \right), \quad (3)$$

which we use in the present work. For ordinary GMCs with $n(\text{H}_2) \sim 500 \text{ cm}^{-3}$, $T_{\text{b},1-0} \sim 10 \text{ K}$, and $K_{\text{vir}} \sim 1-2$ the latter yields $X_{\text{co}} \sim (3-6) X_1$ (where $X_1 = M_{\odot} (\text{K km s}^{-1} \text{ pc}^2)^{-1}$).

The optically thin limit for CO J=1–0 line emission is often adopted to provide a lower limit on the total molecular gas mass (e.g. Bryant & Scoville 1996; Solomon et al. 1997). The availability of several CO lines allows a more robust such limit without assuming LTE:

$$X_{\text{co}}^{(\text{thin})} = 0.078 \left[1 + \frac{1}{3} e^{5.5/T_{\text{ex},10}} + \frac{5}{12} r_{21} + \frac{7}{27} r_{32} + \dots \frac{2J+3}{3(J+1)^2} r_{J+1J} + \dots \right] \left(\frac{M_{\odot}}{\text{K km s}^{-1} \text{ pc}^2} \right), \quad (4)$$

(see Appendix), which makes obvious that, unless the CO line ratios become significantly larger than unity (which they can in optically thin emission), most of the contributions come from the low J levels. The LTE expression is:

$$X_{\text{co}}^{(\text{thin})}(\text{LTE}) = 9.45 \times 10^{-3} \left[\left(\frac{T_{\text{k}}}{\text{K}} \right) e^{5.5/T_{\text{k}}} \right] \left(\frac{M_{\odot}}{\text{K km s}^{-1} \text{ pc}^2} \right), \quad (5)$$

which gives a higher (and less reliable) lower limit since the LTE partition function can be significantly larger than the non-LTE one. The optically thin approximation can be used also for the realistic case of significant CO line optical depths as long as large velocity gradients keep the photon escape probability local throughout the bulk of the molecular gas mass. Then Equation 4 is modified to

$$X_{\text{co}}^{(\beta)} = 0.078 \beta_{10}^{-1} \left[1 + \frac{1}{3} e^{5.5/T_{\text{ex},10}} + \frac{5}{12} \left(\frac{\beta_{10}}{\beta_{21}} \right) r_{21} + \frac{7}{27} \left(\frac{\beta_{10}}{\beta_{32}} \right) r_{32} + \dots \right. \\ \left. + \dots \frac{2J+3}{3(J+1)^2} \left(\frac{\beta_{10}}{\beta_{J+1J}} \right) r_{J+1J} + \dots \right] \left(\frac{M_{\odot}}{\text{K km s}^{-1} \text{ pc}^2} \right), \quad (6)$$

where $\beta_{J+1J} = [1 - \exp(-\tau_{J+1J})] / \tau_{J+1J}$ is the photon escape probability (see Appendix). The last equation provides a more robust lower limit than Equation 4, as it accounts for finite line optical depths (computed from radiative transfer models). If enough line ratios are available, the estimate from Equation 6 will approach that of Equation 3 as long as one average gas phase dominates the emergent CO line emission.

In Figure 1 we show the X_{co} and $X_{\text{co}}^{(\text{thin})}(\text{LTE})$ distributions, computed from Equations 3 and 5 and the results of one radiative transfer models for the CO SLEDs and ^{13}CO lines for all the LIRGs in our sample (see Paper I). Most X_{co} values are $\lesssim 1.5 X_1$, with $\langle X_{\text{co}} \rangle \sim 0.60 X_1$ obtained for the main distribution (excluding the few outliers beyond $3 X_1$). The $X_{\text{co}}^{(\text{thin})}(\text{LTE})$ distribution gives similar results, indicating that most of the states compatible with the CO SLEDs have optically thin or moderately optically thick CO J=1–0 line ($\tau_{10} \sim 1-3$). This has been noted in the past in the context of a two-phase ISM model and attributed to the high temperatures of a turbulent “envelope” phase in molecular clouds (Aalto et al. 1995).

The X_{co} range obtained using our one-phase models of global CO SLEDs is similar to that reported by DS98 and Yao et al. 2003. Moreover in Figure 2 the distribution of

$\sqrt{n(\text{H}_2)}/T_{\text{b},1-0}$ demonstrates that unlike often stated, the effects of density and temperature do not always cancel out but are responsible for much of the X_{co} variations over different ISM environments (compare Figure 2, with the X_{co} distribution in Figure 1). Nevertheless the average dynamical state of the gas (i.e. K_{vir}) remains the most important factor affecting the average X_{co} . This is shown in Figure 3 where the X_{co} distributions for virial/near-virial and unbound average gas dynamical states are shown. In the merger-driven starbursts of ULIRGs highly non-virial gas velocities can be caused by significant amounts of stellar mass concomitant with a continuous molecular gas distribution as noted by DS98 (see also Solomon et al. 1997), albeit without using radiative transfer models to constrain K_{vir} . Strong tidal fields acting on GMC cloud envelopes and/or a diffuse intercloud molecular gas distribution whose velocity field traces the combined potential of the surviving dense GMC cores as well as stars will both raise the average K_{vir} , and further reduce the corresponding X_{co} (Equation 3).

In Figure 4 the distribution of $X_{\text{co}}^{(\beta)}$ computed from Equation 6 is shown which, unlike that deduced from Equation 3, uses the CO line ratios explicitly. This makes it more suitable when fully-sampled CO SLEDs from $J=1-0$ up to high- J (e.g. $J=6-5$, $7-6$) are available, and when the turbulent models of the hierarchical density structures of molecular clouds (e.g. Ossenkopf 2002) become refined enough to provide global CO and ^{13}CO SLEDs as well as the corresponding $\beta_{J+1,J}$ values per density “sub-phase”. For well-sampled ^{13}CO SLEDs the $X_{\text{co}}^{(\beta)}$ expression (using the appropriate $[^{13}\text{CO}/\text{H}_2]$ abundance) is even more useful as $\beta_{J+1,J}(^{13}\text{CO})\sim 1$. In our current study using the output $\beta_{J+1,J}$ values from our one-phase models in Equation 6 yields an $X_{\text{co}}^{(\beta)}$ distribution similar to that of X_{co} from Equation 3.

Interestingly the X_{co} distributions, while concentrated within $\sim(0.3-1.5) X_1$, do extend out to Galactic values $\sim(2.5-6) X_1$. These are found for disk-dominated LIRGs (e.g. NGC 157 and Mrk 1048), (U)LIRGs with unexpectedly “cold” CO ratios (e.g. IRAS 05189-2524) where cool (~ 15 K) gas with low/modest densities ($\sim(10^2-10^3) \text{cm}^{-3}$) dominates their average ISM state. Surprisingly, *Galactic X_{co} values can be found also in some ULIRGs*, whose “hot” CO ratios (e.g. IRAS 08572+3915) indicate a dominant warm ($\sim(100-150)$ K) and dense ($\sim(3\times 10^4-10^6) \text{cm}^{-3}$) phase, or other evidence (e.g. multi- J HCN lines) suggest a massive dense, gas phase (e.g. Mrk 231). Thus large X_{co} values are possible for both high and low excitation gas phases and thus cannot be used as indicators of Galaxy-type ISM conditions in distant star forming disks (e.g. Daddi et al. 2010b). This also suggests that in many local ULIRGs and similar systems at high redshifts *the widely adopted $X_{\text{co}}\sim(0.8-1) X_1$ values underestimate their molecular gas mass.*

2.3. Eddington-limited star formation and a minimum molecular gas mass

Recent studies of SF feedback suggest a maximum $\epsilon_{g,*} = L_{\text{IR}}^{(*)}/M_*(\text{H}_2) \sim 500 (L_{\odot}/M_{\odot})$ for the dense and warm gas $M_*(\text{H}_2)$ near SF sites in galaxies as a result of strong radiation pressure from the nascent O, B star clusters onto the concomitant dust of the accreted gas fueling these sites (Scoville 2004; Thompson et al. 2005; Thompson 2009). Thus, provided that average dust properties (e.g. its effective radiative absorption coefficient per unit mass) remain similar in metal-rich star-forming systems such as LIRGs, a near-constant $\epsilon_{g,*}$ is expected among them. A value of $\epsilon_{g,*} \sim 500 (L_{\odot}/M_{\odot})$ is actually measured in individual SF sites of spiral disks such as M 51 and entire starbursts such as Arp 220 (Scoville 2003), while $\sim(440 \pm 100) (L_{\odot}/M_{\odot})$ is obtained for CS-bright star-forming cores in the Galaxy (Shirley et al. 2003). Further evidence for a near-constant $\epsilon_{g,*}$ is the tight linear $L_{\text{IR}}\text{-HCN}(1\text{-}0)$ correlation found for individual GMCs up to entire ULIRGs (Wu et al. 2005) with HCN $J=1\text{-}0$ used as a dense gas mass tracer. However the intermittency expected for galaxy-sized molecular gas reservoirs (i.e. at any given epoch of a galaxy's evolution some dense gas regions will be forming stars while others will not) will lower the global $\epsilon_{g,*}$ to $\sim 1/3\text{-}1/2$ of the Eddington value (Andrews & Thompson 2011).

Similar $\epsilon_{g,*}$ values can be obtained without explicit use of the Eddington limit (and the detailed dust properties it entails), but from the typical $L_*/M_{\text{new},*}$ in young starbursts where $M_{\text{new},*}$ is the mass of the new stars and L_* their bolometric luminosity ($\sim L_{\text{IR}}^{(*)}$ for the deeply dust-enshrouded SF sites). For $\epsilon_{\text{SF},c} = M_{\text{new},*}/[M_{\text{new},*} + M_*(\text{H}_2)]$ as the SF efficiency of the dense gas regions where the new stars form it is

$$\epsilon_{g,*} = \frac{\epsilon_{\text{SF},c}}{1 - \epsilon_{\text{SF},c}} \left(\frac{L_{\text{IR}}^{(*)}}{M_{\text{new},*}} \right). \quad (7)$$

For $\epsilon_{\text{SF},c} \sim 0.3\text{-}0.5$ typical for dense SF regions, and $L_{\text{IR}}^{(*)}/M_{\text{new},*} = (300\text{-}400) (M_{\odot}/L_{\odot})$ (Downes & Solomon 1998 and references therein), Equation 7 yields $\epsilon_{g,*} \sim (130\text{-}400) (M_{\odot}/L_{\odot})$. Here we choose $\epsilon_{g,*} = 250 (L_{\odot}/M_{\odot})$, close to the average values from Equation 7 and the black body limit deduced for compact CO line emission concomitant with an optically thick ($\tau_{100\mu\text{m}} > 1$) dust emission (Solomon et al. 1997). Eddington-limited star formation in LIRGs implies a *minimum molecular gas mass* $M_{\text{SF}} = L_{\text{IR}}^{(*)}/\epsilon_{g,*}$ fueling their observed star formation rates. In Figure 5 we show the M_{SF} distribution which, for the ULIRGs in our sample, reaches up to $\sim 5 \times 10^9 M_{\odot}$ i.e. surpassing the total molecular gas reservoirs of typical spirals.

2.4. Computing X_{co} in a two-component approximation

In some cases where one-phase LVG models of global CO line ratios of LIRGs do not converge to a well-defined range of physical conditions, a simple two-phase model can be used to examine the underlying ISM conditions and the corresponding X_{co} factors. The total CO J=1–0 luminosity can then be expressed as

$$L'_{\text{CO},1-0} = L_{\text{CO},1-0}^{(h)'} + L_{\text{CO},1-0}^{(l)'} = (\epsilon_{g,*} X_{\text{co}}^{(h)})^{-1} L_{\text{IR}}^{(*)} + L_{\text{CO},1-0}^{(l)'} \quad (8)$$

where (h) and (l) indicate the high and the low excitation phases, $X_{\text{co}}^{(h)}$ is the CO-H₂ conversion factor for the former, and $\epsilon_{g,*} = 250(L_{\odot}/M_{\odot})$. This assumes that the high excitation phase fuels Eddington-limited star formation. For any other transition

$$L'_{\text{CO},J+1-J} = \left[\frac{L_{\text{IR}}^{(*)}}{\epsilon_{g,*} X_{\text{co}}^{(h)}} \right] r_{J+1,J}^{(h)} + L_{\text{CO},J+1-J}^{(l)'} \quad (9)$$

The molecular gas near H II regions and interfaces between molecular clouds and O,B stellar associations is an obvious choice for obtaining template high-excitation CO SLEDs. The beam-matched CO line survey of the Orion A and B GMCs found $r_{21} = 1.2\text{--}1.3$ and $R_{21} = 10$ (the CO/¹³CO J=2–1 ratio) in such “hot” spots (Sakamoto et al. 1994). These ratios along with $T_{\text{kin}} \geq 100$ K (expected from the high CO line brightness temperatures in such SF spots) set as constraints to a one-phase LVG model yield: $T_{\text{kin}} = (125\text{--}150)$ K, $n(\text{H}_2) = 3 \times 10^5 \text{ cm}^{-3}$, $K_{\text{vir}} = 7$, and corresponding line ratios: $r_{21}^{(h)}(3) = 1.35$, $r_{32}^{(h)} = 1.33$, $r_{43}^{(h)} = 1.30$, $r_{54}^{(h)} = 1.27$, $r_{65}^{(h)} = 1.25$, and $r_{76}^{(h)} = 1.22$. For this LVG solution set we compute (Equation 3) $X_{\text{co}}^{(h)} \sim 2.2 X_1$, and from Equations 8 and 9 the CO line ratios of the low-excitation (l)-phase. These can then be used as constraints on 1-phase LVG models to obtain the average ISM conditions and $X_{\text{co}}^{(l)}$. For such a 2-phase decomposition the effective $X_{\text{co}}^{(2\text{-ph})}$ factor would be

$$X_{\text{co}}^{(2\text{-ph})} = \frac{X_{\text{co}}^{(h)} + \rho_{\text{co}}^{(1-h)} X_{\text{co}}^{(l)}}{1 + \rho_{\text{co}}^{(1-h)}} \quad (10)$$

with $\rho_{\text{co}}^{(1-h)} = L_{\text{co},1-0}^{(l)'}/L_{\text{co},1-0}^{(h)'}$. Using the Eddington-limit normalization for $L_{\text{co},1-0}^{(h)'}$ yields

$$X_{\text{co}}^{(2\text{-ph})} = X_{\text{co}}^{(l)} + \frac{L_{\text{IR}}^{(*)}}{\epsilon_{g,*} L'_{\text{CO},1-0}} \left(1 - \frac{X_{\text{co}}^{(l)}}{X_{\text{co}}^{(h)}} \right), \quad (11)$$

When lines such as higher-J CO transitions (J=4–3, 6–5) and/or heavy rotor molecular lines

(e.g. HCN) are available, they are used to set constraints on the (h)-phase, $\rho_{\text{co}}^{(1-h)}$, and $X_{\text{co}}^{(2-ph)}$ without assuming the (h)-phase CO SLED and $X_{\text{co}}^{(h)}$ deduced from the Orion GMC star-forming “spots”.

3. The X_{co} factor in LIRGs

The average ISM conditions deduced using the CO lines available per LIRG (see Paper I) encompasses the $[n(\text{H}_2), T_{\text{kin}}, K_{\text{vir}}]$ parameter space where most of the mass is expected to reside in ordinary GMCs. Thus the narrow X_{co} distribution around $\langle X_{\text{co}} \rangle \sim 0.6 X_1$ (Figs 1, 4), does not seem as the result of an excitation bias induced by the particular molecular lines used. This is not to say that other high-J CO or e.g. HCN line luminosities are expected to be compatible with the average ISM states deduced from our current CO line dataset but rather than that such lines with their higher critical densities will probe much smaller gas mass fractions per typical GMC to be of any consequence when it comes to the global X_{co} .

It is tempting to consider the aforementioned picture as complete. It is certainly compatible with models of supersonic turbulence in ordinary GMCs where most molecular gas mass is found at densities $< 10^4 \text{ cm}^{-3}$, its conditions thus “accessible” to the CO, ^{13}CO lines used to constrain them (and X_{co}) in our study. In the merger-driven starbursts of ULIRGs however GMCs may be far from ordinary. Stripping of their outer envelopes by strong tidal fields and/or the large pressures from a hot ionized gas phase resulting from HI cloud collisions, both expected in merger environments (e.g. Solomon et al. 1997), can dramatically alter the $M(\text{H}_2)$ - $n(\text{H}_2)$ distribution towards most mass being at $n(\text{H}_2) \geq 10^4 \text{ cm}^{-3}$. This actually occurs in the Galactic Center (e.g. Güsten & Philipp 1994), and in ULIRGs it can involve their entire molecular gas reservoirs. In such cases low-J CO, ^{13}CO lines are no longer sensitive to the average ISM conditions and may thus yield inaccurate “corrections” to the global X_{co} factor with respect to its Galactically calibrated value.

3.1. The X_{co} in ULIRGs: theoretical expectations for highly turbulent gas

The high pressures in the highly turbulent gas disks in ULIRGs (DS98) will: a) result to much larger average gas densities at all scales, and b) “relocate” large mass fractions of their GMCs to densities $n(\text{H}) > 10^4 \text{ cm}^{-3}$. The latter can be easily shown from the probability distribution function (pdf) of the density in supersonically turbulent clouds. This is well-approximated by a log-normal distribution with a dispersion:

$$\sigma_\rho \approx \left[\ln \left(1 + \frac{3M^2}{4} \right) \right]^{1/2}, \quad (12)$$

where $M=\sigma_v/c_s$ is the average 1-dim Mach number (Padoan & Nordlund 2002). The mass fraction contained in cloud structures with overdensities $x \geq x_o$ ($x=n/\langle n \rangle$) is then given by

$$f = \frac{M(x \geq x_o)}{M_{\text{tot}}} = \frac{1}{2} \left[1 + \text{erf} \left(\frac{-2 \ln(x_o) + \sigma_\rho^2}{2^{3/2} \sigma_\rho} \right) \right]. \quad (13)$$

The high velocity dispersions $\sigma_v \sim (30-140) \text{ km s}^{-1}$ measured in the molecular disks of ULIRGs (DS98; see also Swinbank et al. 2011 for a recently discovered such disk at $z \sim 2.3$) versus those in spiral disks ($\sim (5-10) \text{ km s}^{-1}$) correspond to $M(\text{ULIRGs}) \sim (3-30) \times M(\text{spirals})$. For $M(\text{spiral})=10$ then $\sigma_\rho(\text{spirals}) \sim 2$, while $\sigma_\rho(\text{ULIRGs}) \sim 2.55-3.33$, which dramatically extends the gas density pdf expected in ULIRGs towards high values where much of the gas mass will now lie. Indeed for the GMCs in spiral disks only $\sim 3\%$ of the mass will be found at overdensities of $x > x_o = 500$ ($= 5 \times 10^4 \text{ cm}^{-3}$ for typical GMC with $\langle n \rangle = 100 \text{ cm}^{-3}$) while for ULIRGs this is $\sim 45\%$ (Figure 6). This difference can be even larger since the *average* molecular gas density in disks is lower ($\langle n \rangle \sim (100-500) \text{ cm}^{-3}$) than in ULIRGs where it can reach up to at least $\sim 10^4 \text{ cm}^{-3}$ (Greve et al. 2009). Thus gas at $n \geq 5 \times 10^4 \text{ cm}^{-3}$ corresponds to an overdensity of $x_o = 100-500$ (containing $\lesssim 10\%$ of gas mass) for GMCs in spirals, and only $x_o = 5$ (and 90% of the mass) for GMCs in ULIRGs. The typical CO SLED available for LIRGs in our sample ($J=1-0, 2-1, 3-2$) would then be insensitive to the state of the molecular gas in ULIRGs and thus unable to constrain the corresponding X_{co} factor, while it would remain adequate for such a task for the molecular gas in isolated spirals.

Interestingly the few cases of near-Galactic X_{co} in ULIRGs were found when either higher-J CO lines were available or when a dense and warm gas phase was massive enough to be obvious even in low-J CO SLEDs (Paper I, and section 4). The X_{co} for such dense gas can be high, approaching and even surpassing Galactic values. Indicatively, for $n = 5 \times 10^4 \text{ cm}^{-3}$ and warm gas with a thermalized CO $J=1-0$ line $T_{b,1-0} \sim T_{\text{kin}} \sim (100-150) \text{ K}$, it is: $X_{\text{co}} \sim (4-6) K_{\text{vir}}^{-1} X_{\text{I}}$ (Eq. 3), which for self-gravitating gas ($K_{\text{vir}}=1$) corresponds to Galactic values.

Moreover, for the highly turbulent, high-pressure ISM environments in ULIRGs the notion of molecular gas reservoirs reducible to ensembles of discrete GMCs may no longer apply, with much of the gas in the pre-merger GMCs redistributed in continuous disks of $\sim (100-300) \text{ pc}$ diameter (DS98; Sakamoto et al. 2008). A warm, low-density, molecular gas phase, with large K_{vir} (> 10) can then be generated, *alongside* the denser one, by the tidal disruption of GMC “envelopes” in merger environments, the high pressures turning intercloud CNM HI into H_2 , and the effects of supersonic turbulence driven at the largest

scales (e.g. Ossenkopf 2002). Such a diffuse phase, even if containing little mass, can easily dominate the emergent global CO J=1–0, 2–1 line emission of ULIRGs, yielding “cold” CO(2-1)/(1-0) ratios and low X_{co} factors (a result of its low densities, high temperatures, and large K_{vir} values). These low X_{co} values, *while appropriate for the diffuse gas mass, may not be so for the bulk of the molecular gas that now resides at much higher densities.*

Thus in the very turbulent molecular gas reservoirs of ULIRGs a combination of: a) most of their mass residing at high densities (with potentially large X_{co} factors), and b) the existence of a diffuse, warm, and unbound phase with little mass (and low X_{co}) dominating low-J CO SLEDs (and the average X_{co} determined from them), can easily result to *a systematic underestimate of their total molecular gas mass.* All current observational studies likely suffer from this bias, expected to be most prominent in ULIRGs with high molecular gas surface densities. This includes the present study as mostly low-J CO SLEDs (up to J=3–2) are typically available per LIRG. The only exceptions are the few ULIRGs for which, a highly excited CO J=3–2 line, CO J=4–3, 6–5 lines, and/or HCN lines from the literature allowed the revealing of their massive dense gas reservoirs (see Section 4). Studies of X_{co} in similar systems at high redshifts (e.g. Tacconi et al. 2008) will be similarly affected. Only molecular SLEDs with high critical densities can overcome such an X_{co} bias in ULIRGs and see how many actually lie on the high end of the X_{co} distributions shown in Figures 1 and 4.

3.1.1. Numerical simulations and the X_{co} factor: important caveats, and ways forward

Recently GMC-sized numerical simulations that include H_2 and CO formation/destruction and radiative transfer in MHD turbulent models were used to explore X_{co} and its dependence on average ISM conditions (Shetty et al. 2011a,b). These simulations also include chemistry and thermodynamical effects but not SF-driven heating (via photons or CRs) or turbulent heating which could dominate in ULIRGs. Currently such studies explore Galactic-type GMCs whose X_{co} values they found similar to the one observed. Extending such numerical models to ISM conditions expected in ULIRGs is not straightforward as GMC boundary conditions such as ambient radiation fields, surface pressure, external gravitational field and its tidal terms (important for galactic centers of spirals and ULIRGs) are set constant in GMC-sized simulations or, in the case of tidal fields, are omitted altogether. Nevertheless in any realistic setting of GMCs in galaxies these boundary conditions do change, sometimes faster than internal cloud evolutionary timescales, and especially so in ULIRGs.

Galaxy-sized numerical studies of X_{co} in disks and mergers recently presented by Narayanan et al. 2011 address the aforementioned important point of coupled GMC-galaxy evolution by tracking the evolution of GMC boundary conditions, but do so by necessarily adopting

some subresolution methods to follow in-cloud physics and keep the problem computationally tractable. They recover Galactic X_{co} values for disks, but ~ 5 - 10 times lower ones in mergers, with a large spread that makes a single ULIRG-appropriate X_{co} factor impractical. Nevertheless, for ULIRGs in particular, these simulations do not have (and could not have) the resolution necessary to track gas with $n \geq 10^4 \text{ cm}^{-3}$ (where most of their gas mass resides). Resolving the all-important kinematic state of such a dense gas component (self-gravitating or not?) within their compact gas reservoirs ($\sim (100\text{-}300) \text{ pc}$) is currently impossible with galaxy-sized simulations, as is the explicit tracking of the large turbulence-regulated range of densities expected in ULIRGs. There the *average* densities can surpass $\sim 10^4 \text{ cm}^{-3}$, while the high levels of turbulence will maintain $\gtrsim 60\%$ of the mass at $n \geq 10^5 \text{ cm}^{-3}$ (Figure 6). With the T_{kin} values computed in such simulations likely to be lower limits (as CR and mechanical SNR-driven heating are omitted), gas densities and the corresponding kinematic states remain the only parameters affecting the average X_{co} in metal-rich environments that can push its values either way. Indeed while additional heating can only raise T_{kin} and thus the CO J=1–0 brightness temperature (reducing X_{co}), high densities ($>10^4 \text{ cm}^{-3}$) and self-gravitating states ($K_{\text{vir}} \sim 1$) will act to raise X_{co} .

GMC-sized simulations of the much more turbulent and denser molecular gas in ULIRGs are necessary for computing the corresponding X_{co} but these must now use new initial conditions with: a) much higher volumed-averaged gas densities (current ones use $\sim 150 \text{ cm}^{-3}$), b) higher velocity dispersions (current ones use $\sigma_v \sim 2.4 \text{ km s}^{-1}$), and c) higher background CR energy densities (and thus non-negligible CR gas heating). Such simulations and their emergent line intensities can be compared to much richer molecular SLEDs available now than in the past. These include the typical CO lines from J=1–0 up to J=4–3 observed from the ground, rising up to J=13–12 using the Herschel Space Observatory (van der Werf et al. 2010), further complemented by multi-J observations of heavy rotor molecules like HCN, HCO⁺, CS (e.g. Greve et al. 2009) as sensitivities vastly improve in the era of ALMA. Thus, rather than simply trust the X_{co} yielded by GMC-sized simulations as is currently done, these simulations will yield X_{co} values as a by-product of the much more difficult task of reproducing relative strengths of molecular line luminosities with critical densities ranging from $\sim 100 \text{ cm}^{-3}$ up to $\sim 10^7 \text{ cm}^{-3}$. These encompass the entire range of hierarchical structures in turbulent GMCs, from a highly turbulent low-density possibly non self-gravitating “GMC-envelope” phase at large scales up to self-gravitating compact dense gas cores with dissipated supersonic turbulence (e.g. Ossenkopf 2002). GMC-sized numerical simulations exploring a dense grid of ULIRG-type GMC boundary conditions and determining the corresponding X_{co} grid can then be used to inform galaxy-sized numerical simulations where such boundary conditions are tracked, while resolving the hierarchical structures of individual GMCs (and thus determining $f(x_o)$ from the simulations) remains out of reach.

3.2. High X_{co} in ULIRGs: past observational evidence ignored?

As discussed in the previous sections, by relying on low-J CO SLEDs, most observational studies of X_{co} may have imparted a bias towards low values in ULIRGs. Nevertheless past observations of heavy rotor molecules such as HCN J=1–0 have given early hints of a large scale $M(\text{H}_2)$ - $n(\text{H}_2)$ redistribution in these merger systems, which placed large fractions ($\gtrsim 50\%$) of their total molecular gas mass at much higher densities ($\geq 10^4 \text{ cm}^{-3}$) than in isolated gas-rich disk systems (e.g. Solomon et al. 1992; Gao & Solomon 2004). However a single transition of a heavy rotor molecule cannot set constraints on the gas temperature and density (let alone on its average dynamical state) useful enough to constrain the corresponding X_{mol} factor well. Thus these early estimates of the dense molecular gas mass in ULIRGs are necessarily very uncertain as they relied on an X_{HCN} factor derived for $n \sim n_{\text{crit}}[\text{HCN}(1-0)]$, self-gravitating gas, and HCN J=1–0 brightness temperatures typical of the IR color temperatures of SF galaxies (e.g. Gao & Solomon 2004). Indicatively for $n(\text{H}_2) = 5 \times 10^4 \text{ cm}^{-3}$, $T_{\text{b},1-0}(\text{HCN}) = 40 \text{ K}$ and $K_{\text{vir}} = 1$ Equation 3 applied for HCN J=1–0 yields $X_{\text{HCN}} = 15 X_{\text{I}}$, which can be higher still for higher gas densities, as indicated by multi-J HCN, CS and HCO^+ line observations of Arp 220 and NGC 6240 and where $X_{\text{HCN}} \sim (20-35) X_{\text{I}}$ (Greve et al. 2009).

For such high X_{HCN} values and $L'_{\text{HCN},1-0}/L'_{\text{co},1-0} = 1/4-1/6$ observed in ULIRGs (e.g. Solomon et al. 1992; Gao & Solomon 2004; Gracia-Burillo et al. 2012) it is easy to show that $X_{\text{co}}^{(2-\text{ph})}$ (Equation 10) will yield near-Galactic or higher values in such systems. Indeed, assuming that the only contribution to the (h)-phase in Equation 10 comes from the HCN-bright gas (i.e. the HCN emission from the low-excitation (l) phase is negligible) we can determine $\rho_{\text{co}}^{(1-\text{h})}$ from

$$\rho_{\text{co}}^{(1-\text{h})} = \frac{L'_{\text{co},1-0}}{L_{\text{co},1-0}^{(\text{h})'}} - 1 = \frac{r_{\text{CO}/\text{HCN}}^{(\text{obs})}}{r_{\text{CO}/\text{HCN}}^{(\text{h})}} - 1, \quad (14)$$

where $r_{\text{CO}/\text{HCN}}^{(\text{obs})} = L'_{\text{co},1-0}/L'_{\text{HCN},1-0}$ in ULIRGs (=4-6), and $r_{\text{CO}/\text{HCN}}^{(\text{h})}$ that of the (h)-phase. The latter can be found using a radiative transfer model for densities typical of HCN-bright gas, an assumed gas temperature, and setting $K_{\text{vir}}^{(\text{h})} = 1$. For $n = 10^5 \text{ cm}^{-3}$, and $T_{\text{kin}} = 100 \text{ K}$ using an LVG model for HCN and CO lines we compute $T_{\text{b},\text{HCN}1-0} = 41 \text{ K}$ and $T_{\text{b},\text{co}1-0}^{(\text{h})} = 96 \text{ K}$. Thus $r_{\text{CO}/\text{HCN}}^{(\text{h})} = 2.34$, while $X_{\text{HCN}} \sim 20 X_{\text{I}}$ and $X_{\text{co}}^{(\text{h})} \sim 8.6 X_{\text{I}}$, with $\rho_{\text{co}}^{(1-\text{h})} \sim 0.71-1.56$. Setting $X_{\text{co}}^{(1)} = 0.5 X_{\text{I}}$ (Figs. 1, 4) for the low-excitation (CO-bright but HCN-dark) phase, we obtain $X_{\text{co}}^{(2-\text{ph})} \sim (4-5) X_{\text{I}}$, i.e. Galactic values. These are now due to much higher fractions of dense HCN-bright gas than in the Galaxy, with large X_{HCN} (and $X_{\text{co}}^{(\text{h})}$). If such $X_{\text{co}}^{(2-\text{ph})}$ values are the norm in the high-pressured turbulent gas disks of ULIRGs, *their dynamical masses would be dominated by the molecular gas*, quite unlike isolated SF spirals. Indeed for all the ULIRGs in the

DS98 study whose dynamical mass is reasonably well-constrained (with both CO 1-0 and 2-1 imaging) Galactic X_{co} values would yield $M_{\text{gas}}/M_{\text{dyn}} \sim 0.6-1$, and compatible with the obvious limitation of $M_{\text{gas}}/M_{\text{dyn}} \leq 1$ within the observational uncertainties of M_{dyn} estimates. Regarding the latter it is worth pointing out that low S/N for extended CO line emission regions in current interferometric maps as well as dynamically unrelaxed, non-circular, molecular gas motions (expected in strong mergers) typically cause *underestimates* rather than overestimates of the actual M_{dyn} . Surprisingly such a bias was deduced even for gas-rich but otherwise isolated disks with numerical simulations showing an observationally-determined M_{dyn} to be typically be $\sim 30\%$ less than the actual value (Daddi et al. 2010b). Needless to say this state of affairs becomes worse still of CO-imaged systems at high redshifts.

Multi-J observations of heavy rotor molecules and/or high-J CO lines in ULIRGs can produce dense gas mass estimates via a (radiative transfer model)-constrained X_{mol} factor. However the few such studies available (Papadopoulos 2007; Papadopoulos et al. 2007; Krips et al. 2008; Gracia-Carpio et al. 2008; Greve et al. 2009) are a testimony of how hard it is to overcome the degeneracies inherent in radiative transfer models of optically thick line emission from heavy rotor molecules. The n- T_{kin} solution degeneracies of the Large Velocity Gradient (LVG) radiative transfer models typically used in such studies translate to a wide range of X_{HCN} factors, ranging from $\sim 10 X_1$ and reaching up to $\sim (50-90) X_1$ (Krips et al. 2008; Gracia-Carpio et al. 2008). Tellingly even the two studies with the largest number of dense gas tracer lines available per ULIRG, that of Mrk 231 (Papadopoulos et al. 2007) and of Arp 220, NGC 6240 (Greve et al. 2009) cannot overcome such degeneracies, and yield LVG solutions that produce $X_{\text{HCN}} \sim (10-20) X_1$ and $\sim (17-37) X_1$ respectively. Nevertheless most X_{HCN} values deduced in such studies are high enough to yield dominant amounts of dense gas mass in ULIRGs, with a near-Galactic or even larger than Galactic $X_{\text{co}}^{(2-\text{ph})}$.

This apparent contradiction of the low X_{co} factor advocated for ULIRGs by past low-J CO line studies (e.g. Solomon et al. 1997; DS98; Yao et al. 2003), and the larger effective $X_{\text{co}}^{(2-\text{ph})}$ implied by heavy rotor molecular line emission (mostly HCN) in such galaxies has not been much noted in the literature. In the rare cases where this discrepancy was discussed, the argument went for a downward revision of X_{HCN} by $\sim 1/5$ rather than a boost of the widely adopted ULIRG-value of $X_{\text{co}} \sim 1 X_1$ (e.g. Papadopoulos et al. 2007). It must be noted however that the possibility of HCN-based molecular gas mass estimates raising the effective X_{co} in ULIRGs is mentioned in the seminal interferometric work by DS98.

3.2.1. What could lower X_{co} in ULIRGs

Lower X_{HCN} values than those reported in existing studies are possible if higher gas temperatures and/or unbound gas motions ($K_{\text{vir}} > 1$) prevail for the bulk of the dense gas in ULIRGs. In the most detailed such study Greve et al. (2009) do find warm and non-virial LVG solutions for the HCN-bright gas in Arp 220 and NGC 6240 with $n(\text{H}_2) = 3 \times 10^5 \text{ cm}^{-3}$, $T_{\text{kin}} = (45\text{-}120) \text{ K}$ (Arp 220) and $T_{\text{kin}} = (60\text{-}120) \text{ K}$ (NGC 6240) while $K_{\text{vir}} \sim 2, 5$ for Arp 220 and NGC 6240 respectively. Choosing $T_{\text{kin}} = 100 \text{ K}$ as indicative for both systems (for a given density and K_{vir} high T_{kin} 's yield small X_{mol} 's), we find $T_{\text{b,HCN1-0}}$ (Arp 220) $\sim 60 \text{ K}$, $T_{\text{b,co1-0}}^{(\text{h})}$ (Arp 220) $\sim 96 \text{ K}$ and $T_{\text{b,HCN1-0}}$ (NGC 6240) $\sim 40 \text{ K}$, $T_{\text{b,co1-0}}^{(\text{h})}$ (NGC 6240) $\sim 86 \text{ K}$ (for their corresponding K_{vir} values). Then from Equation 3: $X_{\text{HCN}} \sim 12 X_1$, $X_{\text{co}}^{(\text{h})} \sim 7.6 X_1$ for Arp 220 and $X_{\text{HCN}} \sim 7.3 X_1$, $X_{\text{co}}^{(\text{h})} \sim 3.4 X_1$ for NGC 6240. Thus using $r_{\text{CO/HCN}}^{(\text{obs})} = 5.9$ (Arp 220), 12.5 (NGC 6240), and the LVG-computed: $r_{\text{CO/HCN}}^{(\text{h})} \sim 1.6$ (Arp 220), 2.15 (NGC 6240), we find $\rho_{\text{co}}^{(1-\text{h})} \sim 2.68$ (Arp 220), 4.81 (NGC 6240). Then from Equation 10 and the aforementioned numbers (and setting $X_{\text{co}}^{(1)} = 0.5 X_1$) it is: $X_{\text{co}}^{(2-\text{ph})}$ (Arp 220) $\sim 2.4 X_1$ and $X_{\text{co}}^{(2-\text{ph})}$ (NGC 6240) $\sim 1 X_1$.

In the aforementioned example the warm “end” of a degenerate range of LVG solutions to a multi-J heavy rotor molecular line dataset yields an $X_{\text{co}} \sim (1/5) X_{\text{co,Gal}}$ for NGC 6240 while reducing that of Arp 220 to $\sim (1/2) X_{\text{co,Gal}}$. Nevertheless such sets of solutions, with $K_{\text{vir}} > 1$ and T_{kin} significantly higher than T_{dust} are not typically considered optimal in most studies. Indeed $K_{\text{vir}} \sim 1$ is often used as a constraint on the LVG solution range of molecular lines tracing dense gas (e.g. HCN, CS) while solutions with $T_{\text{kin}} \sim T_{\text{dust}}$ are considered as more appropriate for such a gas component since gas-dust thermal coupling is expected to be strong (e.g. see the dense gas model in Mrk 231 by Papadopoulos et al. 2007). On the other hand recent theoretical and observational work has shown that in ULIRGs large temperatures with $T_{\text{kin}} > T_{\text{dust}}$ are possible even with most of the gas mass at high densities ($n \geq 10^5 \text{ cm}^{-3}$) because of dominant CR and/or turbulent heating, both powered by the large SNR number densities in these galaxies (Papadopoulos 2010; Paper I; Rangwala et al. 2011). Nevertheless, while high T_{kin} certainly contributes in lowering $X_{\text{co}}^{(\text{h})}$ of the dense gas phase, it is the high K_{vir} values that are mostly responsible for this, a result noted also by previous studies (e.g. DS98). Indeed, setting $K_{\text{vir}} = 1$ for the aforementioned LVG solutions for the dense gas phase in Arp 220 and NGC 6240 brings their $X_{\text{co}}^{(2-\text{ph})}$ factors back up to $\sim 4.5 X_1$ (Arp 220) and $\sim 3.3 X_1$ (NGC 6240).

Clearly good constraints on the dynamical state of the dense gas in ULIRGs is of utmost importance since while $K_{\text{vir}} \sim 1$ may be a safe assumption for the SF-fueling dense gas component of individual GMCs in typical spirals, it may not be so for the extreme ISM environments of ULIRGs. Strong tidal fields and/or “bottom”-stirred ISM by strong SF feedback (via multiple SNR shocks and the radiative feedback implied by Eddington-limit-

regulated SFRs) could induce $K_{\text{vir}} > 1$ even for the dense gas in such systems (see Paper I), lowering X_{HCN} and hence the corresponding $X_{\text{CO}}^{(2-\text{ph})}$ factor.

3.3. Cold SF-quiescent molecular gas and large X_{CO} in LIRGs

Gas-rich disks containing a starburst in their central $\sim(1-2)$ kpc, but also large amounts of SF-quiescent ISM at larger galactocentric radii are often found in LIRGs with $L_{\text{IR}} < 10^{12} L_{\odot}$, and such configurations are even expected for weakly perturbed systems (e.g. Maiolino et al. 1997 and references therein). Large amounts of cold ($\sim(10-15)$ K) molecular gas beyond a warm component ($\sim(35-40)$ K) confined within a star-forming central ~ 1 kpc has been shown as a general feature of LIRGs using CO J=2–1, 1–0 lines (Papadopoulos & Seaquist 1998). Sensitive dust submm continuum and CO J=1–0 imaging in individual LIRGs found cold dust and concomitant molecular gas with low CO J=1–0 brightness extending out to radii of at least ~ 3 kpc (Papadopoulos & Seaquist 1999; Papadopoulos & Allen 2000). Submm continuum and HI imaging studies of nearby spirals also suggest cold molecular gas as a general feature of their disks at large galactocentric distances (Thomas et al. 2004).

Extended, SF-quiescent, molecular gas reservoirs in the disks of LIRGs can be undetected because of low CO J=1–0 line brightness and/or lack of CO in the lower metallicity environments found at large galactocentric distances. Two SF-idle GMCs with $n \sim 10^2 \text{ cm}^{-3}$ and potentially very low kinetic temperatures (~ 5 K) have been found in M31 (Allen & Lequeux 1993; Loinard et al. 1995; Allen et al. 1995). For $K_{\text{vir}} \sim 1-2$ (i.e. self-gravitating or nearly so) such clouds will have $T_{\text{CO},1-0}^{(l)} \sim 1.4$ K and a corresponding $X_{\text{CO}}^{(l)} \sim 19 X_{\text{I}}$. In the global CO SLEDs of LIRGs such a cold SF-idle component, even if massive, it will be completely inconspicuous, outshined by the much more CO-luminous SF molecular gas where typical $T_{\text{CO},1-0}^{(h)} \geq 15$ K. The global X_{CO} of a LIRG, computed using models of its global CO SLED, will then invariably be biased by the average ISM properties of its central starburst, often having a genuinely low $X_{\text{CO}}^{(h)} \sim (1/3-1/5) X_{\text{CO,Gal}}$ factor (e.g. Papadopoulos & Seaquist 1999; Papadopoulos & Allen 2000). Thus its adoption for the entire LIRG can much underestimate the contribution from a massive cold, SF-quiescent component where a Galactic X_{CO} applies, as indicated by submm, HI and CO J=1–0 imaging for such galaxies.

We can compute an indicative $X_{\text{CO}}^{(2-\text{ph})}$ in such a LIRG for a given $\rho_{\text{CO}}^{(1-h)}$ by setting $X_{\text{CO}}^{(l)} = X_{\text{CO,Gal}}$ for the cold, extended, SF-quiescent component, and $X_{\text{CO}}^{(h)} = (1/5) X_{\text{Gal,CO}}$ for the warm, nuclear, star-forming one. Using the results by Papadopoulos & Seaquist (1998) where “stacked” CO(2–1)/(1–0) ratios for LIRGs were used to determine a generic warm versus cold molecular gas distribution in their disks (their Figure 6) we set $L_{\text{h}} \sim 0.9$ kpc as the diameter of the warm SF component and $L_{\text{s}} \sim 20$ kpc as that of the entire CO-bright gas

distribution in the “average” LIRG. With a warm/cold CO brightness temperature ratio of $t_b = T_{\text{co},1-0}^{(h)}/T_{\text{co},1-0}^{(l)} \sim 3$ it is: $\rho_{\text{co}}^{(1-h)} = (1/t_b) \times [(L_s/L_h)^2 - 1] \sim 164$. Thus $X_{\text{co}}^{(2-ph)} \sim X_{\text{co}}^{(l)} = X_{\text{co,Gal}}$, i.e. dominated by the cold disk component. Given that $\rho_{\text{co}}^{(1-h)}$ can vary greatly among LIRGs, it is instructive to also obtain $X_{\text{co}}^{(2-ph)}$ in a LIRG where the relative distributions of the warm SF versus the cold SF-idle gas are well known. For the Sy2 NGC 1068: $L_h \sim 2.7$ kpc and $L_s \sim 6$ kpc (Papadopoulos & Seaquist 1999), while $t_b \sim 5$. Thus $\rho_{\text{co}}^{(1-h)} \sim 0.79$ and $X_{\text{co}}^{(2-ph)} \sim 0.6 X_{\text{co,Gal}}$, which is $\sim 3x$ higher than $X_{\text{co}}^{(h)}$ (that would be deduced from its global CO SLED).

3.4. Molecular gas inventories in LIRGs: critical observations

Highly turbulent molecular gas in the merger-driven starbursts of ULIRGs, and extended, cold, SF-quiescent gas in the disks of isolated or slightly perturbed LIRGs represent the two extremes where current CO line studies may systematically underestimate the total molecular gas mass. In both cases global CO SLEDs often show a low-excitation component, seen as small CO J=1–0, 2–1 line flux “excess” (often with a subthermal CO (2–1)/(1–0) ratio) on top of the dominant CO line emission of a warm and dense SF gas phase with high CO line excitation to much higher J levels. In ULIRGs such a diffuse low-excitation phase is typically unbound, warm, and contains little mass. In the disks of LIRGs it consists of SF-quiescent, gravitationally bound (or nearly so), Galaxy-type GMCs extending beyond a central starburst. In the latter case spatially resolving the CO SLEDs and/or dust emission of the nuclear SF region versus the extended cold disk can yield proper molecular gas mass estimates not dominated by the (usually) low X_{co} of the CO-bright nuclear SF region. In practice CO and ^{13}CO J=1–0, and J=2–1 imaging of those SF and SF-idle areas of LIRGs is adequate to determine the nature of the residing ISM (SF: $r_{21} \sim 1$, $R_{10,21} \sim 10-15$, SF-quiescent: $r_{21} \sim 0.4-0.6$, $R_{10,21} \sim 3-6$, the corresponding X_{co} values, and the areas over which they apply.

In the upcoming era of ALMA such spatial separations of SF and non-SF ISM in LIRG disks along with estimates of the corresponding molecular line ratios and X_{co} values will be straightforward. For ULIRGs though the low-density and the high density gas components can be concomitant or very closely associated, especially if the former is the outcome of the disruption of GMC outer layers. Thus high resolution CO observations, even with ALMA, may be unable to separate their distributions and their corresponding CO line ratios, leaving their X_{co} factors still uncertain. In such galaxies, with the bulk of the molecular gas mass at $n \gtrsim 10^4 \text{ cm}^{-3}$, observations of rotational transitions of heavy rotor molecules such as HCN are of paramount importance, even without spatial information. For example a high global HCN/CO J=1–0 brightness temperature ratio of $\sim 1/4-1/6$ would immediately indicate an unusually high $M_{\text{dense}}/M_{\text{tot}}(\text{H}_2)$, contrasting the $\sim 10\times$ lower such ratio in disk GMCs. Then

multi-J observations of heavy rotor molecules can be used to determine the corresponding X_{mol} , $X_{\text{co}}^{(\text{h})}$ factors and eventually $M_{\text{tot}}(\text{H}_2)$.

High resolution interferometric imaging of at least two rotational transitions of a heavy rotor molecule (e.g. HCN J=1–0, 3–2) along with at least one of its isotopologues (e.g. H^{13}CN J=1–0) remains an invaluable resource for better determining the distribution and mass of the dense gas in the compact disks of ULIRGs. This can be achieved using radiative transfer models of the emergent HCN line emission as a function of position within these disks, as done earlier for the CO J=1–0, J=2–1 interferometric study by DS98. The focus will now be on the dense gas where much of the molecular gas mass resides, while its all-important average dynamical state (i.e. the K_{vir}) will be determined as part of the modeling. Imaging of the rare isotopologues can much reduce the radiative transfer modeling degeneracies affecting $K_{\text{vir}}(\mathbf{r})$, and yield improved constraints on the dense gas surface densities $\Sigma_{\text{dense}}(\mathbf{r})$ of the gas disks in ULIRGs. Their total gas mass can then be determined from integrating the resulting $\Sigma_{\text{dense}}(\mathbf{r})$ over the best-fit disk models.

Here we must note that any molecular line observations that involve the $[\text{C}/^{13}\text{C}]$ isotope ratio such as $\text{CO}/^{13}\text{CO}$ or $\text{HCN}/\text{H}^{13}\text{CN}$, while necessary for reducing LVG modeling degeneracies and better constraining K_{vir} , they involve the additional assumption of the $[\text{C}/^{13}\text{C}]$ abundance ratio (which we assumed to be 50 in our LVG models). The latter can be particularly uncertain in ULIRGs where their large $\text{CO}/^{13}\text{CO}$ line ratios have also been attributed to a higher $[\text{C}/^{13}\text{C}]$ abundance than in spiral disks, a result of early starburst ages and/or accretion of relatively unprocessed (by star-formation) molecular gas (Henkel & Mauersberger 1993). If enhanced $[\text{C}/^{13}\text{C}]$ abundances are indeed the norm in ULIRGs this will have the general effect of *increasing the various X_{co} , X_{HCN} factors* since the deduced K_{vir} values per gas phase can now be lower. This will be so simply because larger $[\text{C}/^{13}\text{C}]$ abundances rather than low CO line optical depths (and thus high K_{vir} , see Equation 11 in Paper 1) can be also responsible for the observed high $\text{CO}/^{13}\text{CO}$ line ratios in ULIRGs.

3.4.1. *Molecular gas mass estimates of ULIRGs: the promise of Herschel*

In ULIRGs a massive, warm, and dense gas phase can have a luminous CO SLED that remains prominent up to very high-J rotational transitions. Since J=1–0, 2–1 transitions can have significant contributions from a low-excitation diffuse gas component containing small fraction of the total molecular gas mass, this leaves only J=3–2 and higher-J CO lines as useful probes of the bulk of the molecular gas mass and its properties. The SPIRE/FTS aboard the HSO can provide access to CO lines from J=4–3 up to J=13–12 for local luminous ULIRGs (e.g. van der Werf et al. 2010; Rangwala et al. 2011) and thus yield a critical dataset

for obtaining better total molecular gas mass estimates in such systems.

Once a fully-sampled global CO SLED from $J=1-0$ up to $J=13-12$ is available, a multi-component analysis can decompose it into a series of gas components, constraining their properties, and using them to obtain the corresponding X_{co} factors. Such multi-phase models could eventually be produced by theoretical advancements in GMC-sized numerical simulations (see 3.1.1). Thus HSO observations of high- J CO lines will allow better inventories of molecular gas mass in ULIRGs since much of that mass resides in a dense, and presumably SF and warm phase. We note however that serious degeneracies will remain, especially regarding the all-important dynamical state of each gas component upon which the corresponding X_{co} factor strongly depends. Multi- J observations of the much fainter (especially in ULIRGs) ^{13}CO isotopologue lines, necessarily using the much larger mm/submm telescopes available from the ground (and thus limited by the atmosphere up to $J=6-5$, $7-6$) are important for reducing those degeneracies, and better constraining K_{vir} , or equivalently (for a given density and temperature), the escape probabilities $\beta_{J+1,J}$ per gas component that enter the expressions of the X_{co} factors (Equations 3 and 6).

4. Probing the extremes: individual (U)LIRGs, their molecular gas, and X_{CO}

Several (U)LIRGs in our sample merit an individual study either because a larger than average number of available CO lines permits it (see Table 7 in Paper I), and/or because very high line excitation make their CO SLEDs irreducible to superpositions of star-forming and (non-SF) molecular gas (see also Paper I for a discussion on the implication about ISM power sources). Finally there are LIRGs whose global $\text{CO}(J+1-J)/(1-0)$ ratios suggest the cold SF-quiescent clouds found at large galactocentric distances in the Galaxy and the disk of M 31. Such globally “cold” yet star-forming galaxies are very few, as expected for an IR-selected (and thus SFR-selected) LIRG sample, and thus also deserve a closer look as they represent the low-excitation range in LIRGs. The detailed model(s) per galaxy and the associated discussion are in the Appendix, while here we summarize the most important findings.

The extreme range of CO SLEDs found for the molecular gas reservoirs of LIRGs discussed in Paper I is now marked by individual objects. On the high end are galaxies like IRAS 00057+4021, Arp 299, IRAS 12112+305 and others whose extremely high CO line excitation implies large amounts of very dense ($\sim(1-3) \times (10^4-10^6) \text{ cm}^{-3}$ and (often) very warm ($T_{\text{kin}} \gtrsim 100 \text{ K}$) gas. The large $f_{\text{d}} = M(n \geq 10^4 \text{ cm}^{-3}) / M_{\text{tot}}(\text{H}_2)$ deduced for such (U)LIRGs independently recovers, using mid/high- J CO lines, a well-known result for merger-driven starbursts obtained using the HCN/CO $J=1-0$ ratio as an f_{d} proxy (Gao & Solomon 2004). These earlier studies (see also Gracia-Carpio et al. 2008; Krips et al. 2008) found ~ 10

times higher dense gas mass fractions in ULIRGs than in isolated spirals. Isofar as the dense molecular gas phase closely tracks the dense and warm gas associated with SF sites, the mid-J/high-J CO lines of ULIRGs are also expected to show clear indications of a high f_d , as it is indeed found, and quite unlike what is expected from typical GMCs ($f_{d,GMC} \sim 0.02-0.03$).

Furthermore, the very warm and strongly unbound ($K_{vir} \geq 20$) states uncovered for the massive dense gas reservoirs of some LIRGs can make their global CO SLEDs surpass even those expected for SF “hot”-spots in the Orion A and B clouds. While in some distinct cases this can be due to strong AGN feedback (e.g. Mrk 231), for all other galaxies with such extreme ISM conditions (e.g. IRAS 00057+4021, IRAS 08572+3915, IRAS 23365+3604) the cause is unclear. It remains to be explored whether the much higher SFR *densities* of the compact SF regions of ULIRGs (e.g. Sakamoto et al. 2008) can create such extraordinary ISM states where turbulence-injection by SNRs no longer remains confined in small regions but encompasses much more molecular gas mass (see discussion in Paper I). This, along with CRs (also SNR-generated) may set up powerful global mechanisms that can volumetrically heat large amounts of gas, unhindered by the large dust extinctions and high average gas densities that will keep PDRs very localized around SF sites.

On the low excitation end only a few cases of low global CO line ratios are found (e.g. IRAS 05189–2524, IRAS 03359+1523). This is expected for IR-selected (and thus SFR-selected) galaxies (see Dunne et al. 2000 on the limitations of such samples in finding (cold-ISM)-dominated systems). In Arp 193 a low-excitation ISM state and the lack of large amounts of dense and warm gas is actually suggested by HCN rather than CO lines. Indeed despite the presence of a young merger with substantial IR luminosity and a significant HCN/CO J=1–0 line ratio, its global HCN line emission is consistent with the absence of a dense gas phase, possibly a case of strong SF feedback momentarily dispersing its dense gas supply (Papadopoulos 2007). Such IR-luminous/(dense-gas)-deficient galaxies will be rare (see discussion in B.17) and thus valuable for studying the effects of SF feedback onto the dense ISM where the initial conditions of star formation are set. The case of IRAS 05189–2524 on the other hand stands out as one where a massive cold molecular gas-rich disk is implied but unlike other LIRGs (e.g. I Zw 1) there are no morphological indications whatsoever for the presence of such a disk in this very compact ULIRG/AGN system. Moreover its “warm” CO(6-5)/(3-2) ratio, warm IR “colors”, and compact size in cm, near-IR, and optical wavelengths would argue for the presence of only a warm, dense, SF gas phase, and thus this object represents a cautionary tale about such conclusions drawn for similar high-z ULIRG/AGN systems using only high-J CO lines (e.g. Tacconi et al. 2006).

We note that massive cold molecular gas disks are implied for other LIRGs as well (e.g. I Zw 1, VII Zw 031, NGC 7469) but without strongly affecting their global CO SLEDs or

CO/ ^{13}CO line ratios which remains dominated by the warm SF phase. This simply mirrors, for molecular lines, a result well-known for dust continuum emission, though in practice global CO SLEDs are somewhat more sensitive to the presence of cold diffuse gas than the global dust SEDs are to the concomitant cold dust mass (Papadopoulos & Allen 2000).

4.1. Effects of average ISM conditions on the X_{co}

In Table 1 we tabulate the total molecular gas mass estimates as produced by Equations 3, 10, the corresponding X_{co} factors, the minimum molecular gas mass implied for Eddington-limited star formation (section 2.3), and the mass of the high-excitation (h)-phase when a 2-component model is used to interpret the CO, ^{13}CO lines (see Appendix). A mere inspection of the third column demonstrates that in several galaxies ($\sim 40\%$) *significantly larger X_{co} factors than the so-called (U)LIRG values of $\sim (0.6-1) X_l$ may apply*. For ULIRGs this is due to large and even dominant fractions of their molecular gas mass being at much higher densities than in disk-dominated LIRGs while for the latter because extended cold molecular disks (with a Galactic X_{co}) can contain much of the molecular gas mass while remaining inconspicuous in the global CO SLEDs used to constrain the global X_{co} . For ULIRGs this low-mass bias includes some very well-known systems such as Mrk 231 and Arp 220. For lower IR luminosity galaxies underestimates of their total molecular gas by the X_{co} deduced from one-phase radiative transfer models of their CO SLEDs can be important in disk-dominated systems (e.g. NGC 7469), but also in seemingly compact star-forming galaxies that nevertheless have “cold” CO SLEDs and Galactic X_{co} values (IRAS 05189–2524).

The computed $X_{\text{co}}^{(2-\text{ph})}$ and $M_{\text{tot}}^{(2-\text{ph})}$ in Table 1 also make clear that in the case of ULIRGs global molecular line SLEDs can reveal the aforementioned mass bias, provided that they include mid/high-J CO and/or heavy rotor molecular lines (e.g. HCN). For less IR-luminous galaxies with nuclear starbursts and cold SF-quiescent gas-rich disks global SLEDs cannot easily identify the presence of the latter except in a few cases (e.g. IRAS 05189-2524). This becomes possible only when additional spatial information (e.g. CO 1-0, submm dust continuum, or cm imaging) is available for such a disk (e.g. NGC 7469). In the absence of such information even good one-phase models of global CO SLEDs for a (starburst)+(cold disk) system may be unable to reveal the disk component leaving the deduced average X_{co} dominated by the starburst phase (e.g. IRAS 02483+4302). In the era of ALMA routine CO multi-J and ^{13}CO line imaging will provide much better molecular gas mass estimates for disk-dominated LIRGs with strong ISM excitation gradients (see 3.4). For ULIRGs on the other hand multi-J observations of heavy rotor molecules (e.g. HCN, CS) and their rare isotopologues are necessary for confirming the high total X_{co} and molecular gas masses

implied by our results in Table 1, by constraining the all-important dynamic state of the massive dense gas phase as discussed in 3.2.1.

5. Conclusions

In this work our large CO, ^{13}CO line survey of Luminous Infrared Galaxies (LIRGs) detailed in Paper I (Papadopoulos et al. 2011) is used to examine the impact of the wide range of average ISM conditions found for these galaxies on their total molecular gas mass estimates via the so-called $X_{\text{co}} = M(\text{H}_2)/L'_{\text{CO},1-0}$ factor. Our sample includes some of the most prominent local ULIRGs (e.g. Arp 220, Mrk 231, IRAS 17208–0014), often used as templates for merger-driven starbursts at high redshifts, as well as less IR luminous disk-dominated galaxies. We find that one-phase radiative transfer models of the global CO, ^{13}CO line ratios yield $\langle X_{\text{co}} \rangle \sim (0.6 \pm 0.2) M_{\odot} (\text{K km s}^{-1} \text{pc}^2)^{-1}$, similar to that obtained by past studies. The average gas temperature and density strongly influence X_{co} , but the gas average dynamical state is the most important influencing factor with unbound gas corresponding to low X_{co} values while self-gravitating gas to higher ones.

Nevertheless higher $X_{\text{co}} \sim (2-6) M_{\odot} (\text{K km s}^{-1} \text{pc}^2)^{-1}$ values are deduced for (U)LIRGs whenever adequate molecular line data exist to determine the mass contribution of gas at densities $n \geq 10^4 \text{ cm}^{-3}$ (high-J CO lines from our survey and/or HCN lines from the literature). Theoretical expectations for the highly turbulent molecular gas in the merger-induced starbursts of ULIRGs indicate that, with most of the gas at such high densities, the aforementioned large X_{co} values maybe the rule rather than the exception in such systems. Past observational studies were unable to determine this, yielding instead much lower X_{co} values (and often considered as ULIRG-appropriate standard ones), because the molecular lines used (mostly CO J=1–0, 2–1) could not constrain the properties of the dominant (i.e. the dense) gas phase in ULIRGs. Our results indicate that only high-J CO lines and multi-J observations of heavy rotor molecules (e.g. HCN, CS) can overcome this mass bias, placing the Herschel Space Observatory and ALMA front and center in the quest for improved molecular gas mass estimates in ULIRGs in the local and the distant Universe. Of particular importance are good constraints on the dynamical state of the dense molecular gas in such systems (self-gravitating or not?) since strongly unbound states for this phase seem to be the only possible way that X_{co} in ULIRGs could be much lower than a Galactic value. Observations of high-density tracing rare isotopologues (e.g. high-J ^{13}CO , H^{13}CN) will be of crucial importance in yielding such constraints. On the theoretical front, GMC-sized numerical simulations of the turbulent molecular gas with ULIRG-type of boundary conditions are needed in order to obtain the dense gas mass fraction and its temporal evolution. This

in turn can inform galaxy-sized simulations of merger systems which recently have included molecular gas, but cannot track the dynamical state and mass of the dense gas.

We also find LIRGs where underestimates of their total molecular gas are the result of a massive, cold, gas-rich, disk existing beyond their central starburst. In such cases the global CO SLED, and the X_{CO} factor determined from it, remains dominated by the central starburst and its often low X_{CO} . Spatially resolving the CO, ^{13}CO line and dust continuum emission of such disks in LIRGs with strong ISM excitation gradients is indispensable in accounting for their total molecular gas mass. In such cases, provided that adequate resolution is employed to separate the cold gas disk from the nuclear starburst, even low-J CO and ^{13}CO lines (J=1–0, 2–1, 3–2) are adequate to yield much improved molecular gas mass estimates.

Finally our study unfolds the wide range of the global CO SLEDs of LIRGs presented in Paper I over a subsample of individual systems. We find galaxies whose extreme CO SLEDs indicate ISM conditions that surpass those expected for star-forming regions and suggest ISM energy sources other than photons from PDRs (as already discussed in Paper I). These can be AGN, extreme turbulence, and/or very large cosmic ray energy densities. Moreover we find LIRGs where extreme SF feedback may have momentarily fully disrupted their dense molecular gas reservoirs, and LIRGs where large amounts of cold SF-quietest molecular gas are present despite the absence of an extended disk, their compact near-IR/cm emission size, and “warm” CO (6-5)/(3-2) ratios. The latter type of objects can be particularly worrying if encountered at high redshifts where such characteristics can readily lead towards large underestimates of their total molecular gas mass. The wide range of the average ISM conditions and the intriguing possibilities that may lie behind it, make our subsample of individually-studied LIRGs an excellent target for future ALMA and NOEMA (for the northern objects) molecular line imaging observations leading towards a complete picture about ISM energetics, AGN and SF feedback on the molecular gas in galaxies.

We would like to thank the referee Santiago Burillo for his comments, and particularly for bringing into our attention two important issues namely, the uncertainties of [CO/ ^{13}CO] abundance ratio in ULIRGs, and the reliability of dynamical mass estimates, which resulted in our corresponding clarifications included in this paper. Padelis P. Papadopoulos would like to dedicate this long-coming work to his 10-month old son *Λεωνίδα-Χρηστο*, for late night inspirations, and to his wife *Μαργαριτα* for her enduring support. The project was funded also by the John S. Latsis Public Benefit Foundation. The sole responsibility for the content lies with its authors.

A. The X_{CO} factor in an LVG setting

The CO J=1–0 line luminosity $L'_{\text{CO}}(1-0)$ (in $\text{K km s}^{-1} \text{ pc}^2$, see Equation 5, Paper I) can be re-expressed as

$$L'_{\text{CO}(1-0)} = \int_{\Delta V} \int_{A_s(V)} T_{b,1-0}(\vec{r}, V) da dV = \int_{\Delta R_s} \int_{A_s(R)} \left[T_{b,1-0}(\vec{r}, R) \left(\frac{dV}{dR} \right)_{\vec{r},R} \right] da dR \quad (\text{A1})$$

where any given velocity V is assumed to correspond uniquely to a source surface $A_s(V)$, emitting at $T_b(\vec{r}, V)$. In turn this can be parametrized by a “depth-in-the-source” parameter $R(V)$ so that these iso-velocity surfaces completely scan the entire source volume for a range ΔR_s (which corresponds to the FWZI of the source velocity field), and without any radiative coupling (the LVG assumption). The latter implies that the line luminosities emanating from these surfaces simply add up. Thus we can write

$$L'_{\text{CO}(1-0)} = \langle T_{b,1-0} \left(\frac{dV}{dR} \right) \rangle \Delta V_s = \langle T_{b,1-0} \rangle \left(\frac{dV}{dR} \right) \Delta V_s, \quad (\text{A2})$$

where $\langle \dots \rangle$ denotes averaging over the entire source volume ΔV_s , and for an assumed constant velocity gradient. Thus for

$$\frac{dV}{dR} = K_{\text{vir}} \times \left(\frac{dV}{dR} \right)_{\text{vir}} \sim 0.65 \sqrt{\alpha} K_{\text{vir}} \left(\frac{\langle n(\text{H}_2) \rangle}{10^3 \text{ cm}^{-3}} \right)^{1/2} \text{ km s}^{-1} \text{ pc}^{-1}, \quad (\text{A3})$$

and $M(\text{H}_2) = \mu m(\text{H}_2) \langle n(\text{H}_2) \rangle \Delta V_s$ ($\mu=1.36$ accounts for the He mass) Equations A1, A2, and A3 along with substituting astrophysical units yield for the X_{CO} factor

$$X_{\text{CO}} = \frac{\mu m(\text{H}_2) \langle n(\text{H}_2) \rangle K_{\text{vir}}^{-1}}{\langle T_{b,1-0} \rangle} \left(\frac{dV}{dR} \right)_{\text{vir}}^{-1} = \frac{3.25 \sqrt{\langle n(\text{H}_2) \rangle}}{\sqrt{\alpha} \langle T_{b,1-0} \rangle} K_{\text{vir}}^{-1} \left(\frac{M_{\odot}}{\text{K km s}^{-1} \text{ pc}^2} \right). \quad (\text{A4})$$

The last expression (used in the main text with the averaging symbols omitted for simplicity) for $\alpha=1.5$ becomes identical to that derived by Solomon et al. 1997 (their Equation 21 for $f=1$). For virialized gas motions ($K_{\text{vir}}=1$), and typical conditions in Galactic GMCs with $\langle n(\text{H}_2) \rangle = (100-500) \text{ cm}^{-3}$ and $T_{b,1-0} = 10 \text{ K}$ yields $X_{\text{CO}} \sim (3-6) M_{\odot} (\text{K km s}^{-1} \text{ pc}^2)^{-1}$, in good accord with the average Galactic value and its uncertainties. Finally, expression A4 is valid for any optically thick molecular line emission used as a mass tracer of a particular gas phase (e.g. HCN J=1–0 tracing dense gas with $n(\text{H}_2) > 10^4 \text{ cm}^{-3}$), while multi-J observations of the particular molecule and its isotopologues can be used to constrain $\langle n(\text{H}_2) \rangle$, $T_{b,1-0}$, and K_{vir} .

A.1. The optically thin approximation for X_{CO}

From standard formalism the integrated line luminosity for an optically thin CO $J+1 \rightarrow J$ line, omitting the CMB for simplicity, is given by

$$L_{J+1,J} = N_{J+1} A_{J+1,J} h \nu_{J+1,J}, \quad (\text{A5})$$

where N_{J+1} is the total number of CO molecules at the $J+1$ state and $A_{J+1,J}$ is the Einstein coefficient of the $J+1 \rightarrow J$ transition. This line luminosity can be re-expressed in terms of $L'_{J+1,J}$ (in $L_1 = K \text{ km s}^{-1} \text{ pc}^2$ units, see A1) using

$$L_{J+1,J} = \frac{8\pi k_B \nu_{J+1,J}^3}{c^3} L'_{J+1,J}, \quad (\text{A6})$$

which combined with A5 yields

$$N_{J+1} = \frac{8\pi k_B \nu_{J+1,J}^2}{hc^3 A_{J+1,J}} L'_{J+1,J}. \quad (\text{A7})$$

The total molecular gas mass is then given by

$$M(\text{H}_2) = (N_0 + N_1 + N_2 + N_3 + N_4 \dots) R_{\text{CO}} \mu m_{\text{H}_2}, \quad (\text{A8})$$

where $R_{\text{CO}} = [\text{H}_2/\text{CO}] = 10^4$ is the CO abundance and $\mu = 1.36$ accounts for He mass. The molecule population at the $J=0$ level obviously cannot be estimated from a line transition, and we thus compute it from $N_0 = (g_0/g_1) \exp[E_1/(k_B T_{\text{ex},10})] N_1$ where $g_J = 2J + 1$ denotes the J -state degeneracy factor, $E_1/k_B \sim 5.5 \text{ K}$, and $T_{\text{ex},10}$ is the excitation temperature of the CO $J=1-0$ transition. Substituting this in A8 yields

$$M(\text{H}_2) = \left(1 + \frac{1}{3} e^{5.5/T_{\text{ex},10}} + \frac{N_2}{N_1} + \frac{N_3}{N_1} + \dots \right) R_{\text{CO}} \mu m_{\text{H}_2} N_1, \quad (\text{A9})$$

which after substituting the expressions from A7 yields

$$X_{\text{co}}^{(\text{thin})} = \frac{8\pi k_B \mu m_{\text{H}_2} \nu_{10}^2 R_{\text{CO}}}{hc^3 A_{10}} \times \left[1 + \frac{1}{3} e^{5.5/T_{\text{ex},10}} + \left(\frac{\nu_{21}}{\nu_{10}} \right)^2 \frac{A_{10}}{A_{21}} r_{21} + \left(\frac{\nu_{32}}{\nu_{10}} \right)^2 \frac{A_{10}}{A_{32}} r_{32} + \dots \right] \quad (\text{A10})$$

where r_{J+1J} are the $L'_{\text{CO}}(J+1-J)/L'_{\text{CO}}(1-0)$ ratios observed (Equations 5, 6). The Einstein coefficients scale as a function of J as

$$A_{J+1J} = 3 \frac{(J+1)^4}{2J+3} A_{10} \quad (\text{A11})$$

while $\nu_{J+1J}=(J+1)\nu_{10}$. Thus equation A10 finally becomes

$$X_{\text{co}}^{(\text{thin})} = \frac{8\pi k_B \mu m_{\text{H}_2} \nu_{10}^2 R_{\text{CO}}}{hc^3 A_{10}} \times \left[1 + \frac{1}{3} e^{5.5/T_{\text{ex},10}} + \frac{5}{12} r_{21} + \frac{7}{27} r_{32} + \dots \frac{2J+3}{3(J+1)^2} r_{J+1J} + \dots \right]. \quad (\text{A12})$$

Substituting the various physical constants and introducing astrophysical units yields,

$$X_{\text{co}}^{(\text{thin})} = 0.078 \left[1 + \frac{1}{3} e^{5.5/T_{\text{ex},10}} + \frac{5}{12} r_{21} + \frac{7}{27} r_{32} + \dots \frac{2J+3}{3(J+1)^2} r_{J+1J} + \dots \right] \left(\frac{M_{\odot}}{\text{K km s}^{-1} \text{ pc}^2} \right). \quad (\text{A13})$$

In the literature the LTE approximation is often used by setting $\sum_{k=0} N_k = Z_{\text{LTE}}/g_1 N_1$ and $Z_{\text{LTE}} \sim 2(k_B T_k/E_1) = 2[T_k/(5.5 \text{ K})]$ in Equation A8, which then yields

$$X_{\text{co}}^{(\text{thin})}(\text{LTE}) = 9.45 \times 10^{-3} \left[\left(\frac{T_k}{\text{K}} \right) e^{5.5/T_k} \right] \left(\frac{M_{\odot}}{\text{K km s}^{-1} \text{ pc}^2} \right). \quad (\text{A14})$$

For optically thick CO emission where the optical depths arise in small gas cells with respect to molecular cloud sizes CO line emission remains effectively optically thin (i.e. traces the entire emitting gas mass) but with $A_{ik} \rightarrow \beta_{ik} A_{ik}$ in all the previous equations, with $\beta_{ik} = [1 - \exp(-\tau_{ik})]/\tau_{ik}$ being the photon escape probability (for a spherical cloud). In such a case Equation A10 can be trivially modified for finite CO line optical depths to yield

$$X_{\text{co}}^{(\beta)} = 0.078 \beta_{10}^{-1} \left[1 + \frac{1}{3} e^{5.5/T_{\text{ex},10}} + \frac{5}{12} \left(\frac{\beta_{10}}{\beta_{21}} \right) r_{21} + \frac{7}{27} \left(\frac{\beta_{10}}{\beta_{32}} \right) r_{32} + \dots \right. \quad (\text{A15}) \\ \left. + \dots \frac{2J+3}{3(J+1)^2} \left(\frac{\beta_{10}}{\beta_{J+1J}} \right) r_{J+1J} + \dots \right] \left(\frac{M_{\odot}}{\text{K km s}^{-1} \text{ pc}^2} \right).$$

B. Models of individual LIRGs

Here we describe the radiative transfer models in selected galaxies from our sample. The details of the Large Velocity Gradient (LVG) radiative transfer code used, and the parameter space explored by its $[T_{\text{kin}}, n, K_{\text{vir}}]$ variables can be found in Paper I. In the several cases where a one-phase gas LVG model manifestly fails to reproduce the available line ratios we use a two-phase approximation (see 2.4) to better represent the underlying average molecular gas properties, and compute the corresponding $X_{\text{CO}}^{(2\text{-ph})}$ (Equation 10). The (h)-phase properties and its $X_{\text{CO}}^{(h)}$ are constrained using CO J=4–3, 3–2 and ^{13}CO lines, with the 6–5 transition placing constraints as a lower limit of the true emergent line luminosity (see Paper I), with higher CO J=6–5 luminosities typically yielding even denser gas LVG solutions with larger $X_{\text{CO}}^{(h)}$. The “residual” CO line ratios (determined from Equations 8, 9) are used as inputs into our LVG radiative transfer code in order to constrain the physical properties and corresponding $X_{\text{CO}}^{(l)}$ factor of the low-excitation (l)-phase. In the cases where a two-phase ISM model is necessary but inadequate CO line observations exist to constrain the (h)-phase, we assume one based on the model defined by the Orion star-formation “hot-spots”, their SLED, and molecular gas mass normalization (see 2.4). Finally in the very few cases where heavy rotor molecular lines (mostly HCN transitions) exist, they are often used to determine the (h)-phase. For all the LIRGs studied, their measured CO line ratios, computed SF-powered IR luminosities $L_{\text{IR}}^{(*)}$, and the dust temperatures used to constrain the LVG model (i.e. $T_{\text{kin}}/T_{\text{dust}} \gtrsim 1$) can be found in Paper I.

B.1. IRAS 00057+4021

There are only a few studies of this LIRG, and the only available CO J=1–0 interferometric map shows a very compact nearly face-on source with most of the gas in a $\lesssim 1''$ (~ 864 pc) core (DS98). Its luminous CO J=4–3 line emission cannot be accounted by one-phase LVG models, with the best such model: $T_{\text{kin}}=90$ K, $n(\text{H}_2)\sim 3 \times 10^2 \text{ cm}^{-3}$, $K_{\text{vir}}=1$, reproducing well the observed r_{21} , r_{32} and the R_{21} lower limit, but yielding $r_{43}^{(\text{lvg})}=0.48$, which is $\sim 1/3$ of the observed value. Moreover the fact that $r_{43} > r_{43}^{(h)}$ (Orion) (see 2.4) and $r_{43} > r_{32}$, makes obvious that a superposition of low-excitation (SF-quiescent) and high-excitation Orion-type SF “hot” spots cannot produce such a highly-excited global CO SLED, and that even extreme GMCs consisting solely of such “hot” spots are inadequate. Thus the *average* state of the molecular gas in IRAS 00057+4021 “out-excites” even the SF regions in Orion A and B. The existence of such ULIRGs, and the implications for an ISM energy input other than far-UV/optical/IR photons from SF sites (i.e. turbulent and/or CR heating) has already been noted in Paper I (see also Rangwala et al. 2011).

Using $r_{43}\text{-}\sigma=0.89$ along with the other CO line ratios still does not yield an average ISM state that can reproduce them. The best LVG solution ranges then are: $T_{\text{kin}}=(35\text{-}65)\text{ K}$, $n(\text{H}_2)=10^3\text{ cm}^{-3}$, $K_{\text{vir}}\sim 1\text{-}4$, and $T_{\text{kin}}=(70\text{-}150)\text{ K}$, $n(\text{H}_2)=3 \times 10^2\text{ cm}^{-3}$, $K_{\text{vir}}\sim 1$. These reproduce the observed r_{32} , r_{21} and the R_{21} lower limit, but yield $r_{43}(\text{lvg})\sim 0.45\text{-}0.50$, i.e. still significantly lower than $r_{43}\text{-}\sigma$. A 2-phase model using an Orion-defined (h)-phase (and SLED) gives $r_{21}^{(l)}=0.91$, $r_{32}^{(l)}=0.53$, $r_{43}^{(l)}=0.83$ (Equations 8, 9), and remains unable to fit these residual line ratios, failing to account for the $J=4\text{-}3$ line ($r_{43}^{(l)}(\text{lvg})\sim 0.3\text{-}0.4$). Using only the $J=3\text{-}2$, $J=4\text{-}3$ transitions as constraints ($r_{43/32}=2.23 \pm 0.97$) of the (h) phase and restricting LVG solutions with $T_{\text{kin}}\geq T_{\text{dust}}(=37\text{ K})$ and $K_{\text{vir}}\geq 1$, yields $T_{\text{kin}}\gtrsim 95\text{ K}$, $n(\text{H}_2)=3 \times 10^4\text{ cm}^{-3}$, and $K_{\text{vir}}\sim 20$. The fit yields no upper limit on T_{kin} , as expected since the maximum possible $r_{43/32}$ (attained for optically thin thermalized CO lines) is $(4/3)^2 e^{-E_{32}/(k_B T_{\text{kin}})}=1.77 e^{-16.6/T_{\text{kin}}}\rightarrow 1.77$ for $16.6/T_{\text{kin}}\rightarrow 0$. Using the lower $r_{43/32}=1.26$ value ($=(\text{observed})-\sigma$) as input in the LVG code yields identical results. Thus *a very warm, dense, and strongly kinematically stirred gas phase is present in IRAS 00057+4021*. An estimate of its mass can be obtained from the measured $L'_{\text{CO}(4-3)}=(5.84 \times 10^9)\text{ L}_1$, and $L'_{\text{CO}(1-0)}=1/\langle r_{43}^{(\text{h-ex})} \rangle \times L'_{\text{CO}(4-3)}$, where $\langle r_{43}^{(\text{h-ex})} \rangle=3.4$ is the average $\text{CO}(4\text{-}3)/(1\text{-}0)$ ratio computed from the range of LVG solutions compatible with the observed one. Thus for $L'_{\text{CO}(1-0)}=(1.72 \times 10^9)\text{ L}_1$, and $X_{\text{co}}^{(\text{h})}\sim 0.92\text{ X}_1$ (computed from the LVG solutions compatible with $r_{43/32}$) it is $M_{\text{h-ex}}(\text{H}_2)\sim 1.6 \times 10^9\text{ M}_\odot$, comparable to the total $(\text{HI}+\text{H}_2)$ gas mass of the Milky Way and the minimum $M_{\text{SF}}(\text{H}_2)=L_{\text{IR}}^{(*)}/\epsilon_{\text{g},*}\sim 1.2 \times 10^9\text{ M}_\odot$ expected for “fueling” star formation in this LIRG. In Table 1 we comprehensively list all these gas mass estimates for IRAS 00057+4021, along with $M_{\text{total}}(\text{H}_2)$ computed using 1-phase and 2-phase LVG models (Eqs 3 and 10). We must note however that for IRAS 00057+4021 and most (but not all) LIRGs where 2-phase models are used, the large degeneracy that exists for LVG solutions of the “residual” CO line ratios of the (l)-phase (cool and near-virial versus warm and strongly gravitationally unbound states) translates to a large range of $X_{\text{co}}^{(l)}$, and thus $X_{\text{co}}^{(2\text{-ph})}$, values (Table 1). This in effect is the low-J CO SLED degeneracy described in 3.4, which the global CO SLEDs available in our study cannot “break”.

The high-excitation (h)-phase in IRAS 00057+4021 contains $\sim(20\text{-}50)\%$ of $M_{\text{tot}}(\text{H}_2)$ (Table 1), which is at least $\sim 10\times$ larger than what would be expected if its ISM was reducible to typical Galactic GMCs. Moreover its $r_{21}^{(\text{h})}(\text{lvg})\sim 2.5$, $R_{21}^{(\text{h})}(\text{lvg})\sim 23$ ratios (for $T_{\text{kin}}=100\text{ K}$, $n(\text{H}_2)=3 \times 10^4\text{ cm}^{-3}$, and $K_{\text{vir}}=22$) are higher than those in the Orion SF “hot-spots” near HII regions and O,B star associations (Sakamoto et al. 1994). This further corroborates the irreducibility of the observed CO SLED of IRAS 00057+4021 to ordinary photon-powered ISM states. On the other hand strong mechanical feedback from SNR-driven shocks could in principle yield such highly excited CO SLEDs (Arikawa et al. 1999; Bolatto et al. 2003), but just like radiative feedback from O, B stars, such SNR-driven “hot” spots involve only small fractions of a typical GMC mass. Indicatively, in the Galactic SNRs W 44 and IC 443

a warm, dense, and very kinematically stirred component with $r_{21} \sim 1.3-4$ (Seta et al. 1998) involves only $\sim 1\%$ of the impacted GMCs, with negligible effect on their global CO line ratios ($\langle r_{21} \rangle_{\text{GMC}} \sim 0.6$). We must also note however that IRAS 00057+4021 is a Seyfert 2 and its AGN, if X-ray luminous, can induce such extreme conditions to a large molecular gas mass, if distributed close to it (Schleicher et al. 2010).

B.2. IRAS 00509+1225 (IZw 1)

This LIRG hosts an optically and X-ray luminous QSO in the center of a molecular gas-rich disk, the site of a vigorous circumnuclear starburst (Barvainis et al. 1989; Eckart et al. 1994 and references therein). The latter has been imaged interferometrically (Schinnerer et al. 1998; Staguhn et al. 2004) revealing a disk of $\sim 8-12$ ($\sim 12-14$ kpc) with cold ISM but increasing ISM excitation towards its central ~ 1.5 (~ 2 kpc) SF circumnuclear ring.

In terms of global CO line excitation while its $r_{21} = 0.84 \pm 0.24$ ratio can be (barely) compatible with that of a SF-quiescent disk like the Milky Way (~ 0.6), its luminous J=3–2 line with $r_{32} = 1.16 \pm 0.40$ is clearly dominated by much higher ISM excitation, typical of a SF phase (even $r_{32}-\sigma = 0.76$ is 2.5x higher than $r_{32} = 0.3$ typical for SF-quiescent ISM). A one-phase LVG model yields an acceptable fit within the measurement uncertainties, with $r_{21}(\text{lvg}) \sim 1$, $r_{32}(\text{lvg}) \sim 0.90-0.95$, and $R_{10} \sim 8$, $R_{21} \sim 5-7$ while $K_{\text{vir}} \sim 1-2$ (a result of the modest R_{10} and R_{21}). The best one-phase LVG solutions yield $X_{\text{co}} \sim 1.5 X_1$ (Equation 3), and a total molecular gas mass $M(\text{H}_2) \sim 8.5 \times 10^9 M_{\odot}$. The minimum dense gas mass fueling an Eddington-limited SF is $M_{\text{SF}}(\text{H}_2) = 4 \times 10^8 M_{\odot}$, which only $\sim 5\%$ of the $M_{\text{tot}}(\text{H}_2)$ and typical for ordinary SF GMCs found in galactic disks. Thus IZw 1 stands as an example of a LIRG with star formation occurring in an isolated gas-rich disk, fueled by ordinary molecular clouds.

The reasonable 1-phase LVG fit of the observed global CO line ratios in IZw 1 make a 2-phase decomposition unnecessary. Nevertheless the available observational information on the presence of a cold molecular gas-rich disk and a circumnuclear ring starburst allow such a decomposition as a useful test on the limitations of global CO SLEDs and their fit by a single average ISM state, to yield reliable total molecular gas mass estimates. Using the CO J=3–2, 6–5 and ^{13}CO J=1–0 lines to constrain the (h)-phase we find the best LVG solution range at $T_{\text{kin}} = (65-75)$ K, $n = 10^4 \text{ cm}^{-3}$ and $K_{\text{vir}} = 13$ that yield $X_{\text{co}}^{(\text{h})} = 0.65 X_1$. Adopting a Galactic $X_{\text{co}}^{(1)} = 5 X_1$ for the computed residual CO J=1–0 emission, which we attribute to the extended gas disk, yields $X_{\text{co}}^{(2-\text{ph})} = 1.65 X_1$ (Equation 10), similar to that computed from the one-phase LVG model. We caution however that the CO J=6–5 line luminosity is highly uncertain and along with it the current 2-phase decomposition.

B.3. NGC 828

This is a disturbed spiral galaxy with a prominent dust lane and H α emission in its center and two sources symmetrically around the center source along the major axis (Hattori et al. 2004). VLA imaging of its cm continuum emission show it elongated along the disk, as would be expected for star formation, with no signs of AGN activity such as a radio core or jets (Parma et al. 1986). Its single dish CO J=1–0 detection showed abundant molecular gas (Sanders et al. 1986) while subsequent interferometric CO 1-0 imaging with OVRO recovered all the single dish flux and showed it to be extended $\sim 10'' \times 20''$ ($\sim 7.5 \text{ kpc} \times 3.6 \text{ kpc}$) with the longest dimension lying along the optical disk (Wang et al. 1991). The same study obtained a dynamical mass of $M_{\text{dyn}} \sim 4 \times 10^{10} M_{\odot}$ within a CO disk radius of 3.9 kpc (for the adopted cosmology). However at $\sim 4''$ (1.4 kpc) south-east of its nucleus the CO-derived velocity field deviates from that of a normal rotating spiral, possibly indicating the presence of another molecular gas concentration brought in as part of a merger (Wang et al. 1991).

The available CO lines are consistent with a star-forming disk with a well-excited CO J=3–2 line ($r_{32}=0.70 \pm 0.15$, Paper I) but whose modest $R_{10}=10 \pm 2$ and $R_{21}=12 \pm 3$ ratios indicate that any merger activity has not disturbed the average dynamical state of the molecular clouds. This is reflected in the one-phase LVG solutions found for $T_{\text{kin}} \geq 35 \text{ K}$ which invariably have $K_{\text{vir}} \sim 2-4$. These solutions remain highly degenerate however with $T_{\text{kin}}=(35-50) \text{ K}$, $n=10^3 \text{ cm}^{-3}$, and $K_{\text{vir}} \sim 4$ almost as good as $T_{\text{kin}}=(55-150) \text{ K}$, $n=3 \times 10^2 \text{ cm}^{-3}$, and $K_{\text{vir}} \sim 2$. The corresponding $X_{\text{co}} \sim (0.8-1.1) X_1$, yields $M_{\text{tot}} \sim (4.6-6.3) \times 10^9 M_{\odot}$, while $M_{\text{SF}} \sim 3 \times 10^8 M_{\odot}$ is necessary to fuel an Eddington-limited star formation.

Thus the dense and warm gas fueling SF sites in this low IR luminosity galaxy will amount to only $\sim 5\%-6.5\%$ of the total molecular gas mass, consistent also with its small HCN/CO J=1–0 ratio of $r_{\text{HCN/CO}}^{(\text{obs})}=0.022$ (Gao & Solomon 2004). Nevertheless global CO SLED can still be easily dominated by even small amounts of star forming gas whose often modest X_{co} may be much smaller than that of an incospicuous SF-quiescent cold gas reservoir. For NGC 828 there is apriori knowledge of an extended molecular gas disk with $\sim 8 \text{ kpc}$ diameter. However a 2-phase fit with an assumed (h)-phase SLED and mass normalization (see 2.4) leaves the (l)-phase properties largely undetermined with $X_{\text{co}}^{(l)} \sim (0.7-2.5) X_1$ ($\sim X_{\text{co}}^{(2-\text{ph})}$ since the (l)-phase CO J=1–0 luminosity dominates), and $M_{\text{tot}} \sim (4-14) \times 10^9 M_{\odot}$.

B.4. IRAS 02483+4302

This two-nuclei system is a gas-poor/gas-rich merger of an elliptical (nucleus A) going through the disk of a former spiral containing nucleus B (Kollatschny et al. 1992) and all of

the molecular gas detected in a CO J=1–0 interferometer map (DS98). The optically bright nucleus A hosts an AGN with a Sy2 spectrum, and is located 3.8'' (~ 3.76 kpc) to the west of nucleus B. The latter is where star formation occurs in this system, “activated” by the merger event which also likely triggered the QSO activity in the gas-poor merger progenitor.

Its CO line ratios up to J=3–2 can be well-fitted by a wide range of conditions with even a cold $T_{\text{kin}}=15$ K but highly unbound ($K_{\text{vir}}=22$) phase yielding a good fit. Most solutions are found at warmer temperatures though with $T_{\text{kin}}=(35-55)$ K, and $T_{\text{kin}}=(90-120)$ K, low densities of $n\sim(3\times 10^2-10^3)$ cm^{-3} , and strongly unbound states $K_{\text{vir}}=7-40$. Such a wide degeneracy of LVG solutions representing the average conditions of the molecular gas in IRAS 02483+4302 is typical for LIRGs where $r_{J+1,J}<1$, and no CO/ ^{13}CO ratios are available to constrain line optical depths (and thus K_{vir}). For this LIRG a lower limit of $R_{10}\gtrsim 13$ is not enough to eliminate the aforementioned degeneracy, though it does preclude SF-quiescent *and* virialized states. For all the LVG solutions compatible with its global line ratios we obtain $X_{\text{co}}=(0.25-0.70) X_1$ (Equation 3). Restricting the admissible range of LVG solutions with $T_{\text{kin}}/T_{\text{dust}}\gtrsim 1$, and $K_{\text{vir}}\lesssim 20$ yields $X_{\text{co}}\sim 0.45 X_1$ and a total molecular gas mass $M(\text{H}_2)\sim 1.6\times 10^9 M_{\odot}$, similar to that obtained using the optically thin, LTE, approximation $M_{\text{thin}}^{(\text{LTE})}\sim 2\times 10^9 M_{\odot}$ (Equation 5 for $T_{\text{kin}}=55$ K) a result of the low/moderate optical depths of the LVG solutions used to deduce X_{co} in this LIRG.

The minimum gas mass for an Eddington-limited star formation in IRAS 02483+4302 is $M_{\text{SF}}(\text{H}_2)\sim 1.4\times 10^9 M_{\odot}$, which is $\sim 90\%$ of its total molecular gas mass (for $X_{\text{co}}=0.45 X_1$). This is rather puzzling as the SF phase, with its expected high densities ($\geq 10^4 \text{cm}^{-3}$) and near gravitationally bound states ($K_{\text{vir}}\sim 1-5$) can easily have CO lines thermalized and with substantial optical depths up to at least J=3–2. Thus if the SF phase indeed dominates the total molecular gas mass in this ULIRG, one would expect $M_{\text{thin}}^{(\text{LTE})}\ll M(\text{H}_2)$ rather than $M_{\text{thin}}^{(\text{LTE})}\sim M(\text{H}_2)$ as the latter implies small/moderate optical depths for the bulk of the molecular gas mass. Moreover the physical states compatible with the global CO line ratios of IRAS 02483+4302 while highly degenerate, are hardly indicative of a dense SF gas phase dominating its total molecular gas mass. It is also telling that all one-phase LVG solutions fail to reproduce the CO J=6–5 line luminosity of this LIRG, indicating the presence of another, potentially massive, gas component whose higher CO line excitation becomes prominent beyond J=3–2. Using only its CO J=3–2, 6–5, and the upper limits on the ^{13}CO J=1–0, 2–1 lines as constraints of the (h)-phase in a 2-phase model still yields a significant range of solutions though all have $n\sim(10^4-10^5) \text{cm}^{-3}$ with $T_{\text{kin}}\geq 60$ K, typical of a dense and warm SF-related phase. Most (but not all) have virial states ($K_{\text{vir}}\sim 1$) with $X_{\text{co}}^{(\text{h})}\sim(1.5-2.5) X_1$. From the corresponding $\langle r_{65}^{(\text{h})} \rangle_{\text{lvg}}\sim 0.90$ and $\langle X_{\text{co}}^{(\text{h})} \rangle_{\text{lvg}}\sim 2.2 X_1$ we obtain $L_{\text{co},1-0}^{(\text{h})}=1.5\times 10^9 L_1$, and $M_{\text{h-ex}}=3.3\times 10^9 M_{\odot}$. Higher CO J=6–5 line luminosities will only make this mass larger (both via a higher $L_{\text{co},1-0}^{(\text{h})}$ and a higher deduced $\langle X_{\text{co}}^{(\text{h})} \rangle_{\text{lvg}}$).

The “residual” global CO line ratios of the (1)-phase in this LIRG cannot distinguish between a cold, SF-quiescent gas at near virial dynamical states (and Galactic $X_{\text{co}}^{(1)}$) versus a warm and highly unbound phase expected in the highly turbulent environments of mergers (and with a low $X_{\text{co}}^{(1)}$ because of the high K_{vir}). Thus for $\rho_{\text{co}}^{(1-h)}=1.43$ computed from our 2-phase model, $X_{\text{co}}^{(h)}=2.2 X_1$ and $X_{\text{co}}^{(l)}=(0.5-2.5) X_1$, we obtain $X_{\text{co}}^{(2-ph)}=(1.2-2.4) X_1$. Higher, near-Galactic, values remain possible if high resolution CO imaging were to reveal the (1)-phase as an extended cold, SF-quiescent gas reservoir, something that global CO SLEDs cannot easily do.

B.5. IRAS 03359+1523

Two interacting galaxies $\sim 10''$ (~ 6.9 kpc) apart can be discerned in optical images, with only the eastern source being bright in radio wavelengths (Condon et al. 1990; Goldader et al. 1997) and containing most ($\gtrsim 75\%$) of the CO J=3–2 emission (Leech et al. 2010, Paper I). This system has the lowest CO(3–2)/(1–0) ratio ($=0.18\pm 0.05$) indicating the lowest-excitation global CO line excitation in our sample, though we cannot exclude the possibility that significant CO J=3–2 flux was “missed” by the 2-point observations of this two-nuclei system.

The best LVG solution indicates SF-quiescent gas ($T_{\text{kin}}=15$ K $n=3\times 10^2$ cm^{-3} and $K_{\text{vir}}\sim 2$), yielding $r_{32}\sim 0.22$ and $R_{21}\sim 18$ which is somewhat higher than the observed value ($=12\pm 3$). The corresponding $X_{\text{co}}\sim 2.5 X_1$ gives $M_{\text{tot}}\sim 2.2\times 10^{10} M_{\odot}$, while the LTE approximation for $T_{\text{kin}}=15$ K gives $M_{\text{thin}}^{(\text{LTE})}=1.8\times 10^9 M_{\odot}$, which is $\sim 10\times$ smaller than M_{tot} as expected given the large CO line optical depths ($\tau_{10}\gtrsim 14$) of the corresponding LVG solution. The SF-related molecular gas mass $M_{\text{SF}}(\text{H}_2)=8.2\times 10^8 M_{\odot}$ amounts to only $\sim 4\%$ of $M(\text{H}_2)$, consistent with the low average CO line excitation of this system and ensembles of ordinary GMCs.

B.6. VII Zw 031

This galaxy has one of the highest CO J=1–0 luminosities in our sample and while early ground-based images were suggestive of an elliptical system (Sanders & Mirabel 1996), near-IR NICMOS images clearly show a spiral disk with very bright asymmetric arms tightly around its nucleus over scales of $R\sim(1-1.4)$ kpc (half-light radii), with numerous star clusters on its disk (Scoville et al. 2000). This is one of the few LIRGs where there is no evidence of what has triggered its starburst activity, namely neither a nearby companion system (indicating an early merger stage), nor tidal tails (signs of an advanced or post-merger

system). High resolution interferometric imaging indicates a nearly face-on source with a rapidly rotating gaseous ring on scales of few hundred parsecs (DS98).

The low-J CO SLED with $r_{21}=0.72\pm 0.12$ and $r_{32}=0.43\pm 0.19$ indicate rather low average line excitation, compatible even with SF-quiescent ISM ($r_{21}\sim 0.5-0.6$, $r_{32}\sim 0.25-0.30$). A radiative transfer model of only the CO J=1–0, 2–1, 3–2, and ^{13}CO J=1–0, 2–1 lines yields $T_{\text{kin}}=(30-65)\text{ K}$, $n=3\times 10^2\text{ cm}^{-3}$ and $K_{\text{vir}}\sim 2$ (near-virial). The corresponding $X_{\text{co}}\sim 1.25 X_1$ factor yields $M(\text{H}_2)=1.5\times 10^{10} M_{\odot}$ while the minimum molecular gas mass needed to fuel an Eddington-limited star formation in this LIRG is: $M_{\text{SF}}(\text{H}_2)\sim 2\times 10^9 M_{\odot}$. On the other hand a luminous CO J=4–3 with $r_{43}=1.46\pm 0.45$ (Paper I) is highly excited, and the reason why one-phase LVG solutions, while reproducing the observed $r_{32,21}$ and $R_{10,21}$ line ratios within their measurement uncertainties, they yield $r_{43}^{(\text{lv})}\lesssim 0.20-0.26$, i.e. $\sim 6-7$ times lower than observed. The CO J=6–5 line luminosity with $r_{65}=0.22\pm 0.07$ is also much higher than predicted by these models ($r_{65}^{(\text{lv})}=0.01-0.02$). Interestingly the ^{13}CO J=1–0, 2–1 lines, with modest $R_{10,21}\sim 10$ and $r_{21}(^{13}\text{CO})\sim 0.72$ ratios, also indicate a low/average excitation state.

Thus only the CO J=4–3 and J=6–5 line luminosities signify the presense of another potentially massive warmer and denser gas phase, demonstrating once more the importance of high-J CO line measurements. Moreover, the $r_{43}>r_{32}$ inequality sets the global CO SLED of VII Zw 031 apart from those reducible to a mixture of a dense and warm gas phase (with a CO SLED typical of Orion hot-spots), and a cooler, diffuse one associated with non-SF gas and a low-excitation SLED. As in IRAS 00057+4021, this implies large amounts of hot *and* dense gas, maintained in a strongly unbound dynamical state as to keep the average optical depth of even high-J CO lines below unity (see also discussion in Paper I). We note however that in VII Zw 031 the CO J=3–2 line luminosity is highly uncertain because of the large system temperature, though even a $3\times$ stronger CO J=3–2 line would maintain the aforementioned inequality and its implications for extraordinary ISM conditions in this galaxy.

We use the CO (4-3)/(3-2) ratio $r_{43/32}$ to constrain the (h)-phase in a 2-phase model while using the CO J=6–5 luminosity only as a lower limit. We also assume the minimum $r_{43/32}=(L'_{\text{CO}(4-3)}-\sigma)/(L'_{\text{CO}(3-2)}+\sigma)=1.67$ value consistent within the measurement uncertainties in order to place limits on the lowest possible average excitation level for the (h)-phase. This will still be high as even that minimum value is close to the theoretical maximum of $(4/3)^2$, attained only for a hot gas phase with fully optically thin and thermalized CO lines. We find good solutions only for $T_{\text{kin}}\geq 95\text{ K}$ which keep improving up to the maximum $T_{\text{kin}}=150\text{ K}$ considered, while $n=3\times 10^4\text{ cm}^{-3}$ and $K_{\text{vir}}=22$. No good solutions can be found for lower temperatures as these have unphysical $K_{\text{vir}}<1$ values. Over the good solution range the corresponding $\langle r_{43}^{(\text{h})} \rangle=3.4$ and $r_{65}^{(\text{h})}\gtrsim 2$. The corresponding $\langle X_{\text{co}}^{(\text{h})} \rangle=0.9 X_1$, and from $L_{\text{CO},1-0}^{(\text{h})}=(1/\langle r_{43}^{(\text{h})} \rangle)L'_{\text{CO}(4-3)}\sim 3.45\times 10^9 L_1$ (we used the CO(4-3)- σ value) we esti-

mate: $M_{\text{h-ex}}=3.1\times 10^9 M_{\odot}$. As expected, with a $^{13}\text{CO}(2-1)/(1-0)$ ratio of ~ 0.73 (subthermal), an (h)-phase model cannot successfully include the ^{13}CO lines, while their modest global $R_{10,21}\sim 10$ (Table 8, Paper I) are typical of disk GMCs rather than of those in starbursts (where $R_{10,21}\geq 15$). This along with the fact that there is very little CO J=2–1 and 3–2 emission left after subtraction of the corresponding (h)-phase line emission suggest a cold disk-like (l)-phase. Assuming an $X_{\text{co}}^{(l)}=4.5 X_1$ (i.e. Galactic), and for $\rho_{\text{co}}^{(l-h)}=2.34$, we obtain $X_{\text{co}}^{(2-ph)}=3.4 X_1$ and a total gas mass of $M_{\text{tot}}^{(2-ph)}=3.9\times 10^{10} M_{\odot}$. Thus despite its prominence in CO J=4–3 and 6–5 lines, the high-excitation component amounts to only $\sim 8\%$ of the total molecular gas mass in VII Zw 031. Interestingly, the CO J=2–1 interferometric map by DS98 resolves out half of the 30-m single dish flux, indicating extended emission beyond the $\sim 2''$ (2 kpc) nuclear region where the bright CO J=1–0 emission is distributed. Indeed in the DS98 interferometric image faint CO J=1–0 emission can be seen out to a radius of $\sim 4''$ (4 kpc). New sensitive CO and ^{13}CO J=1–0 and 2–1 interferometric observations with similar u-v coverage (and thus enabling reliable line ratio maps) can be used to discern the existence of such a massive cold molecular gas disk in this intriguing object.

B.7. IRAS 05189–2524

This is Sy2 galaxy that appears to be a late stage merger with a very red compact nucleus and a tidal tail, (Farrah et al. 2003; Veilleux et al. 2002). This (U)LIRG is the most compact and has the warmest mid-IR colors ($f_{25\mu\text{m}}/f_{60\mu\text{m}}=0.25$) out of a nearly complete ULIRG sample selected for their “warm” mid-IR colors ($f_{25\mu\text{m}}/f_{60\mu\text{m}}>0.2$). Such systems are are thought to represent a critical stage in the so-called ULIRG→(optically luminous QSO) transition scenario (Sanders et al. 1988b,c). The AGN in this ULIRG is X-ray luminous with $L_x(2-10\text{keV})\sim 1.3\times 10^{43} \text{ ergs s}^{-1}$ (Dadina 2007). NICMOS near-IR imaging reveals an unresolved nucleus in all three near-IR bands, with a half light radii of $\sim(100-140)$ pc while CO J=1–0 observations show large amounts of molecular gas (Sanders et al. 1991) but no interferometric CO images are available yet for this southern ULIRG.

Unlike all other mergers/starbursts, IRAS 05189–2524 has a small $R_{21}=6 \pm 2$ ratio, typical of the self-gravitating (or nearly so) GMCs in spiral disks. As a result all LVG solutions within the expected temperature range (i.e. $T_{\text{kin}}/T_{\text{d}}\gtrsim 1$) have $K_{\text{vir}}\sim 1-2$, indicating virialized gas motions, quite unlike the much higher K_{vir} found in merger/starbursts. The observed $r_{21}=0.67 \pm 0.15$ together with the modest R_{21} are actually perfectly compatible with a SF-quiescent phase (where $r_{21}\sim 0.6$), although a SF-active one ($r_{21}\sim 0.8-1$) is certainly not excluded within the measurement uncertainties. The best LVG solutions converge towards conditions typical of Galactic GMCs but at elevated temperatures with $T_{\text{k}}=(30-55)$ K,

$n(\text{H}_2)=3 \times 10^2 \text{ cm}^{-3}$, and $K_{\text{vir}} \sim 1$ and yielding $r_{21}=0.86\text{-}0.91$, $r_{32}=0.50\text{-}0.67$, $r_{43}=0.30\text{-}0.40$ and $R_{21}=9$. Using values within the $r_{J+1,J} \pm \sigma$ range as constraints does not change the basic picture of low-density, somewhat warm gas, in a virialized or nearly so dynamical state. For the best solution it is: $X_{\text{co}} \sim 3.5 X_1$, which yields $M_{\text{tot}}(\text{H}_2)=1.37 \times 10^{10} M_{\odot}$.

Denser and warmer gas must of course be present, associated with the vigorous star formation in IRAS 05189–2524 and the minimum mass needed to fuel it of $M_{\text{SF}}(\text{H}_2) \sim 3.6 \times 10^9 M_{\odot}$. The CO J=6–5 line also indicates gas with significantly higher excitation than that indicated by the lower-J CO lines since, for the optimal LVG solutions for the low-J CO SLED segment: $r_{65}(\text{lvg}) \sim 0.01\text{-}0.05$, much lower than the observed $r_{65}=0.37 \pm 0.14$. Using a 2-phase model with an Orion-derived SLED and an Eddington-limit mass normalization for the (h)-phase (see 2.4) yields (l)-phase ratios of $r_{21}^{(l)}=0.45$, $r_{32}^{(l)}=0.28$ and $R_{21}^{(l)}=3.5$ with the best LVG solution being $T_{\text{kin}}=15 \text{ K}$, $n \sim 300 \text{ cm}^{-3}$ and $K_{\text{vir}} \sim 2.2$, i.e. typical of SF-quiet GMCs found in the disk of the Galaxy. The corresponding $X_{\text{co}}^{(l)}=2.5 X_1$, which for a computed $L_{\text{CO}(1-0)}^{(l')}=2.3 \times 10^9 L_1$, yields a total mass of cold SF-quiet molecular gas of $\sim 6 \times 10^9 M_{\odot}$. For the estimated $\rho_{\text{co}}^{(l-h)}=1.43$ and $X_{\text{co}}^{(h)}=2.2 X_1$ (see 2.4) we find $X_{\text{co}}^{(2-ph)} \sim 2.4 X_1$ and a $M_{\text{tot}}^{(2-ph)} \sim 9.4 \times 10^9 M_{\odot}$ with $\sim 65\%$ of this gas mass in a cold SF-quiet phase.

This merger ULIRG/AGN with its large molecular gas reservoir, nearly-Galactic X_{co} ($\sim 3\text{-}6$ times higher than the so-called ULIRG-values of $\sim (0.6\text{-}0.8) X_1$), and most of its molecular gas mass in a cold reservoir, stands as the clearest counter-example to standard views regarding this class of galaxies in the local Universe. Moreover, unlike I Zw 1 (another prominent “warm” LIRG considered midway in a supposed ULIRG \rightarrow (optical QSO) transition) whose known spiral disk can be the repository of its large SF-quiet molecular gas reservoir, the very compact size of IRAS 05189-2524 in cm continuum, near-IR, and optical wavelengths (Condon et al. 1990; Scoville et al. 2000; Surace et al. 1998) seems to preclude such a configuration. This compactness along with a “warm” CO(6–5)/(3–2) ratio of ~ 0.63 (i.e. dominated by the SF phase) in a ULIRG/AGN whose molecular gas reservoir is dominated by a cold SF-quiet component offer a cautionary tale regarding similar ULIRG/AGN objects at high redshifts where such characteristics were often used (and still are) to argue for the presence of only a dense and warm SF gas reservoir (Tacconi et al. 2006). Future ALMA observations of this southern ULIRG and similar objects would thus be very interesting for revealing the distribution of their large molecular gas reservoir and especially of their cold phase.

B.8. IRAS 08030+5243

This LIRG is one of the very few (=3) appearing as a single undistorted nucleus in a large near-IR ($2.2\mu\text{m}$) and optical imaging survey of 56 ULIRGs selected from the IRAS 2 Jy sample (Murphy et al. 1996). Its CO line ratios reveal a low average excitation state but lack of ^{13}CO observations permit a very wide range of conditions to reproduce its low global r_{32} and r_{21} ratios. In turn these conditions yield a large range of X_{co} values, from $X_{\text{co}}\sim 4.6 X_1$ (for $T_{\text{kin}}=15\text{ K}$, $n\sim 300\text{ cm}^{-3}$ and $K_{\text{vir}}\sim 1$), to $X_{\text{co}}\sim (1.5-1.7) X_1$ (for $T_{\text{kin}}=(55-90)\text{ K}$, $n\sim 100\text{ cm}^{-3}$ and $K_{\text{vir}}\sim 1$) and also down to $X_{\text{co}}\sim 0.61 X_1$ (for $T_{\text{kin}}=[20\text{ K}, (40-50)\text{ K}]$, $n\sim [10^3, 300\text{ cm}^{-3}]$ and $K_{\text{vir}}\sim [13, 7]$ respectively). For a set of very warm ($T_{\text{kin}}=(95-130)\text{ K}$) and strongly unbound ($K_{\text{vir}}=22$) diffuse gas ($n=3\times 10^2\text{ cm}^{-3}$) solutions the X_{co} factor can become as low as $\sim 0.3 X_1$. It is worth remembering that such gas may indeed exist in most ULIRGs as an “envelope” phase of a much denser dense phase, a result of disrupted GMCs during a strong merger. Its high brightness in low-J CO lines (a result of its high T_{kin} and K_{vir} values) is responsible for the low X_{co} deduced for such systems (which nevertheless can have most of their molecular gas mass in a much denser phase with high X_{co} , see discussion in 3.2).

Demonstrating the importance of ^{13}CO line measurements we note that the CO/ ^{13}CO $J=1-0$ ratio changes dramatically among the aforementioned LVG solutions groups, from $R_{10}\sim 5$ for cold virialized gas, to $R_{10}\sim 30$ for the warm highly non-virial ISM states. Nevertheless lack of such measurements makes it impossible to constrain the LVG solution groups and thus X_{co} in this ULIRG. Values as low as $X_{\text{co}}=0.3 X_1$ are likely excluded however as they yield $M_{\text{tot}}\sim 3\times 10^9 M_{\odot}$, comparable to $M_{\text{SF}}(\text{H}_2)=2.4\times 10^9 M_{\odot}$. In such a case the global CO SLED would be that of dense warm SF gas (i.e. highly excited) rather than of low-excitation.

B.9. IRAS 08572+3915

This is another prominent ULIRG from the “warm” ULIRG sample (Sanders et al. 1988c) consisting of a close pair of interacting spirals with their nuclei separated by $5''$ ($\sim 5.6\text{ kpc}$) and clearly discernible in cm, near-IR and optical images (Condon et al. 1990; Scoville et al. 2000; Surace et al. 1998). Its NW nucleus is unresolved in near-IR and is the only one detected in CO $J=1-0$ interferometer maps where it appears unresolved with $\theta_{\text{co}}\leq 2.1''$ ($\sim 2.3\text{ kpc}$) (Evans et al. 2002). Mid-IR ($12-25\mu\text{m}$) imaging showed all the mid-IR emission also emanating from the NW nucleus and a region $\lesssim 330\text{ pc}$ in diameter (Soifer et al. 2000, and for the adopted cosmology).

The discovery of very luminous CO $J=6-5$ emission towards the NW nucleus (Paper I, Figure 2), corresponds to second highest r_{65} ratio in our entire sample (~ 1), indicating ex-

treme ISM excitation conditions, with average gas densities of $\sim(10^5\text{-}10^6)\text{ cm}^{-3}$, and LVG fits that keep improving past $T_{\text{kin}}=150\text{ K}$. The 3σ upper limit on $r_{32}\lesssim 2.54$ is certainly compatible with such conditions, albeit not imposing any useful additional constraints (high T_{sys} because of $\nu_{\text{sky}}(3\text{-}2)$ near the 325 GHz atmospheric absorption feature prevented sensitive CO J=3–2 observations of this system). The high r_{65} ratio measured for the NW nucleus of this ULIRG is actually perfectly compatible with a pure Orion “hot-spot” CO SLED (see 2.4), further emphasizing the truly extraordinary levels of ISM excitation. The corresponding molecular gas mass is at least $M_{\text{SF}}(\text{H}_2)\sim 3.9\times 10^9 M_{\odot}$ (assuming an Eddington-limited SF). *A Galactic $X_{\text{co}}\sim(3\text{-}6)M_{\odot}(K\text{ km s}^{-1}\text{ pc}^2)^{-1}$ factor is deduced* from the LVG solutions with $T_{\text{kin}}\geq 65\text{ K}$, which corresponds to $M(\text{H}_2)\sim(4.8\text{-}9.6)\times 10^9 M_{\odot}$. Thus $M_{\text{SF}}/M_{\text{tot}}\sim 0.41\text{-}0.81$, among the highest such fractions for the individually-studied LIRGs (see Table 1).

B.10. Arp 55

This is another clear merger having double nuclei as IRAS 08572+3915, but more widely separated ($\sim 12''$, 9.3 kpc) seen in radio continuum maps (Condon et al. 1990) as well as optical and CO J=1–0 interferometric maps (Sanders et al. 1988). A tidal tail emerging from the eastern nucleus (also the most gas-rich one) is clearly visible in H α emission (Hattori et al. 2004). The two nuclei have been separately detected in CO J=3–2 (Leech et al. 2010, Paper I) while the NE nucleus may have been tentatively detected also in CO J=6–5 (Paper I), with an implied high CO(6–5)/(3–2) brightness temperature ratio of $r_{65/32}=0.75$ indicating a highly excited molecular ISM phase. On the other hand the global HCN/CO J=1–0 brightness temperature ratio is ~ 0.03 (Gao & Solomon 2004), typical of the molecular gas found in isolated spiral disks and quite unlike the much higher such ratios in merger/starbursts.

Using the global r_{21} and r_{32} , along with the lower limit on the CO/ ^{13}CO J=2–1 ratio (see Paper I) yields a large range of possible average ISM states, all with $n\sim(1\text{-}3)\times 10^3\text{ cm}^{-3}$ and most with surprisingly large K_{vir} ($\sim 70\text{-}126$). Restricting K_{vir} to values ≤ 40 yields a much narrower range of solutions with $T_{\text{kin}}=(45\text{-}70)\text{ K}$ and corresponding $X_{\text{co}}\sim(0.25\text{-}0.8)X_1$. This still considerable X_{co} range yields $M_{\text{tot}}\sim(2.9\text{-}9.2)\times 10^9 M_{\odot}$, while $M_{\text{SF}}\sim 0.9\times 10^9 M_{\odot}$. The latter is $\sim 1/10\text{-}1/3$ of the total molecular gas mass, leaving ample room for a SF-quiescent molecular gas reservoir. In Arp 55 however SF-quiescent is not the cool and mostly gravitationally bound gas found in the GMCs of isolated disks. Indeed the large temperatures and K_{vir} values needed to fit its highly-excited CO lines and $R_{21}\gtrsim 13$ suggest warm and strongly unbound gas which, unlike in most other ULIRGs, contains most of the molecular gas mass. The low HCN/CO J=1–0 ratio then may not be due to the prevalence of Galactic-type SF-quiescent GMCs rather than to a disrupted ISM state that has, momentarily, a

low (dense)/(total) molecular gas mass fraction. Short periods during which the dense gas reservoir of a LIRG can be strongly disrupted by SF feedback while its IR luminosity remains intact are expected in strongly evolving mergers (Loenen 2009). In such a scenario Arp 55 would be one of the few mergers “caught” in a very short act (see also Arp 193). Interestingly its HCN(3–2)/(1–0) ratio is <0.3 (Juneau et al. 2009), much lower than in some classical (U)LIRGs such as Arp 220 and NGC 6240 (Greve et al. 2009). More sensitive ^{13}CO and higher-J HCN observations of Arp 55 are necessary to confirm such a tantalizing picture of global ISM dynamics.

B.11. IRAS 09320+6134 (UGC 05101)

Near-IR NICMOS observations show a single extremely red and unresolved nucleus with $\theta_s \leq 0.22''$ (~ 170 pc), surrounded by a strongly perturbed spiral structure (Scoville et al. 2000) with a tidal tail and a large ring seen in the optical (Sanders et al. 1988b). The half-light source radius at $2\mu\text{m}$ is ~ 450 pc while an interferometric CO J=3–2 image reveals a gas distribution of $\sim 2''$ (1.5 kpc) in size (Wilson et al. 2008). Its disturbed morphology is interpreted as the result of an interaction with another gas-rich spiral (Sanders et al. 1988b) and even with a gas-poor dwarf galaxy $17''$ to the southeast (Majewski et al. 1993). This ULIRG contains an AGN luminous in hard X-rays (Imanishi et al. 2003) and is deeply dust-enshrouded along most lines of sight, with $N(\text{H}) > 10^{24} \text{ cm}^{-2}$ (Imanishi et al. 2001).

Its CO SLED betrays the presence of a high-excitation gas component already from the low-J lines with $r_{21}=1.23$ and $r_{32}=0.93$ (Paper I). These ratios along with the high CO/ ^{13}CO J=2–1 ratio of $R_{21}=18$ can be well-fitted by two ranges of LVG solutions, namely: $T_{\text{kin}}=(35-65) \text{ K}$, $n=3 \times 10^3 \text{ cm}^{-3}$, $K_{\text{vir}}=22$, and $T_{\text{kin}}=(100-130) \text{ K}$, $n=10^3 \text{ cm}^{-3}$, $K_{\text{vir}}=4$. The corresponding average X_{co} factors are $X_{\text{co}} \sim 0.4 X_1$ and $X_{\text{co}} \sim 0.6 X_1$ respectively. We note that a small range of solutions with $T_{\text{kin}}=(25-30) \text{ K}$, $n=10^4 \text{ cm}^{-3}$ and $K_{\text{vir}}=40$ also exists but are unlikely to be good representation of the average ISM state in this ULIRG since $T_{\text{kin}}/T_{\text{dust}} < 1$ (considered unlikely, see Paper I). Moreover their very large K_{vir} make it even less likely that these modest gas temperatures can correspond to such highly unbound dynamical states where the molecular gas can be significantly heated by the dissipated supersonic turbulence (see Paper I). Nevertheless adopting this narrow cooler gas solution range would not make much difference when it comes to the corresponding X_{co} factor which is $\sim 0.5 X_1$. The corresponding total molecular gas mass then is $M_{\text{tot}} \sim (1.9-2.9) \times 10^9 M_{\odot}$ while $M_{\text{SF}} \sim 1.6 \times 10^9 M_{\odot}$.

The large fraction of SF gas mass in UGC 05101 ($\sim (55-84)\%$) is further corroborated by the high HCN/CO J=1–0 brightness temperature ratio of ~ 0.2 (Gao & Solomon 2004) (for typical spiral disks this ratio is $\sim 0.02-0.03$) isofar as HCN J=1–0 is a linear proxy for dense

gas mass and most of that gas is involved in star formation. This dense gas reservoir is likely confined into the small (near-IR)-bright nucleus fueling a compact starburst. Such compact, ~ 100 pc-sized gas-disk/starburst configurations have been revealed for Arp 220 (Sakamoto et al. 2008; Mathushita et al 2004) where extremely high extinctions ($N(\text{H}) \geq 10^{25} \text{ cm}^{-3}$) correspond to significant dust optical depths even at submm wavelengths (Sakamoto et al. 2010, Papadopoulos et al. 2010a). These can be responsible for Compton-thick AGN, and a suppression of high-J CO lines in such systems. This may be the case also for UGC 05101 as indicated by its low CO(6-5)/(1-0) yet high HCN/CO J=1-0 ratio (see Figure 11, Papadopoulos et al. 2010b).

Despite the good one-phase fit obtained for the global CO SLED (and R_{21}) of this ULIRG, the observed CO line emission may still be dominated by a phase that does not contain the bulk of its molecular gas mass. Indeed, neither the modest densities nor the potentially highly unbound average dynamical states implied by the one-phase LVG fits would be typical of the HCN-bright star-forming phase. As discussed in 3.2 the X_{co} obtained from the global low-J CO SLED may thus be suitable only for a gas phase that does not contain much of the molecular gas mass. Using the observed $r_{\text{CO/HCN}}^{(\text{obs})} = 5$ in the context of a 2-phase model along with $r_{\text{CO/HCN}}^{(\text{h})} = 2.34$ (see 3.2) yields $\rho_{\text{co}}^{(\text{l-h})} = 1.136$ (Eq. 14). In the absence of multi-J HCN observations that could constrain X_{HCN} we set $X_{\text{HCN}} = 10 X_1$, the smallest value produced by such studies (e.g. Papadopoulos 2007; Gracia-Carpio et al. 2008). Thus $X_{\text{co}}^{(\text{h})} = (r_{\text{CO/HCN}}^{(\text{h})})^{-1} X_{\text{HCN}} \sim 4.3 X_1$, and for $X_{\text{co}}^{(\text{l})} = 0.5 X_1$ it would be $X_{\text{co}}^{(\text{2-ph})} = 2.3 X_1$, which is $\sim (4-6) \times$ higher than that deduced from one-phase LVG models of the low-J CO SLED. Multi-J observations of HCN or other heavy rotor molecules (e.g. CS, HCO⁺) can confirm such potentially high masses of molecular gas at high densities.

B.12. NGC 3310

The young and intense star formation activity of this UV-bright galaxy is on par with M82, and the likely result of a recent merger with a smaller galaxy (Balick & Heckman 1981; Concelice et al. 2000; Elmegreen et al. 2002). Its gas and dust are warmed and disrupted by the presence of the starburst in its central 1-2 kpc. Tidal HI tails, unusually large HI velocity dispersions ($\sim 40 \text{ km s}^{-1}$) for a spiral galaxy (Kregel & Sancisi 2001), and large velocity offsets (up to 150 km s^{-1}) between molecular cloud and adjacent HII regions (Kikumoto et al. 1993) provide further evidence for a dynamically disturbed gas typical of mergers.

This galaxy has been extensively studied by Zhu et al. 2009 as a template of a highly-excited ISM, indicated by $r_{21,32} > 1$ ratios and warm IR “colors” ($S_{100\mu\text{m}}/S_{60\mu\text{m}} = 1.28$). Despite

its low IR luminosity ($L_{\text{IR}}^{(*)} \sim 2.7 \times 10^{10} L_{\odot}$, Paper I) its global $r_{21}=1.47$ and $r_{32}=1.21$ ratios surpass those of Orion cloud SF “hotspots”, and are among the highest observed in our sample. Its proximity allowed spatially resolved studies of its molecular gas with single-dish telescopes obtaining beam-matched observations of the CO(3–2)/(1–0) ratio (see Zhu et al. 2009 for details). These high global CO line ratios of NGC 3310 can be fitted well by a single phase provided $T_{\text{kin}} \geq 35 \text{ K}$ ($\sim T_{\text{dust}}$), but remain highly degenerate over the $[T_{\text{kin}}, n, K_{\text{vir}}]$ domain up to the highest temperature searched (150 K). Interestingly for $T_{\text{kin}}=(35-50) \text{ K}$ a class of dense ($n \sim (1-3) \times 10^4 \text{ cm}^{-3}$) and strongly unbound ($K_{\text{vir}} \sim 20-40$) states are possible, though only higher-J and/or ^{13}CO line observations could reduce the wide degeneracy of the LVG solutions and designate such phases as those most likely representing the actual ISM conditions. Other solution ranges are: $T_{\text{kin}}=(70-90) \text{ K}$, $n=3 \times 10^3 \text{ cm}^{-3}$ and $K_{\text{vir}}=22$ while near-virial solutions can be found at high temperatures $T_{\text{kin}}=95 \text{ K}$, (140-145) K, $n=(1-3) \times 10^4 \text{ cm}^{-3}$ and $K_{\text{vir}}=4, 2.2$. The large degeneracy of possible average ISM conditions translates to a significant one for the X_{co} factors, ranging from $\sim 0.4 X_1$ (for the highly unbound states with $K_{\text{vir}}=22-40$) and up to $\sim (1.2-2.2) X_1$ (for the near-virial states with $K_{\text{vir}}=4, 2.2$).

For $X_{\text{co}}=(0.4-2.2) X_1$ the corresponding $M_{\text{tot}}=(0.3-1.5) \times 10^8 M_{\odot}$ while $M_{\text{SF}}=1.1 \times 10^8 M_{\odot}$. The latter seems to rule out the lowest X_{co} values while even for the highest ones it is: $M_{\text{SF}}/M_{\text{tot}} \sim 0.73$, i.e. most of the molecular gas in NGC 3310 is directly involved in star formation (for an Eddington-limited SF process), leaving little room for a massive low-excitation molecular gas reservoir. Interestingly the LVG solutions corresponding to the highest X_{co} values are those indicative of a SF phase with $n \sim 3 \times 10^4 \text{ cm}^{-3}$, $K_{\text{vir}}=2.2$ and large $T_{\text{kin}}=(140-145) \text{ K}$. We caution though that all this pertains only to the inner $\sim 40''$ of this galaxy where the starburst takes place, a massive molecular gas reservoir with low densities, highly unbound gas motions, and low CO line excitation can still exist beyond it, a situation actually encountered in M 82 in the form large scale molecular gas outflows (Weiss et al. 2005).

B.13. IRAS 10565+2448

This is a ULIRG with HII region-type line ratios (Armus, Heckman, & Miley 1989) implying an optical spectrum dominated by young stars rather than an AGN. Nevertheless a weak contribution from an AGN seems necessary in order to fit its IR/submm dust continuum SED (Farrah et al. 2003). Early r-band (6550Å) imaging has shown this object to be a possible triple merger galaxy system (Murphy et al. 1996), while near-IR imaging with the HST NICMOS camera shows a luminous primary galaxy interacting with a much fainter one $\sim 8''$ ($\sim 6.7 \text{ kpc}$) to the southeast (Scoville et al. 2000). The primary galaxy is compact with

a half-light source diameter at $2\mu\text{m}$ of $\sim 650\text{ pc}$, and the only source where luminous CO J=1–0 line emission is detected (DS98) with a diameter of $1.5''$ (1.25 kpc). Moreover this ULIRG along with VII Zw 031 and Arp 193 are the only galaxies where kinematic models of the CO emission indicate a rotating ring rather than a filled disk gas distribution (DS98).

Its low-J CO lines (J=1–0, 2–1, 3–2) indicate a well-excited low-J CO SLED ($r_{21}=1.06$, $r_{32}=0.80$) expected for a starburst while the large $R_{10}=15$ and $R_{21}\gtrsim 18$ are typical for merger systems. Two ranges of one-phase LVG solutions that can be found for $T_{\text{kin}}/T_{\text{dust}}\geq 1$ (with $T_{\text{dust}}=40\text{ K}$) namely: $[T_{\text{kin}}, n, K_{\text{vir}}]=[(40 - 50)\text{ K}, 3 \times 10^3\text{ cm}^{-3}, 7]$ and $[T_{\text{kin}}, n, K_{\text{vir}}]=[(80 - 140)\text{ K}, 10^3\text{ cm}^{-3}, 4]$, with the best ones obtained for $T_{\text{kin}}=45\text{ K}$ and 115 K respectively. Both also reproduce the CO J=6–5 line luminosity with $r_{65}^{(\text{lv})}\sim 0.15$ (observed value: 0.18 ± 0.055).

The resulting X_{co} factors are: $X_{\text{co}}=0.75 X_1$ (for $T_{\text{kin}}=45\text{ K}$) and $0.60 X_1$ (for $T_{\text{kin}}=115\text{ K}$), yielding a total molecular gas mass of $M_{\text{tot}}=(3.8\text{--}4.80)\times 10^9 M_{\odot}$. The minimum such mass needed for Eddington-limited SF is $M_{\text{SF}}=2.6\times 10^9 M_{\odot}$, which is $\sim 54\%$ – 68% of M_{tot} . As in UGC 05101 the aforementioned large fraction of molecular gas mass directly involved in star formation in IRAS 10565+2448 is corroborated by a high HCN/CO J=1–0 brightness temperature ratio of $r_{\text{HCN/CO}}\sim 0.17$ (Gao & Solomon 2004). However all the 1-phase LVG solutions obtained are hardly representative of a dominant dense and self-gravitating gas phase but more typical of the “cloud-envelope” warm and diffuse gas often found in the ISM of mergers. Moreover all one-phase LVG fits fail to reproduce the $R_{21}\gtrsim 18$ lower limit, with $R_{21}^{(\text{lv})}=12$ being the highest value obtained (for the $T_{\text{kin}}=115\text{ K}$ solution). A 2-phase model with an assumed (h)-phase alleviates this and yields an (l)-phase with $T_{\text{kin}}=65\text{ K}$, $n=10^3\text{ cm}^{-3}$, and $K_{\text{vir}}=13$ that has $R_{21}\sim 20$ and $X_{\text{co}}^{(\text{l})}=0.4 X_1$. The computed $X_{\text{co}}^{(2\text{-ph})}\sim 0.75 X_1$ is within the range of the one-phase values, a result of the low $X_{\text{co}}^{(\text{l})}$, the large luminosity contribution of the (l)-phase ($\rho_{\text{co}}^{(\text{l-h})}\sim 4.5$), and the modest $X_{\text{co}}^{(\text{h})}=2.2 X_1$ of the (h)-phase (see 2.4).

Setting constraints on the (h)-phase and $X_{\text{co}}^{(\text{h})}$ by using the observed CO J=3–2, 6–5 and ^{13}CO J=1–0 lines (assumed emanating mostly from that phase), does not change the aforementioned picture, at least when it comes to the values of $X_{\text{co}}^{(2\text{-ph})}$. Indeed while the corresponding LVG models do recover dense gas solutions ($n\sim 10^4\text{ cm}^{-3}$), substantial K_{vir} values (~ 13) keep the corresponding $X_{\text{co}}^{(\text{h})}$ well below Galactic. In this model the (l)-phase contribution, and thus the influence of $X_{\text{co}}^{(\text{l})}$ on the $X_{\text{co}}^{(2\text{-ph})}$, is negligible. We must stress however that other high-J CO line observations, and crucially multi-J HCN observations are necessary to confirm this picture. If luminous such lines were to be discovered for this ULIRG, they could substantially raise $X_{\text{co}}^{(\text{h})}$ and thus $X_{\text{co}}^{(2\text{-ph})}$ as discussed in 3.2.

B.14. Arp 299

This is a spectacular merger of two galaxies, IC 694 and NGC 3690, with luminous CO J=1–0 emission detected in the nuclei of both (which are $22'' - 4.4$ kpc, apart), and the interface between them (Sargent et al. 1987; Sargent & Scoville 1991). A long HI tidal tail is also seen extending out to ~ 180 kpc (Hibbard & Yun 1999). Along with the Antennae galaxy this (U)LIRG has been considered an early template for mergers, documenting their ability to rapidly funnel the gas in the disks of the progenitors into compact regions (Sargent & Scoville 1991). Indeed the two nuclei in Arp 299 contain $\sim 80\%$ of its molecular gas reservoir, fueling intense star-formation, while the nucleus of IC 694 contains also an AGN (Sargent & Scoville 1991 and references therein), and is the primary source of the bolometric luminosity of this spectacular system (Charmandaris et al. 2002). The most detailed molecular line study of this template merger system is the interferometric study of CO, ^{13}CO and HCN J=1–0 line emission by Aalto et al. 1997 which finds most of the HCN-bright emission located in compact regions ($\lesssim 310$ pc) in the two nuclei of the merging galaxies, and unusually large CO/ ^{13}CO line ratio variations (from ~ 60 in the IC 694 nucleus, to $\sim 5-10$ in its disk). Actually the state of the gas in the IC 694 nucleus with the largest HCN/CO *and* CO/ ^{13}CO ratios *exemplifies the effects of highly turbulent environments found in mergers*, with much of the molecular gas mass “resettled” at high densities (boosting the HCN/CO ratio) while the violent disruption of GMCs creates a diffuse warm and highly unbound “envelope” phase dominating the low-J CO lines (boosting the CO/ ^{13}CO ratios).

While we have no CO J=6–5 measurements for this galaxy (too extended for the narrow JCMT beam at 690 GHz) our CO J=3–2 and J=4–3 measurements indicate high CO line excitation. A one-phase LVG model of the global CO (3–2)/(1–0), (4–3)/(1–0) and CO/ ^{13}CO J=1–0 line ratios gives the best fit for $T_{\text{kin}}=30$ K, $n=10^4$ cm^{-3} and $K_{\text{vir}}=40$ which indicates strongly unbound gas motions. Other average gas states are also possible (e.g. $T_{\text{kin}}=40$ K, $n=3 \times 10^3$ cm^{-3} and $K_{\text{vir}}=22$) but all have $K_{\text{vir}} \gtrsim 22$. The corresponding X_{co} factor over the LVG solution range is $X_{\text{co}}=(0.35-0.42) X_1$, with the largest value corresponding to the dense gas solution. These yield $M_{\text{tot}} \sim (1-1.2) \times 10^9 M_{\odot}$ while $M_{\text{SF}} \sim 1.9 \times 10^9 M_{\odot}$, which clearly favors the higher X_{co} values and indicates that $\sim 100\%$ of the molecular gas mass is associated with SF sites. Larger values of X_{co} (and M_{tot}) remain possible however if most of the molecular gas mass in Arp 299 is contained in the HCN-bright phase with large X_{HCN} factors. Multi-J CO, ^{13}CO and HCN, H^{13}CN line imaging would be ideal in determining this as a function of position within a template merger whose ISM conditions seem to encompass the full range possible, from quiescent disks to compact starburst nuclei.

B.15. IRAS 12112+0305

This ULIRG consists of a strongly interacting pair of galaxies whose nuclei are $\sim 2.9''$ (~ 4 kpc) apart (Carico et al. 1990; Scoville et al. 2000), while tidal tails and “plumes” are visible both in optical (Surace et al. 2000) and near-IR (Scoville et al. 2000) wavelengths. CO J=1–0 interferometry finds the bulk ($\sim 75\%$) of the emission emanating from the NE nucleus of this system (Evans et al. 2002), which is unresolved with a size of $\lesssim 2''$ ($\lesssim 2.7$ kpc), and also the only one tentatively detected in CO J=6–5 (see Paper I). Thus our one-phase LVG radiative transfer modeling pertains only to the NE nucleus of this strongly interacting system. The observed $r_{32}=1.58$ ratio is the second highest in our sample (the highest one found in another double nuclei system: IRAS 22491-1808) and indicates the presence of high-excitation molecular gas. This surpasses the corresponding ratio of the SF “hot-spots” in the Orion molecular cloud, while the $r_{32}>r_{21}$ inequality is another indication of a qualitatively different CO SLED, irreducible to a mixture of SF and SF-quiescent gas (see Paper I).

All one-phase LVG solutions for IRAS 12112+0305 indicate average gas states with $n \sim (3 \times 10^4 - 10^6) \text{ cm}^{-3}$. Nevertheless lack of ^{13}CO line observations leaves serious degeneracies with e.g. $[T_{\text{kin}}(\text{K}), n(\text{cm}^{-3}), K_{\text{vir}}] = [60, 10^5, 13], [125, 10^4, 1]$ being nearly equivalent. The corresponding $X_{\text{co}} \sim (1.5-5.3) X_1$, with *Galactic values of $\sim (4-5) X_1$ obtained for the warmest ($= (120-150) \text{ K}$) and densest ($= (10^5-10^6) \text{ cm}^{-3}$) states.* The presence of such high densities is corroborated by a high HCN/CO J=1–0 ratio of $r_{\text{HCN/CO}}=0.16$ (HCN from Gracia-Carpio et al. 2008, CO from Paper I), though without offering any constraints on the temperatures of the dense gas or its all-important kinematic state. However even the warmest and densest one-phase solutions remain rather poor fits of the “hot” $r_{32} \sim 1.6$ and comparatively “cooler” $r_{21} \sim 0.9$ ratio. Indicatively such a solution ($n=10^6 \text{ cm}^{-3}$) with $T_{\text{kin}}=150 \text{ K}$ and $K_{\text{vir}}=4$ yields $r_{32} \sim r_{21} \sim 1$ as the high density, and modest K_{vir} act to keep the CO lines well-thermalized but also optically thick up to high-J levels.

A two-phase model of the global CO line ratios in this intriguing ULIRG cannot use an Orion-derived (h)-phase CO SLED as the observed $r_{32} > r_{32}^{(\text{h})}$ (Orion). Using only the CO (3-2)/(2-1) ratio $r_{32/21}=1.76 \pm 0.48$ to constrain the high-excitation (h)-phase yields: $n=3 \times 10^4 \text{ cm}^{-3}$, $K_{\text{vir}}=22$, and $T_{\text{kin}} \gtrsim 140 \text{ K}$ (for $T_{\text{kin}}=140 \text{ K}$, $r_{32/21}^{(\text{avg})}=1.28 \sim r_{32/21} - \sigma$), with a fit that keeps improving past $T_{\text{kin}}=200 \text{ K}$ (where $r_{32/21}=1.41$). This is expected since $r_{32/21} > 1$ indicates a thermalized J=3–2 line (and thus $n \gtrsim n_{\text{crit},3-2} \sim 10^4 \text{ cm}^{-3}$), with low/modest optical depths (ensured in part by the large K_{vir}), and warm enough gas to populate the J=3 level. The molecular gas mass of this phase can be estimated from $L_{\text{CO}(1-0)}^{(\text{h})'} = (1/r_{32}^{(\text{h})}) L'_{\text{CO}(3-2)} \sim 4 \times 10^9 L_1$ (where $r_{32}^{(\text{h})} \sim 4$) and the computed $X_{\text{co}}^{(\text{h})} \sim 1 X_1$, thus $M_{\text{h-ex}}(\text{H}_2) \sim 4 \times 10^9 M_{\odot}$, and similar to that needed to fuel an Eddington-limited SF in this ULIRG of $M_{\text{SF}}(\text{H}_2) \sim 5 \times 10^9 M_{\odot}$. For the (l)-phase $L_{\text{CO}(1-0)}^{(\text{l})'} \sim 6.1 \times 10^9 L_1$ luminosity there are no constraints on its corresponding $X_{\text{co}}^{(\text{l})}$

factor. Setting $X_{\text{co}}^{(l)} = (0.5-5) X_1$ yields $X_{\text{co}}^{(2-\text{ph})} = (0.7-3.4) X_1$ and a corresponding $M_{\text{tot}} \sim (7.1-34.3) \times 10^9 M_{\odot}$. Multi-J HCN and H^{13}CN as well as ^{13}CO line observations are critical for reducing the degeneracies of the radiative transfer models for the dense and the low-excitation gas, and their X_{co} factors.

B.16. Mrk 231

This is an archetypal ULIRG/QSO and the most IR luminous galaxy in the Revised IRAS Bright Galaxy Survey (RBGS; Sanders et al. 2003). It has a compact nucleus, surrounded by irregular incomplete rings of star formation along with a small tidal arm that contains numerous blue star-forming ‘knots’ (Farrah et al. 2003 and references therein). It has large amounts of molecular gas in a compact ($0.85''$, 700 pc) nearly face-on disk (Bryant & Scoville 1996; DS98) which allows nearly unobscured view towards an optically luminous AGN which classifies this object also as a Seyfert 1 galaxy. Mrk 231 was also the first ULIRG for which high-J CO lines (J=4–3, 6–5) were detected (Papadopoulos et al. 2007) while recent SPIRE/FTS observations with the HSO revealed luminous high-J CO lines up to J=13–12 emanating from AGN-induced X-ray Dissociated Regions (XDRs) (van der Werf et al. 2010). Its well-excited high-J CO lines, the largest HCN/CO J=1–0 ratio ($r_{\text{HCN/CO}} \sim 0.29$) observed among ULIRGs (Papadopoulos et al. 2007), and a very high CO/ ^{13}CO J=2–1 ratio exemplify the extraordinary *average* molecular gas states possible in such systems (similar to the IC 694 core in the Arp 299 merger system). Finally the availability of HCN J=4–3, 1–0 measurements along with the high-J CO lines allowed a detailed study of its dense gas phase (Papadopoulos et al. 2007), and make Mrk 231 a good case study for the effects of the large $M(n > 10^4 \text{ cm}^{-3})/M_{\text{tot}}$ fractions on the global X_{co} of ULIRGs.

A one-phase LVG fit predictably fails to converge on any average state as it cannot accommodate both the high densities needed to excite the CO J=3–2, 4–3, and 6–5 lines *and* maintain the very low optical depths needed for reproducing the very large $R_{10}=47$ ratio. Indicatively the best one-phase LVG solutions: $T_{\text{kin}} = (115-150) \text{ K}$, $n \sim (300-10^3) \text{ cm}^{-3}$ and $K_{\text{vir}} = 7-40$ yield $r_{21}^{(\text{lv})} \sim 0.83-1.1$ (obs= 0.89 ± 0.12), $r_{32}^{(\text{lv})} \sim 0.5-0.7$ (obs= 0.72 ± 0.13), $r_{43}^{(\text{lv})} \sim 0.22-0.3$ (obs= 0.8 ± 0.2) and $r_{65}^{(\text{lv})} \sim 0.03$ (obs= 0.42 ± 0.12 , but not used for the LVG fit), while $R_{21}^{(\text{lv})} = 25-32$ (obs= 47 ± 16). Thus the average ISM state deduced by a one-phase LVG model can be responsible for up to J=3–2 (and the ^{13}CO J=2–1) line emission but severely underpredicts the CO J=4–3, and 6–5 line luminosities. The corresponding $X_{\text{co}} \sim (0.25-0.45) X_1$ is low but within what was thought as the ULIRG-appropriate range (for Mrk 231 DS98 give $X_{\text{co}} \sim (0.7-0.8) X_1$). These yield $M_{\text{tot}} \sim (1.8-3.2) \times 10^9 M_{\odot}$, but a minimum $M_{\text{SF}} = 5.5 \times 10^9 M_{\odot}$ clearly favors the higher M_{tot} (and X_{co}) among those computed with the one-phase model.

For a 2-phase model we use the results by Papadopoulos et al. 2007 of warm ($\sim(85-140)$ K), diffuse gas ($\sim 300 \text{ cm}^{-3}$) that is highly unbound ($K_{\text{vir}} \gg 1$), and dense gas ($\sim(1-3) \times 10^4 \text{ cm}^{-3}$, $T_{\text{kin}}=(40-70)$ K) responsible for the bright CO J=6–5, HCN J=1–0, 4–3 lines. The latter phase is virialized with $X_{\text{HCN}} \sim (10-25) X_1$ (for our numerical factor in Equation 3 rather than the one in Papadopoulos et al. 2007) and $r_{\text{CO/HCN}}^{(\text{h})} \sim 2-2.54$ (high value corresponding to the lower X_{HCN} values). Thus $X_{\text{co}}^{(\text{h})} = (1/r_{\text{CO/HCN}}^{(\text{h})}) X_{\text{HCN}} \sim (3.94-12.5) X_1$ while for the diffuse and HCN-dark phase: $X_{\text{co}}^{(\text{l})} \sim (0.4-1) X_1$. For an $r_{\text{CO/HCN}}^{(\text{obs})} = 3.45$ we then find $\rho_{\text{co}}^{(\text{l-h})} \sim 0.36-0.73$ (yielding $X_{\text{co}}^{(\text{h})} = (3.94-12.5) X_1$), and an $X_{\text{co}}^{(2-\text{ph})} \sim (3-7) X_1$ (for the smallest $X_{\text{co}}^{(\text{l})}$). Thus *a Galactic X_{co} factor applies in Mrk 231*, a result of a large mass of dense gas with high $X_{\text{co}}^{(\text{h})}$ values, themselves a result of the high gas densities *and* their virial dynamical states.

B.17. Arp 193

This galaxy is a template of a young merger-induced starburst with an age of $\text{few} \times 10^7$ yr and near-IR imaging showing a highly dust-enshrouded nucleus, and tidal tails (Smith et al. 1995). A disturbed highly inclined disk is also seen in NICMOS near-IR imaging with reddening increasing towards the NW within the disk (Scoville et al. 2000), and a similar extinction distribution implied by a CO J=1–0 interferometer map (Bryant & Scoville 1999). Extended radio continuum emission ($\sim 3'' \times 3.7''$) is seen at cm wavelengths with two nuclei $\sim 1''$ apart and a spectral index of $\alpha \sim 0.6$ ($S_\nu \propto \nu^{-\alpha}$), consistent with SF-related non-thermal synchrotron emission (Clements & Alexander 2004). The latter study also finds significant decoupling of the HI and CO-bright H_2 gas motions and distributions. The young age of this disk-disk merger/starburst is corroborated by several extra-planar highly luminous star clusters (Scoville et al. 2000) and many bright HII regions (Clements & Alexander 2004).

High S/N CO J=1–0 and 2–1 interferometric imaging confirmed a highly inclined $2.8'' \times 0.8''$ ($\sim 1.3 \text{ kpc} \times 0.37 \text{ kpc}$) gas disk whose CO emission is best fit by a molecular ring (DS98). A compact southeast CO source coinciding with the secondary cm continuum emission peak in Arp 193 has the properties of a giant molecular core, and is much warmer and denser than the rest of the disk. Along with a region in Mrk 273, and the western nucleus of Arp 220 (DS98), it is one of the most extreme SF regions in the local Universe, forming stars very near or at the Eddington-limit set by the radiation pressure from young massive stars on the dust of the dense molecular gas (i.e. $L_{\text{IR}}/M_{\text{dense}}(\text{SF-region}) \sim (250-500) L_\odot/M_\odot$). One-phase LVG solutions to its CO line ratios yield low-density solutions with $n \sim (1-3) \times 10^3 \text{ cm}^{-3}$ but large temperature degeneracies with $T_{\text{kin}} = 40$ K, (60-75) K, (80-115) K and corresponding $K_{\text{vir}} = 22, 4$ and 13 values. Warmer solutions with $T_{\text{kin}} = (120-150)$ K and even larger $K_{\text{vir}} (=40)$

values also exist. Considering only the gas states with $K_{\text{vir}} \lesssim 20$ yields $X_{\text{co}} \sim (0.35-0.75) X_1$ and $M_{\text{tot}} \sim (1.6-3.5) \times 10^9 M_{\odot}$, with the highest X_{co} (and M_{tot}) values corresponding to the states with the smallest K_{vir} . The minimum molecular gas mass for an Eddington-limited star formation is $M_{\text{SF}} \sim 0.9 \times 10^9 M_{\odot}$.

A young starburst and the strong SF feedback expected in such extreme SF events could be responsible for Arp 193 being the only LIRG where, despite a large SF-powered IR luminosity ($\sim 2.2 \times 10^{11} L_{\odot}$) and HCN/CO J=1–0 ratio (~ 0.044 , with HCN J=1–0 from Carpio-et al. 2008, and CO J=1–0 from Paper I), the average state of its molecular ISM, is compatible with a complete absence of a dense molecular gas reservoir (Papadopoulos 2007). This is indicated by its low HCN (4–3)/(1–0) and (3–2)/(1–0) line ratios of $r_{43} \lesssim 0.12$ (3σ) and $r_{32} = 0.22 \pm 0.03$ (Papadopoulos 2007; Gracia-Carpio et al. 2008). Using them as constraints yields a narrow temperature range of dense gas solutions with $T_{\text{kin}} = (50-60) \text{ K}$, $n = 3 \times 10^4 \text{ cm}^{-3}$ and $K_{\text{vir}} = 14$ (rather large for a dense gas phase). The widest range of solutions is at: $T_{\text{kin}} = (65-95) \text{ K}$, $n = 3 \times 10^3 \text{ cm}^{-3}$ and $K_{\text{vir}} \sim 1$. Unlike the former set of solutions the latter reproduces also the CO(3-2)/HCN(1-0) line ratio of $\sim 17 \pm 4$ (which can be reasonably assumed as an additional constraint on the denser SF gas phase²). Using the upper limit of the HCN(4–3)/(1–0) ratio as a detection (as to obtain the densest possible LVG solutions) only pushes the aforementioned set of dense gas solutions to $T_{\text{kin}} = (90-105) \text{ K}$, while the lower density/virial ones are now found at $T_{\text{kin}} = (110-150) \text{ K}$ (both sets of solutions can now reproduce the CO(3-2)/HCN(1-0) ratio).

For a 2-phase model where the HCN-bright gas is set as the (h)-phase we obtain $X_{\text{co}}^{(2\text{-ph})} \sim (0.70-1.75) X_1$ (with the low values corresponding to the dense/unbound solutions). This is $\sim (0.9-2) \times X_{\text{co}}(\text{DS98})$, and yields $M_{\text{tot}} \sim (3.3-8.1) \times 10^9 M_{\odot}$. Thus Arp 193 stands as a case where multi-J line observations of high-density tracers such as HCN do not significantly change the picture obtained by the low-J CO lines regarding the global X_{co} factor. This may be because this LIRG is a rare merger, “caught” in the act of having momentarily dispersed/consumed its dense gas mass while still having large SF-powered IR luminosities, a brief state of affairs expected because of SF-feedback during the evolution of merger starbursts (Loenen 2009). We note however high-resolution CO imaging revealing the “excess” CO J=1–0 line emission of the (l)-phase to be a cold SF-quiescent phase can still push the global X_{co} towards near-Galactic values via a higher $X_{\text{co}}^{(l)}$.

²the non-detection of CO J=6–5 in this LIRG is likely due to a pointing offset of the JCMT

B.18. NGC 5135

Optical and near-IR *HST* observations reveal this Sy2 galaxy to be a grand design spiral with star formation across its arms but being most intense in its central ~ 1 kpc (Martini et al. 2003). The inner 1.6 kpc is also where most of its cm radio continuum emerges (Condon et al. 1996). Optical and UV studies by Gonzalez Delgado et al. (1998) reveal a young nuclear starburst with gas likely provided by a bar instability. Its HCN/CO J=1–0 line ratio of ~ 0.087 (Gao & Solomon 2004), while not as high as in ULIRGs, it is nevertheless $\sim (3-4) \times$ higher than in spiral disks. This indicates a significant dense gas mass fraction, even in the absence of a strong merger and/or galaxy interaction. Lack of the latter makes the large $R_{10}=26$ and $R_{10}=13$ measured in NGC 5135 an exception as these are typical mostly in mergers. Interestingly this galaxy is known for powerful gas outflows of hundreds of km/s, driven by its young starburst (Gonzalez Delgado et al. 1988).

One-phase models of its CO line ratios yield $[T_{\text{kin}}, n, K_{\text{vir}}]=[(30-40)\text{K}, 3 \times 10^3 \text{ cm}^{-3}, 22]$, with warmer (but also more degenerate) solutions such as: $[(60-110)\text{K}, 10^3 \text{ cm}^{-3}, 13]$ also remaining possible. For the entire range of solutions the corresponding $X_{\text{co}} \sim (0.35-0.45) X_{\text{I}}$, similar to $X_{\text{co}}^{(\text{thin})}$ (LTE) for $T_{\text{kin}}=(30-70)$ K (the temperatures of the best solutions), as expected for the low/modest optical depths of the LVG solutions. For these X_{co} values $M_{\text{tot}}=(1.1-1.4) \times 10^9 M_{\odot}$ while $M_{\text{SF}}=3 \times 10^8 M_{\odot}$, which corresponds to $\sim 20\%-30\%$ of the total molecular gas mass. Nevertheless, with the distribution of the molecular gas unknown, a Galactic X_{co} for disk-distributed gas not intimately involved with star-formation remains a distinct possibility. In such a case the true X_{co} and M_{tot} can easily be $\sim (10-15)$ times higher, reducing $M_{\text{SF}}/M_{\text{tot}}$ to only few%, and more typical of spiral disks. As described in 3.4 CO line imaging observations rather than global CO SLEDs can be used to determine the existence of such a cold molecular gas disk.

B.19. Mrk 273

This extraordinary ULIRG shows up as a double-nuclei system in NICMOS near-IR observations where the nuclei are only $\sim 1''$ (740 pc) apart (Scoville et al. 2000). A strikingly long tidal tail ($\sim 1'$, 44 kpc) as well as a decoupling of stellar and gas motions (Tacconi et al. 2002) are the telltale signatures of a strong merger. Its northern nucleus contains a compact hard X-ray luminous Sy2 AGN (Xia et al. 2002), but the dust emission SED of this ULIRG is dominated by a starburst (Farrah et al. 2003). This galaxy actually contains the most extreme starburst region among all ULIRGs imaged in the DS98 study, with an IR luminosity of $\sim 6.7 \times 10^{11} L_{\odot}$ emanating from its core of only $\sim 0.35'' \times (<0.2'')$ ($260 \text{ pc} \times (<149 \text{ pc})$) diameter. This makes the compact nuclear CO line source of Mrk 273

akin to the west nucleus of Arp 220, and along with Arp 193 these three ULIRGs host the most prodigious SF events in the local Universe (DS98). For the core of Mrk 273 the IR brightness is: $\sigma_{\text{IR}} \sim L_{\text{IR}} / (\pi R_{\text{co}}^2) \sim 10^{13} L_{\odot} \text{ kpc}^{-2}$, i.e. the Eddington limit for radiation-pressure-regulated star formation (Thompson 2009). In the framework of an Eddington-limited SF this makes the compact nuclear starburst in Mrk 273 a maximal SF event, and its astounding CO linewidth of $\sim 1060 \text{ km s}^{-1}$ (DS98) may be a direct outcome of radiation pressure becoming dynamically important as to affect bulk gas motions.

The global CO line ratios, while typical of a star-forming ISM they are not typical of an extreme starburst as Mrk 273 certainly is. The $R_{21} = 7 \pm 2$ ratio in particular is low, found mostly for GMCs in SF-quiet spirals ($R_{21} \geq 20$ is observed for extreme starbursts). The compact starburst core of Mrk 273 is surrounded by extended CO line emission ($\sim 3''$ - $7''$, i.e. $(2.2$ - $5.1) \text{ kpc}$, DS98) where ordinary star-forming and even SF-quiet ISM could be containing significant fractions of the total molecular gas mass. The optimum LVG solutions obtained for the global CO ratios are: $[T_{\text{kin, n}}, K_{\text{vir}}] = [30$ - $70, 3 \times 10^2, 1]$. Apart from the elevated temperatures such conditions are typical of Galactic GMCs, while the $X_{\text{co}} \sim 2 X_1$ of the best LVG solution (at $T_{\text{kin}} = 45 \text{ K}$) is higher than the so-called ULIRG value ($\sim 0.8 X_1$). The corresponding $M_{\text{tot}} \sim 10^{10} M_{\odot}$ while a minimum mass of $M_{\text{SF}} \sim 3.3 \times 10^9 M_{\odot}$ is needed to fuel an Eddington-limited star formation in this system.

The total molecular gas mass of Mrk 273 can be higher still if the mass contributions of a colder low-density and SF-quiet phase, and a warmer denser SF one are accounted separately. A clear indication of a highly-excited SF gas phase is given by the CO J=6–5 line which, while not as bright as in some other (U)LIRGs (e.g. Mrk 231, NGC 6240), yields a r_{65} that is $\sim 5 \times$ higher than that anticipated from the best LVG fit of the lower-J CO lines. A high HCN/CO J=1–0 ratio of $r_{\text{HCN/CO}} = 0.14$ (using the CO J=1–0 value from Paper I and the HCN J=1–0 from Carpio et al. 2008) and a well-excited HCN J=3–2 line with $r_{32}(\text{HCN}) = 0.49 \pm 0.11$ (Gracia-Carpio et al. 2008) offer more evidence for the presence of a dense gas phase. A two-phase decomposition using only the CO 3-2, 6-5 and ^{13}CO J=2–1 lines to constrain the high-excitation phase yields $M_{\text{h-ex}}(\text{H}_2) \sim 6 \times 10^9 M_{\odot}$, and an effective $X_{\text{co}}^{(2\text{-ph})} \sim 2.5 X_1$. The latter yields $M_{\text{tot}}(\text{H}_2) = 1.3 \times 10^{10} M_{\odot}$, of which $\sim 53\%$ correspond to the low CO brightness (l)-phase. Thus despite its spectacular starburst, Mrk 273 is an example of a ULIRG that contains also large amounts of cooler low CO-excitation gas. Use of the two available HCN lines to determine the properties of the (h)-phase does not change this picture, and can actually raise $X_{\text{co}}^{(2\text{-ph})}$ up to $\sim (4$ - $5.5) X_1$.

B.20. 3C 293

This powerful radio galaxy was the first F-R II source (i.e with edge-brightened radio lobes, see Fanaroff & Riley 1974) to be detected in CO locally ($z=0.046$), revealing large amounts of molecular gas distributed in a rotating disk of $7''$ (~ 6.2 kpc) centered in its nucleus, and with a large CO linewidth of $\sim 900 \text{ km s}^{-1}$ (Evans et al. 1999). Its disturbed morphology maybe due to an interaction with a companion galaxy $\sim 40''$ (35 kpc) to the southwest, while a powerful optical/IR-luminous jet interacts with the ambient ISM (Floyd et al. 2006). The SF efficiency of the galaxy is low ($\sim 8 L_{\odot}/M_{\odot}$) and along with a $\text{SFR} \sim (6-7) M_{\odot} \text{ yr}^{-1}$ it is typical of ordinary spirals. The modest global CO $r_{21}=0.74$ and $r_{32}=0.44$ ratios (Paper I) are also consistent with a SF-quiescent ISM. Thus the high excitation levels of the CO J=4–3, and 6–5 discovered in this system were certainly a surprise. Their interpretation as due to an AGN-driven jet-ISM interaction provided the first known example where “mechanical” AGN feedback globally affects galaxy-size molecular gas reservoirs (Papadopoulos et al. 2008, 2010b), though similar examples with lower-power AGN and much smaller molecular gas reservoirs have been reported much earlier (Matsushita et al. 2004).

The physical conditions compatible with the luminous CO J=4–3, 6–5 lines were studied in detail by Papadopoulos et al. 2010b (see their Table 4) where dense ($\sim 3 \times (10^4-10^5) \text{ cm}^{-3}$), warm $T_{\text{kin}} \sim (75-300) \text{ K}$ and strongly unbound $K_{\text{vir}} \sim 15-50$ states have been deduced. The corresponding $X_{\text{co}}^{(\text{h})} \sim (0.8-1.5) X_{\text{I}}$, with computed $r_{43}^{(\text{h})} = 2-3.2$ and $L_{10}^{(\text{h})'} = (1/r_{43}^{(\text{h})}) \times L'_{43} = (1.46-2.33) \times 10^9 L_{\text{I}}$. This AGN-excited gas will have $M_{\text{h-ex}} \sim (1.1-3.5) \times 10^9 M_{\odot}$, much higher than the $M_{\text{SF}} \sim 5 \times 10^7 M_{\odot}$ of warm and dense gas expected fueling its star formation. Setting a Galactic $X_{\text{co}}^{(\text{l})} = 5 X_{\text{I}}$ for the remaining (l)-phase CO J=1–0 luminosity of the SF-quiescent disk phase yields an effective $X_{\text{co}}^{(2\text{-ph})} = (2.9-3.9) X_{\text{I}}$, which are near-Galactic values. Indicatively, a one-phase fit of only the CO 1–0, 2–1, and 3–2 lines (any LVG fit including the CO J=4–3 and/or J=6–5 predictably fails) yields maximum values of $X_{\text{co}} = (1.2-1.6) X_{\text{I}}$, obtained for the solutions with the lowest K_{vir} values ($\sim 2-4$), but values as low as $X_{\text{co}} \sim 0.5 X_{\text{I}}$ also probable.

B.21. IRAS 14348–1447

This is an impressive ULIRG/merger of two gas-rich spirals with their two nuclei $3.4''$ (5.2 kpc) apart, and clear indications of tidal features and strongly disrupted disks seen in *HST* optical and near-IR NICMOS images (Evans et al. 2000; Scoville et al. 2000). Interferometric imaging of CO J=1–0 has shown that both nuclei contain copious amounts of molecular gas but remain unresolved with size $\lesssim 2.5''$ (3.8 kpc) (Evans et al. 2000). Using radio continuum measurements to obtain size estimates for the two star-forming cores of this ULIRG yields very compact regions with diameters of $D \sim 200 \text{ pc}$ (Condon et al. 1991),

similar to the compact molecular gas disks found in Arp 220 and Mrk 231 (DS98).

The observed CO J=1–0, 2–1, 3–2 and ^{13}CO J=2–1 lines (Paper I) are compatible with a wide range of conditions having $T_{\text{kin}} \gtrsim 35$ K with the best ones found for $T_{\text{kin}}=(40-85)$ K, $n=10^3 \text{ cm}^{-3}$, and $K_{\text{vir}}=4$. Quite unlike most merger/ULIRGs, all good LVG solutions correspond to $K_{\text{vir}} \sim 1-4$. Nevertheless $X_{\text{co}} \sim (0.65-1) X_1$, i.e. much lower than Galactic. The corresponding $M_{\text{tot}} \sim (1.1-1.74) \times 10^{10} M_{\odot}$ while the minimum mass needed for Eddington-limited star-formation is $M_{\text{SF}} \sim 5.6 \times 10^9 M_{\odot}$, which amounts to $\sim 30\%-50\%$ of the total molecular gas mass. In IRAS 14348-1447, as in other ULIRGs, such high mass fractions of what is presumably a dense and warm gas phase are not reflected by the global CO SLED and ^{13}CO lines available, dominated by lower-density gas. Unfortunately neither high-J CO nor HCN line observations exist for this ULIRG to set independent constraints on the mass and physical properties of its dense SF molecular gas. A 2-phase model with an assumed (h)-phase CO SLED (section 2.4), while not necessary in this case (as a wide range of good one-phase fits exist), can be used to assess the impact of a massive dense gas phase on X_{co} . Apart from $n \lesssim 10^3 \text{ cm}^{-3}$ the (l)-phase remains essentially unconstrained (as expected), with $X_{\text{co}}^{(l)} \sim (0.5-1.12) X_1$. For the computed $\rho_{\text{co}}^{(l-h)}=0.85$ this yields $X_{\text{co}}^{(2-ph)}=(1.4-1.7) X_1$.

B.22. Zw 049.057

This galaxy has a SF-powered $L_{\text{IR}}^{(*)} \sim 1.2 \times 10^{11} L_{\odot}$ typical for SF spiral disks (e.g. NGC 7469) and is one of the lowest IR luminosity galaxies in the IRAS *BGS*. NICMOS near-IR imaging with the *HST* indeed show a highly inclined disk-dominated system with a heavily dust-enshrouded nucleus (Scoville et al. 2000). Despite its disk-like appearance its near-IR emission is better fitted by a $r^{1/4}$ rather than an exponential disk profile (Scoville et al. 2000), while its $L_{\text{IR}}/L_{\text{B}}$ ratio is almost as extreme as the much more IR-luminous Arp 220 (Planesas et al. 1991). Early interferometric images of CO J=1–0 found large molecular gas mass within a 1.3 kpc-sized region (Planesas et al. 1991, for the cosmology adopted here).

Its CO SLED remains well excited up to J=4–3 and also has substantial J=6–5 emission (see Paper I) while both its ^{13}CO J=1–0, 2–1 lines are detected and yield $R_{10} \sim 16$ and $R_{21} \sim 24$, typical of merger-driven starbursts rather than disk-dominated LIRGs. One-phase LVG models reproduce all CO, ^{13}CO line ratios up to CO J=4–3 though they still underpredict the luminosity of the latter by $\sim 1.2\sigma$. Unfortunately, even with this large set of lines significant degeneracies remain. Indicatively the two best solutions: $[T_{\text{kin}}, n, K_{\text{vir}}]=[35, 3 \times 10^3, 22]$, $[105, 10^3, 13]$ yield CO line ratios: $[r_{21}, r_{32}, r_{43}, r_{65}, R_{10}, R_{21}]_{\text{lvG}}=[1.05, 0.75, 0.41, 0.05, 22, 21]$, $[1.05, 0.76, 0.40, 0.02, 21, 16]$. Much warmer gas with $[T_{\text{kin}}, n, K_{\text{vir}}]=[130 - 140, 10^3, 4]$ is also possible and yields: $[r_{21}, r_{32}, r_{43}, r_{65}, R_{10}, R_{21}]_{\text{lvG}}=[1.06, 0.86, 0.60, 0.17, 14, 13]$, now in

better agreement with the observed r_{65} (even if not used in the fit) but a rather worse fit of R_{21} . Nevertheless the corresponding X_{co} values span a rather narrow range $\sim(0.35\text{-}0.6)X_1$, yielding $M_{\text{tot}}\sim(3\text{-}5.2)\times 10^8 M_{\odot}$. This is comparable to the minimum molecular gas mass required for Eddington-limited star formation of $M_{\text{SF}}(\text{H}_2)\sim 4.7\times 10^8 M_{\odot}$, yet all the densities deduced from the LVG solutions of the global CO SLED are far from being representative of what is typically a much denser SF phase with small/modest K_{vir} values.

A two-phase decomposition of the average ISM state using the CO J=3–2, 4–3, 6–5 and the ^{13}CO transitions to determine the (h)-state converges to $[T_{\text{kin}}, n, K_{\text{vir}}]=[110\text{-}140, 10^3, 4]$, with $T_{\text{kin}}=140\text{ K}$ corresponding to the best solution (and $X_{\text{co}}^{(\text{h})}=0.6 X_1$). Higher density solutions with $n=10^4\text{ cm}^{-3}$ exist over $T_{\text{kin}}=(40\text{-}65)\text{ K}$ but represent poorer fits and correspond to unbound states with $K_{\text{vir}}\sim 13$. This is a general aspect of all (h)-phase LVG solutions (e.g. even if only the CO J=4–3, 6–5 and ^{13}CO lines are used), namely the best fits occur at higher temperatures, lower densities, and more gravitationally bound states. High density solutions ($\sim 10^4\text{ cm}^{-3}$) and thus more typical for the presumably star forming (h)-phase are found at lower temperatures ($\sim(35\text{-}70)\text{ K}$), and strongly unbound states ($K_{\text{vir}}\sim 13\text{-}40$), but yield poorer fits. Moreover the high K_{vir} of the denser/cooler LVG solutions yield similarly low $X_{\text{co}}^{(\text{h})}$ (e.g. for $T_{\text{kin}}=50\text{ K}$, $n=10^4\text{ cm}^{-3}$ and $K_{\text{vir}}\sim 13$ it is $X_{\text{co}}^{(\text{h})}=0.7 X_1$).

It is the combination of weak ^{13}CO J=1–0, 2–1 and well-excited high-J CO lines that nevertheless still have $r_{J+1,J}<1$ which forces LVG solutions to a parameter space with low CO line optical depths and modest gas densities. This is why K_{vir} is high towards the low- T_{kin} /high- n domain (as to keep CO line optical depths low), and why the need for high K_{vir} 's is relaxed towards higher T_{kin} which now becomes partly responsible for the low optical depths. Average gas densities towards the high T_{kin} regime cannot be high as this would yield $r_{J+1,J}>1$ in the optically thin domain. If we omit the CO J=6–5 line from the fit (as its luminosity can be highly uncertain) and also leave out the ^{13}CO J=1–0 line (which may have a larger contribution from a cooler disk phase) we obtain LVG solutions with densities of $\sim(1\text{-}3)\times 10^4\text{ cm}^{-3}$ that are more typical of SF gas, yet with high enough $K_{\text{vir}}\sim 13\text{-}22$ that still yield a low corresponding $X_{\text{co}}^{(\text{h})}\sim(0.65\text{-}0.75) X_1$. Moreover, with an essentially unconstrained (l)-phase, and no evidence for a cold disk, a 2-phase gas would yield $X_{\text{co}}^{(2\text{-ph})}$ similar to that obtained from 1-phase model.

Thus the molecular gas reservoir in this LIRG is expected to be dominated by its SF component, yet neither the average densities nor the strongly unbound dynamical states deduced from its available global CO SLED are typical of the latter. If this is confirmed by future HCN or other heavy rotor molecular line observations (or more high-J CO and ^{13}CO transitions) it may come to resemble the average ISM state deduced for Arp 193.

B.23. Arp 220 and NGC 6240

These are the two (U)LIRGs in our sample that currently have the best molecular line data tracing their dense gas (i.e. multi-J HCN, CS, HCO⁺ lines), which are used in a detailed study of its physical conditions (Greve et al. 2009). The presence of a massive dense gas phase in both of them is well-established with large HCN/CO J=1–0 line ratios (~ 0.19 (Arp 220), ~ 0.08 (NGC 6240)), well-excited HCN and CS higher-J lines, yet also the large CO/¹³CO line ratios typical for merger-driven extreme starbursts (~ 43 -45 for J=1–0). The latter implies very low CO line optical depths, and thus runs counter what is expected for dominant high-density molecular gas reservoir ($\tau_{J+1,J}(\text{CO}) \gg 1$), necessitating the 2-phase models used in such systems (Aalto et al. 1995; Papadopoulos & Seaquist 1998; this work).

Predictably one-phase models of the CO and ¹³CO lines (see Paper I) fail to converge on any good set of solutions for both galaxies, yielding $[T_{\text{kin}}, n, K_{\text{vir}}] = [(30 - 90) \text{ K}, 10^3 \text{ cm}^{-3}, 40]$ (Arp 220) and $[T_{\text{kin}}, n, K_{\text{vir}}] = [(15 - 40) \text{ K}, 3 \times 10^3 \text{ cm}^{-3}, 40]$ (NGC 6240). For Arp 220 even the CO J=1–0, 2–1, 3–2 lines are impossible to fit with one phase since $r_{21} = 0.67 \pm 0.07$ (see Paper I) indicates a diffuse gas phase that leaves even the J=2–1 line subthermally excited, while $r_{21} = 0.97 \pm 0.14$ marks the emergence of another, denser and warmer phase from J=3–2 and higher. The corresponding one-phase $X_{\text{co}} \sim 0.3 X_1$ for both systems, a low value due to the very large K_{vir} values “forced” by the extreme large CO/¹³CO line ratios obtained for these systems. This is comparable to $X_{\text{co}}^{(\text{thin})}$ (LTE) (for the $T_{\text{kin}} = (30-40) \text{ K}$ range of one-phase LVG solutions), as expected for optically thin CO line emission.

This low X_{co} factor yields $M_{\text{tot}} \sim 1.85 \times 10^9 M_{\odot}$ (Arp 220) and $\sim 2.5 \times 10^9 M_{\odot}$ (NGC 6240), while the minimum molecular gas mass needed for fueling Eddington-limited SF in these extreme merger/starbursts is $M_{\text{SF}} \sim 4 \times 10^9 M_{\odot}$ (Arp 220) and $\sim 1.5 \times 10^9 M_{\odot}$ (NGC 6240). Given that $M_{\text{SF}}/M_{\text{tot}} \gtrsim 0.6$, and in the case of Arp 220 actually > 1 , it becomes obvious, even in the absence of heavy rotor molecular line observations that the true X_{co} factor for these two galaxies must be higher. From the analysis detailed in 3.2.1 the multi-J HCN LVG solutions in a 2-phase LVG model yield: $X_{\text{co}}^{(2\text{-ph})} \sim (2.4-4.5) X_1$ (Arp 220) and $X_{\text{co}}^{(2\text{-ph})} \sim (1-3.3) X_1$ (NGC 6240) with the high values corresponding to virial dynamical states for the dense gas. The new M_{tot} estimates are: $\sim (1.5-2.8) \times 10^{10} M_{\odot}$ (Arp 220) and $\sim (0.8-2.8) \times 10^{10} M_{\odot}$ (NGC 6240). In the case of Arp 220 these amount to $\sim 40\%$ - 77% of the dynamical mass of its molecular gas disks (M_{dyn} from DS98), while for NGC 6240 it surpasses the total mass contained within its central radius of $r \lesssim 1''$ (480 pc) and argues for significant molecular gas mass corresponding to the CO line emission seen beyond its central CO J=2–1 peak (see Tacconi et al. 1999 for CO J=2–1 for a high resolution interferometry map). In the latter case the deduced molecular gas mass may actually dominate the mass distribution out to much larger radii than deduced by Tacconi et al. 1999. Multi-J HCN line interferometric maps, along with at

least one H^{13}CN transition, at resolutions of $\lesssim 1''$, will be valuable in determining the X_{HCN} , the effective $X_{\text{CO}}^{(\text{h})}$, and $X_{\text{CO}}^{(2\text{-ph})}$ of these template merger systems.

B.24. IRAS 17208–0014

This classic ULIRG is the most luminous in our sample, it has a compact gas-rich nucleus (Planesas et al. 1991; DS98), a very disrupted disk, and tidal tails indicating a merger (Murphy et al. 1996; Scoville et al. 2000). In the interferometric study by DS98 this is the ULIRG whose compact gas disk (~ 1.4 kpc) has the largest face-on velocity dispersion of $\sigma_{\text{V}} \sim 150 \text{ km s}^{-1}$, indicating a highly turbulent gas environment. This is also suggested by the large $R_{21} \gtrsim 35$ ratio, expected in the high-pressure, highly turbulent ISM environments of strong mergers (Aalto et al. 1995). Its CO SLED is highly excited up to CO J=4–3 while the weak CO J=6–5 reported in Paper I is most likely due to pointing offsets as ZEUS measurements at the CSO indicate a much stronger line (Stacey 2011).

No reasonable one-phase LVG fits were found for this source while attempts to fit the CO J=1–0 up to J=4–3 and $R_{21}=35$ yield highly unbound states ($K_{\text{vir}} \sim 13\text{--}70$). The best such fit: $[T_{\text{kin}}, n, K_{\text{vir}}] = [70, 10^3, 13]$, yields $r_{21}=0.96$, $r_{32}=0.64$, $r_{43}=0.32$, the latter being $\sim 3\times$ smaller than observed. The large $L_{\text{IR}}^{(*)}$ of this system corresponds to $M_{\text{SF}}(\text{H}_2) \sim 6 \times 10^9 M_{\odot}$. On the other hand $X_{\text{CO}} \sim 0.4 X_1$ computed from the best LVG solution yields $M_{\text{tot}} \sim 5.2 \times 10^9 M_{\odot}$, and thus even the minimum mass expected for a dense and warm SF-fueling phase will dominate M_{tot} , as computed by a one-phase X_{CO} factor. One-phase LVG solutions with their low densities, highly unbound dynamical states certainly do not hint this, while their poor fit of the global CO line ratios of this ULIRG suggest that at least two main gas phases are necessary to represent the average ISM state in this system. The presence of a massive gas phase much denser than those implied by one-phase LVG fits is further corroborated by an $r_{\text{HCN/CO}}=0.14$ (HCN J=1–0 from Gracia-Carpio et al. 2008, CO 1-0 from Paper I) and an $\text{HCN}(3\text{--}2)/(1\text{--}0)$ ratio of $r_{32}(\text{HCN})=0.39$ (Gracia-Carpio et al. 2008).

Using only CO J=4–3, 3–2, and $R_{21}=35$ (the lower limit) to constrain the (h)-phase in a 2-phase model yields only warm $T_{\text{kin}}=(90\text{--}150)$ K and dense $n \sim (3 \times 10^4\text{--}10^5) \text{ cm}^{-3}$ gas phases with $K_{\text{vir}} \sim 13\text{--}22$, and $X_{\text{CO}}^{(\text{h})} \sim 0.85\text{--}1.40$ (high values for the denser gas solutions). These solutions yield $r_{\text{J+1,J}}^{(\text{h})} \sim 2.3\text{--}3$ for $\text{J}+1=2,3,4$ indicating CO lines with small/moderate optical depths, a result of the high temperatures and large K_{vir} values which, along with the high densities, are necessary for well-excited CO lines up to high-J levels *and* a high global R_{21} ratio. The mass of such high-excitation gas can be computed from $L_{10}^{(\text{h})'} = (1/\langle r_{43}^{(\text{h})} \rangle) L'_{43} = (4\text{--}4.4) \times 10^9 L_1$ which yields $M_{\text{h-ex}}(\text{H}_2) \sim (3.4\text{--}6) \times 10^9 M_{\odot}$. Thus, as in some other (U)LIRGs studied here (e.g. IRAS 00057+4021), this galaxy contains large reservoirs of dense gas in

thermal and dynamical states much more extreme than those expected for dense gas in SF regions. As detailed in Paper I these could be indicative of other power sources such as turbulent heated regions (THRs) or CR-dominated regions (e.g. Papadopoulos 2010). Future high resolution high-J CO, ^{13}CO imaging of this system with ALMA would be very valuable for confirming and quantifying such mechanisms via determining the level of turbulence present in its disk (i.e. measuring $\sigma_z(\mathbf{r})$ and the average CR energy density permeating its ISM.

Despite the prominence of the dense highly-excited phase in the J=3–2, 4–3 lines, the (l)-phase remains the main contributor of CO J=1–0 line luminosity in IRAS 17208-0014, with $L_{1-0}^{(l)'} \sim (8.7-9) \times 10^9 L_1$ ($\sim(66-68)\%$ of the observed one). LVG fits of the corresponding “residual” ratio $r_{21}^{(l)} \sim 0.5$, while T_{kin} -degenerate (as expected), all indicate low gas densities $n \sim (1-3) \times 10^2 \text{ cm}^{-3}$ and a wide range of $K_{\text{vir}} \sim 1-70$. The corresponding $X_{\text{co}}^{(l)} \sim (0.5-3) X_1$ (over the $K_{\text{vir}}=1-20$ range of LVG solutions) remains essentially unconstrained, with the lowest values corresponding to the most dynamically unbound states as expected. Thus for $X_{\text{co}}^{(h)} = 1.4 X_1$ (densest gas LVG solutions) we find $X_{\text{co}}^{(2-\text{ph})} \sim (0.75-2.5) X_1$.

Using the states compatible with the HCN(3–2)/(1–0) ratio in IRAS 17208–0014 to define the (h)-phase leads to even higher $X_{\text{co}}^{(2-\text{ph})} \sim (2.5-5.9) X_1$, with larger still $M_{\text{h-ex}}$ (see Table 1). These correspond to a high-density ($\sim(3 \times 10^4-10^5) \text{ cm}^{-3}$) phase with $K_{\text{vir}} \sim 1-6$ (unphysical solutions with $K_{\text{vir}} < 1$ were not considered). Nevertheless, for $T_{\text{kin}} = (75-105)\text{K}$, LVG solutions with high-density gas ($\sim 10^5 \text{ cm}^{-3}$) but $K_{\text{vir}} = 20$ are also possible. These strongly unbound dense gas solutions yield $X_{\text{co}}^{(h)} \sim 0.8 X_1$ and similarly low $X_{\text{co}}^{(2-\text{ph})}$ values (unless cold (l)-phase solutions corresponding to a SF-quiescent disk are considered). Observations of more HCN lines and, crucially, of at least one H^{13}CN line can determine whether such extraordinary dynamical states are possible for the HCN-bright dense gas phase (see 3.4).

B.25. IRAS 22491–1808

This is a ULIRG with a spectacular morphology involving two nuclei separated by $1.6''$ ($\sim 2.3 \text{ kpc}$) (Carico et al. 1990), two tidal tails and numerous SF knots embedded in them (Scoville et al. 2000) indicating an advanced merger. It is also one of the very few ULIRGs where an AGN contributes more than half of the total IR luminosity (Farrah et al. 2003). In our sample it stands out as the galaxy with the most highly excited CO J=3–2 line with $r_{32} = 1.88$, though a large applied correction makes this value somewhat uncertain (see Paper I). All one-phase LVG solutions correspond to dense gas $n = (10^4-3 \times 10^5) \text{ cm}^{-3}$, with the best fits obtained for $T_{\text{kin}} \geq 40 \text{ K}$. Unfortunately lack of more CO line ratios and especially at least one ^{13}CO line measurement permits a wide range of $[T_{\text{kin}}, n, K_{\text{vir}}]$ states

up to $T_{\text{kin}}=150$ K and $K_{\text{vir}}\sim 1-20$ to fit the observed ratios. The one-phase X_{co} values remain essentially unconstrained with $X_{\text{co}}\sim(0.7-2.4) X_1$ and the low values associated with strongly unbound states ($K_{\text{vir}}\sim 13-22$), while the low values with states that have $K_{\text{vir}}\sim 1-7$. The corresponding molecular gas mass is $M_{\text{tot}}\sim(6.3-22)\times 10^9 M_{\odot}$ while $M_{\text{SF}}\sim 5.2\times 10^9 M_{\odot}$.

Another extraordinary aspect of IRAS 22491–1808 is that many of the conditions compatible with its global CO line ratios indicate dense gas ($\sim 3\times 10^5$ cm $^{-3}$) with temperatures $T_{\text{kin}}=(100-130)$ K, significantly larger than those of the dust ($T_{\text{dust}}=(32-49)$ K for emissivity of $\beta=1.5, 2$). Such potentially strong decoupling of gas and dust temperatures, especially at high gas densities where $T_{\text{kin}}\rightarrow T_{\text{dust}}$ is expected, are another indicator of other dominant power sources than PDR photons. Turbulent and CR heating are capable of driving large $T_{\text{kin}}/T_{\text{dust}}>1$ inequalities even for the very dense gas mass reservoirs found in ULIRGs (Paper I, Papadopoulos 2010). These mechanisms can easily dominate when strong gas-rich/gas-rich spiral galaxy interactions drive the bulk of the molecular gas into compact regions in the two nuclei of the progenitors. This will inject large amounts of gas kinetic energy into ~ 100 pc-sized regions fueling extreme turbulence, while high SFR densities will establish extreme CRDRs. Interestingly two other double-nuclei systems, IRAS 12112+305 and IRAS 08572+3915, also show very highly excited (i.e. $r_{J+1,J}>1$) CO lines.

The IRAS 22491-1808 and similar systems are thus excellent cases for studying extreme ISM conditions and their drivers using ALMA. Such observations will be crucial for: a) inferring CR energy densities (by finding starburst region sizes), b) measuring velocity dispersions and the turbulence levels of molecular gas disks and c) directly providing key molecular line diagnostics for the presense of CR-dominated regions (CRDRs) and/or turbulent-heated regions (THR) (Papadopoulos 2010; Bayet et al. 2011, Meijerink et al. 2011).

B.26. NGC 7469

This is a well-studied Sy1 spiral galaxy whose AGN is surrounded by a nearly complete ring of powerful starburst activity contributing $\sim 2/3$ of its L_{IR} (Genzel et al. 1995; Riffel et al. 2006 and references therein). Interferometric CO J=1–0 imaging found its central starburst to be very gas-rich (Meixner et al. 1990; Tacconi & Genzel 1996). Its starburst is thought triggered by an interaction with a neighboring galaxy IC 5283 that lies $83''$ (~ 27 kpc) away (projected distance). A $X_{\text{co}}\sim(1/5)X_{\text{co,Gal}}$ was inferred for its inner ~ 1 kpc, and attributed to the effects of strong SF feedback on molecular clouds (Genzel et al. 1995). A small X_{co} for the starburst region of the disk in NGC 7469 is indeed corroborated by CO J=3–2, 1–0 observations and $850\mu\text{m}/450\mu\text{m}$ dust continuum imaging (Papadopoulos & Allen 2000). However the same observations also revealed faint CO J=1–0 and $450\mu\text{m}$ dust

emission extending well beyond the starburst region, and containing a massive SF-quiescent, cold dust and gas reservoir with a Galactic X_{co} .

These two ISM components make a good one-phase LVG fit impossible for the “cold” $r_{21}=0.75$ and the “warm” $r_{43}=0.83$, $r_{65}=0.22$ ratios observed. The best such solution with $T_{\text{kin}}=70$ K, $n(\text{H}_2)=10^3 \text{ cm}^{-3}$, $K_{\text{vir}}=4$ yields: $r_{21}^{(\text{lvG})}=0.97$, $r_{32}^{(\text{lvG})}=0.75$, $r_{43}^{(\text{lvG})}=0.48$, $r_{65}^{(\text{lvG})}=0.08$, and $R_{21}^{(\text{lvG})}=11$. The first two are higher than those observed ($\sim 2\sigma$ higher in the case of r_{21}), while for (4–3)/(1–0) and (6–5)/(1–0) the LVG-computed ratios are ~ 1.7 and ~ 2.75 times smaller than observed. The $X_{\text{co}}=0.72 X_1$ value computed from the optimal one-phase LVG fit to the global CO SLED is dominated by the SF phase, and corresponds to $M_{\text{tot}}\sim 2.5\times 10^9 M_{\odot}$. The minimum SF gas mass expected on the other hand is $M_{\text{SF}}=6.5\times 10^8 M_{\odot}$.

Using only the CO J=3–2, 4–3, 6–5³ and the ¹³CO J=2–1 lines to constrain the high-excitation (h)-phase in a 2-phase models yields a typical LVG solution for $T_{\text{kin}}=60$ K, $n(\text{H}_2)=10^4 \text{ cm}^{-3}$, and $K_{\text{vir}}=13$ with a corresponding $X_{\text{co}}^{(\text{h})}=0.66 X_1$. From this solution we compute $L_{\text{CO},1-0}^{(\text{h})'}=2.51\times 10^9 L_1$, and $L_{\text{CO},1-0}^{(1)'}=0.97\times 10^9 L_1$ which yield $\rho_{\text{co}}^{(1-\text{h})}\sim 0.39$. Then using the Galactic $X_{\text{co}}^{(1)}=5 X_1$ deduced for the extended CO J=1–0 and submm continuum dust emission of the disk in NGC 7469 (Papadopoulos & Allen 2000), we obtain $X_{\text{co}}^{(2-\text{ph})}\sim 1.88 X_1$, which is $\sim 2.6\times$ higher than that obtained by the one-phase LVG fit of the global SLED.

Thus the cold extended disk of NGC 7469, despite containing $\sim 3\times$ more molecular gas mass than its central starburst, is nearly inconspicuous in the global CO SLED, resulting to a significant underestimate of the total molecular gas mass in this galaxy. Only the available spatial information about its presence could rectify this, a state of affairs mirrored in other such systems (e.g. NGC 1068). For disk-dominated LIRGs with strong excitation gradients induced by the presence of central starbursts only CO, ¹³CO line and dust continuum imaging of their ISM can avoid such pitfalls (see 3.4). This is quite unlike ULIRGs where it is the low-excitation “cloud-envelope”-phase that contains the smaller mass fraction and is concomitant or closely follows the distribution of a massive much denser gas component.

B.27. IRAS 23365+3604

Near-IR imaging of this LIRG reveals tidal tails indicating a merger, and a single nucleus embedded into a nearly face-on disk that is nearly $\sim 20\text{kpc}$ ($17.3''$) in diameter, and shows disturbed spiral structure (Surace et al. 2000). The nucleus is classified as a LINER (Veilleux et al. 1995). The gas dynamics as revealed by CO J=1–0 interferometry (DS98) is strongly

³The wide beam of the CSO was used to obtain the CO 6-5 measurement for this extended object

decoupled from stellar dynamics (Genzel et al. 2001), another hallmark of strong mergers. Its molecular gas disk is compact with ~ 1.2 kpc diameter, and a face-on velocity dispersion of $\sim 100 \text{ km s}^{-1}$ (DS98). Its CO SLED has a “cool” CO(2–1)/(1–0) ratio ($=0.75$) but a well-excited CO J=3–2 line with a “warm” CO(3–2)/(1–0) ($=0.82$), while its large R_{21} ($=17$) is typical for mergers. One-phase LVG models yield moderately good but rather degenerate fits with $[T_{\text{kin}}, n, K_{\text{vir}}] = [30\text{--}65, 10^3, 13]$ and $[70\text{--}150, 3 \times 10^2, 2.2]$ being the optimal solution ranges. The best solutions are obtained for $T_{\text{kin}} = 50\text{K}, 70\text{K}$ with corresponding line ratios: $r_{21}^{(\text{lv})} = 0.88, 0.84$, $r_{32}^{(\text{lv})} = 0.56, 0.55$, $r_{43}^{(\text{lv})} = 0.24, 0.27$ and $R_{21}^{(\text{lv})} = 20, 16$. These are compatible with the measured values though the models typically yield “warmer” r_{21} and “cooler” r_{32} ratios than observed, in the latter case by $\sim 1.1\sigma$. The corresponding $X_{\text{co}} \sim (1\text{--}1.3) X_1$, which gives $M_{\text{tot}} \sim (7.3\text{--}9.5) \times 10^9 M_{\odot}$, while $M_{\text{SF}} \sim 2.5 \times 10^9 M_{\odot}$.

The latter represents a substantial fraction of the total molecular gas mass where much higher gas densities must be prevailing. A clear indication of another highly-excited denser gas phase is provided by CO J=6–5 line which is $\sim 9\text{--}16$ times more luminous than expected from the best LVG solutions. The presence of a dense gas phase able to emit such high-J CO lines is also indicated by a high HCN/CO J=1–0 line ratio of $r_{\text{HCN/CO}}^{(\text{obs})} \sim 0.10$ (HCN from Gracio-Carpio et al. 2008, CO from Paper I). Using the CO J=3–2, J=4–3 (upper limit), J=6–5 and ^{13}CO J=2–1 lines to constrain the high-excitation phase yields: $[T_{\text{kin}}, n, K_{\text{vir}}] = [40\text{--}80, 10^4, 40]$ as the optimum solution range, with $T_{\text{kin}} = 60\text{K}$ being the best. The corresponding CO SLED has $r_{21}^{(\text{h})} = 1.94$, $r_{32}^{(\text{h})} = 1.90$, $r_{43}^{(\text{h})} = 1.50$, and $r_{65}^{(\text{h})} = 0.45$, typical of low/modest optical depths (indicatively $\tau_{10} \sim 0.2$, $\tau_{32} \sim 2.5$), a result of the exceptionally large K_{vir} . A less optimal solution range with lower densities and more modest (but still high) K_{vir} values does exist $[T_{\text{kin}}, n, K_{\text{vir}}] = [90\text{--}150, 3 \times 10^3, 22]$, but could not reproduce the high HCN(1–0)/CO(6–5) ratio of $R_{\text{HCN/CO65}} \sim 0.48 \pm 0.18$ observed for this galaxy as such a low-density phase would hardly emit any HCN J=1–0 ($R_{\text{HCN/CO65}} \lesssim 0.08$).

The mass of the dense, warm, and strongly unbound phase can be found from $X_{\text{co}}^{(\text{h})} \sim 0.45 X_1$ (for $T_{\text{kin}} = 60 \text{K}$), and $L_{\text{CO,1–0}}^{(\text{h})'} = (1/r_{32}^{(\text{h})}) L'_{\text{CO,3–2}} \sim 3.15 \times 10^9 L_1$, which yields $M_{\text{h-ex}} \sim 1.4 \times 10^9 M_{\odot}$. This large gas mass with such high K_{vir} and high densities is rather surprising since such strongly unbound states are associated with cloud-envelopes or intercloud diffuse molecular gas whose $n \lesssim 10^3 \text{ cm}^{-3}$. The remaining CO J=1–0 luminosity of the (l)-phase on the other hand is $L_{\text{CO,1–0}}^{(\text{l})'} \sim 4.15 \times 10^9 L_1$ with an essentially unconstrained $X_{\text{co}}^{(\text{l})}$. Setting $X_{\text{co}}^{(\text{l})} = (0.5\text{--}5) X_1$ to encompass the range from a warm, diffuse and unbound gas component to an underlying cold, self-gravitating, disk phase yields $X_{\text{co}}^{(2\text{-ph})} \sim (0.5\text{--}3) X_1$ and $M_{\text{tot}} \sim (3.7\text{--}22) \times 10^9 M_{\odot}$. The low $X_{\text{co}}^{(\text{l})}$ (and thus M_{tot}) values are more probable because of the negligible CO J=2–1 luminosity of the (l)-phase (a cold, self-gravitating, phase would have higher J=2–1 luminosities).

Using the SNR-GMC interfaces as benchmark entities for dense yet highly unbound

(due to the kinetic energy injected by SNR shocks) molecular gas phase makes clear that a mass fraction of $M_{\text{h-ex}}/M_{\text{tot}} \sim 0.06-0.38$ exceeds that expected per GMC for a SNR-impacted gas phase ($\sim 1\%$ of a GMC's mass). It is worth noting that only in the powerful radio galaxy 3C 293 galaxy-sized molecular gas reservoirs at high densities were inferred to be at such strongly gravitationally unbound states, likely caused by the powerful jet-ISM interaction. While no such AGN influence on the ISM is apparent in IRAS 23365+3604 it is interesting to note that it is one of the 3 ULIRGs (the others being Arp 220 and Mrk 273) where molecular gas velocity fields decoupled from those of stars and ionized gas are found, with molecular gas having ~ 2 times larger linewidths (Colina et al. 2005). High-J CO, ^{13}CO and HCN and H^{13}CN line observations are necessary for confirming such extraordinary dynamical states for the massive dense gas reservoir residing in IRAS 23365+3604 and similar systems.

REFERENCES

- Aalto S., Booth R. S., Black J. M., & Johansson L. E. B. 1995 *A&A*, 300, 369
- Aalto S., Radford S. J. E., Scoville N. Z., & Sargent A. I. 1997, *ApJ*, 475, L107
- Allen R. J., & Lequeux J. 1993, *ApJ*, 410, L15
- Allen R. J., Le Bourlot J., Lequeux J., Pineau des Forêts G., Roueff E. 1995, *ApJ*, 444, 157
- Andrews B. H., & Thompson T. A. 2011, *ApJ*, 727, 97
- Arikawa Y., Tatematsu K., Sekimoto Y., & Takahashi T. 1999, *PASJ*, 51, L7
- Armus L., Heckman T. M., & Miley G. K. 1989, *ApJ*, 347, 727
- Barvainis R., Alloin D., & Antonucci R. 1989, *ApJ*, 337, L69
- Balick B., & Heckman T. M. 1981, *A&A*, 96, 271
- Bayet E., Williams D. A., Hartquist T. W., Viti S. 2011, *MNRAS*, 414, 1583
- Bolatto A. D. Leroy A., Israel F. P. & Jackson J. M. 2003, *ApJ*, 595, 167
- Braine J., & Combes F. 1992, *A&A*, 264, 433
- Bryant P. M., & Scoville N. Z. 1996, *ApJ*, 457, 678
- Bryant P. M., & Scoville N. Z. 1999, *AJ*, 117, 2632
- Carico D. P., Sanders D. B., Soifer B. T., Matthews K., & Neugebauer G. 1990, *AJ*, 100, 70

- Colina L., Arribas S., & Monreal-Ibero A. 2005, *ApJ*, 621, 725
- Condon J. J., Helou G., Sanders D. B., & Soifer B. T. 1990, *ApJS*, 73, 359
- Conselice C. J., Gallagher John S., Calzetti D., Homeier N., & Kinney A. 2000, *AJ*, 119, 79
- Clements M. S., & Alexander P. 2004, *MNRAS*, 350, 66
- Charmandaris V., Stacey G. J., & Gull G. 2002, *ApJ*, 571, 282
- Daddi E., Elbaz D., Walter F., et al. 2010a, *ApJ*, 714, L118
- Daddi E., Bournaud F., Walter F., et al. 2010b, *ApJ*, 713, 686
- Dadina M. 2007, *A&A*, 461, 1209
- Dannerbauer H., Daddi E., Riechers, D. et al. 2009, 698, L178
- Devereux N., Taniguchi Y., Sanders D. B., Nakai N., & Young J. S. 1994, *AJ*, 107, 2006
- Dickman R. L., Snell, R. L., Schloerb, F. P. 1986, *ApJ*, 309, 326
- Downes D., Solomon, P. M. & Radford, S. J. E. 1993, *ApJ*, 414, L13
- Downes D., Solomon, P. M. 1998, *ApJ*, 507, 615
- Dumke M., Nieten Ch., Thuma G., Wielebinksi R., & Walsh W. 2001, *A&A*, 373, 853
- Dunne L., Eales S., Edmunds M., Ivison R., Alexander P., & Clements D. L. 2000, *MNRAS*, 315, 115
- Eckart A., van der Werf P., Hofmann R., & Harris I. 1994, *ApJ*, 424, 627
- Evans A. S., Sanders D. B., Surace J. A., & Mazzarella J. M. 1999, *ApJ*, 511, 730
- Evans A. S. Surace J. A., & Mazzarella J. M. 2000, *ApJ*, 529, L85
- Evans A. S., Mazzarella J. M., Surace J. A., & Sanders D. B. 2002, *ApJ*, 580, 749
- Farrah D., Afonso J., Efstathiou A., Rowan-Robinson M., Fox M., & Clements D. 2003, *MNRAS*, 343, 585
- Fanaroff B. L., & Riley J. M. 1974, *MNRAS*, 167, 31
- Floyd D. J. E., Perlman E., Leahy J. P. et al. 2006, *ApJ*, 639, 23
- Gao Y., & Solomon P. M. 2004, *ApJ*, 606, 271

- Genzel R., Weitzel L., Tacconi-Garman L. E. Blietz M., Cameron M., Krabbe A. 1995, ApJ, 444, 129
- Genzel R., Tacconi L. J., Rigopoulou D., Lutz D., & Tecza M. 2001, ApJ, 563, 527
- Genzel R., Tacconi L. J., Gracia-Carpio J., et al. 2010, MNRAS, 407, 2091
- Goldader J. D., Joseph R. D., Doyon R., & Sanders D. B. 1997, ApJS, 108, 449
- González Delgado R. M., Heckman T., Leitherer C. et al. 1998, ApJ, 505, 174
- Güsten R., Philipp S. D. 2004, in *The Dense Interstellar Medium in Galaxies* Proceedings of the 4th Cologne-Bonn-Zermatt Symposium, Zermatt, Switzerland, S.Pfalzner, C. Kramer, C. Staubmeier, and A. Heithausen (Eds) Springer proceedings in physics, Vol. 91. p. 253
- Güsten R., Serabyn E., Kasemann C., et al. 1996, ApJ, 402, 537
- Greve T. R., Bertoldi F., Smail I., et al. 2005, MNRAS, 359, 1165
- Greve T. R., Papadopoulos P. P., Gao Y., & Radford S. J. E. 2009, ApJ, 692, 1432
- Graciá-Carpio J., Graciá-Burillo S., Planesas P., Fuente A., & Usero A. 2008, A&A, 479, 703
- Graciá-Burillo, S., Usero A., Alonso-Herrero A. et al. 2012, A&A, 539, 8
- Henkel C. & Mauersberger R. 1993, A&A, 274, 730
- Hattori T., Yoshida M., Ohtani H. et al. 2004, AJ, 127, 736
- Horellou C., Casoli F., Combes F., & Durpaz C. 1995, A&A, 298, 743
- Hibbard J. E., & Yun M. S. 1999, AJ, 118, 162
- Iono D., Ho P. T., Yun M. S., Matsushita S., Peck B. A., & Sakamoto K. 2004, ApJ, 616, L63
- Imanishi M., Dudley C. C., & Maloney P. R. 2001, ApJ, 558, L93
- Imanishi M., Terashima Y., Anabuki N., & Nakagawa T. 2003, ApJ, 596, L167
- Iono D., Wilson C. D., Takakuwa S. et al. 2007, ApJ, 659, 283
- Iono D., Wilson C. D., Yun M. S. et al. 2009, ApJ, 695, 1537

- Israel F. P., 1988, in *Millimetre and Submillimetre Astronomy*, R. D. Wolstencroft and W. B. Burton eds. Kluwer Academic Publishers, p. 281
- Israel F. P., et al., 1993, *A&A*, 276, 25
- Israel F. P., 1997, *A&A*, 328, 471
- Israel F. P., 1999, in *H₂ in Space*, F. Combes, G. Pineau des Forêts eds. Cambridge University Press, Astrophysics Series
- Jackson J. M., Paglione T. A. D., Carlstrom J. E., & Rieu N.-Q 1995, *ApJ*, 438, 695
- Juneau S., Narayanan D. T., Moustakas J. 2009, *ApJ*, 707, 1217
- Kikumoto T., Taniguchi Y., Suzuki M., Tomisaka K. 1993, *AJ*, 106, 466
- Kregel M., & Sancisi R. 2001, *A&A*, 376, 59
- Krips M., Neri R., Garcia-Burillo S., Martín S., Combes F., Graciá-Carpio J., & Eckart A. 2008, *ApJ*, 677, 272
- Krips M., Martín S., Eckart A. et al. 2011, *ApJ*, 736, 37
- Kollatschny W., Dietrich M., Borgeest U., & Schramm K.-J. 1991, *A&A*, 249, 57
- Kutner M. L., & Ulich B. L. 1981, *ApJ*, 250, 341
- Leech J., Isaak K., Papadopoulos P. P., Gao Y., & Davies G. R. 2010, *MNRAS*, 406, 1364
- Loenen E. 2009, PhD Thesis, University of Groningen, pg. 115
- Loinard L., Allen R. J., & Lequeux J. 1995, *A&A*, 301, L68
- Krips M., Neri R., Graciá-Burillo S., Martin S., Combes F., Graciá-Carpio J., & Eckart A. 2008, *ApJ*, 677, 262
- Mao R. Q., Henkel C., Schulz A., et al. 2000, *A&A*, 358, 433
- Mao R. Q., Schulz A., Henkel C., Mauersberger R., Muters D., & Dinh-V-Trung 2011, *ApJ*, 724, 1336
- Maloney P. M., & Black J. H., 1988, *ApJ*, 325, 389
- Majewski S. R., Hereld M., Koo D. C., Illingworth G. D., & Heckman T. M. 1993, *ApJ*, 402, 125

- Martini P., Regan M. W., Mulchaey J. S., & Pogge R. W. 2003, *ApJS*, 146, 353
- Maiolino R., Ruiz M., Rieke G. H., & Papadopoulos P. 1997, *ApJ*, 485, 552
- Matsushita S., Sakamoto K., Kuo C.-Y., et al. 2004, *ApJ*, 616, L55
- Matsushita S., Iono D., Petitpas G. et al. 2009, *ApJ*, 693, 56
- Mauersberger R., Henkel C., Walsh W., & Schulz A. 1999, *A&A*, 341, 256
- Mazzarella J. M., Graham J. R. Sanders D. B., & Djorgovski S. 1993, *ApJ*, 409, 170
- Meier D. S., Turner J. L., & Crosthwaite L. P. & Beck S. C. 2001, *AJ*, 121, 740
- Meijerink R., Spaans M., Loenen A. F., van der Werf P. P. 2011, *A&A*, 525, 119
- Meixner M., Puchalsky R., Blitz L., Wright M., & Heckman T. 1990, *ApJ*, 354, 158
- Murphy T. W. Jr., Armus L., Matthews K., Soifer B. T., Mazzarella J. M., Shupe D. L. 1996, *AJ*, 111, 1025
- Narayanan D., Krumholz M., Ostriker E. C., & Hernquist L. 2010, *MNRAS*, 418, 664
- Nieten Ch., Dumke M., Beck R., & Wielebinski R. 1999, *A&A*, 347, L5
- Ossenkopf V. 2002, *A&A*, 391, 295
- Padoan P., & Nordlund A. 2002, *ApJ*, 576, 870
- Papadopoulos P. P. & Seaquist E. R. 1998, *ApJ*, 492, 521
- Papadopoulos P. P. & Seaquist E. R. 1999, *ApJ*, 516, 114
- Papadopoulos P. P. & Allen M. L. 2000, *ApJ*, 537, 631
- Papadopoulos P. P. 2007, *ApJ*, 656, 792
- Papadopoulos P. P., Isaak K. G., & van der Werf P. P. 2007, *ApJ*, 668, 815
- Papadopoulos P. P., Kovacs A., Evans A. S., & Barthel P. 2008, *A&A*, 491, 483
- Papadopoulos P. P., Isaak K. G., & van der Werf P. P. 2010a, *ApJ*, 711, 757
- Papadopoulos P. P., van der Werf P. P., Isaak K. G., & Xilouris E. M. 2010b, *ApJ*, 715, 775
- Papadopoulos P. P., van der Werf P. P., Xilouris E. M., Isaak K. G., Gao Y. & Muehle S. 2011, *MNRAS*, (submitted, arXiv:1109.4176)

- Parma P., de Ruiter H. R., Fanti C., & Fanti R. 1986, *A&AS*, 64, 135
- Paglione T. A. D., Jackson J. M., & Ishizuki S. 1997, *ApJ*, 484, 656
- Petitpas G. R., & Wilson C. D. 1998, *ApJ* 503, 219
- Planesas P., Mirabel I. F., & Sanders D. B. 1991, *ApJ*, 370, 172
- Rangwala E., Maloney P. R., Glenn J. et al. 2011, *ApJ*, 743, 94
- Regan M. W. 2000, *ApJ*, 541, 142
- Riffel R., Rodríguez-Ardila A., & Pastoriza M. G. 2006, *A&A*, 457, 61
- Sakamoto S., 1996, *ApJ*, 462, 215
- Sakamoto S., Hayashi M., Hasegawa T., Handa T., & Oka T. 1994, *ApJ*, 425, 641
- Sakamoto S. PhD Thesis, 1994, University of Tokyo, *PASP* 106, 1112
- Sakamoto K., Wang J., Wiedner M., et al. 2008, *ApJ*, 684, 957
- Sanders D. B., Scoville N. Z., Young J. S., Soifer B. T., Schloerb F. P., Rice W. L., & Danielson G. E. 1986, *ApJ*, 305, L45
- Sanders D. B., Scoville N. Z., Sargent A. I., & Soifer B. T. 1988a, *ApJ*, 324, L55
- Sanders D. B., Soifer B. T., Elias J. H. et al. 1988b, *ApJ*, 325, 74
- Sanders D. B., Soifer B. T., Elias J. H., Neugebauer G., & Matthews K. 1988c, *ApJ*, 328, L35
- Sanders D. B., Scoville N. Z., & Soifer B. T. 1991, *ApJ*, 370, 15 8
- Sanders D. B., & Mirabel I. F. 1996, *ARA&A*, 34, 749
- Sanders D. B. Mazzarella J. M., Kim D.-C., Surace J. A., & Soifer B. T. 2003, *AJ*, 126, 1607
- Sanders D. B., & Ishida C. M. 2004, in *The Neutral ISM in Starburst Galaxies*, eds. S. Aalto, S. Hüttemeister, & A. Pedlar, *ASP Conference Series* 320, p. 230
- Sargent A. I., Sanders D. B., Scoville N. Z., & Soifer B. T. 1987, 312, L35
- Sargent A. I. & Scoville N. Z. 1991, *ApJ*, 366, L1
- Schinnerer E., Eckart A., & Tacconi L. J. 1998, 500, 147

- Scoville N. Z., Sanders D. B., Sargent A. I., Soifer B. T., & Tinney C. G. 1989, *ApJ*, 345, L25
- Scoville N. Z. 2004, Evans A. S., Thompson R., Rieke M., Hines D. C., F. J., Dinshaw N., Surace J. A., & Armus L. 2000, *AJ*, 119, 991
- Scoville N. Z. 2004, in *The Neutral ISM in Starburst Galaxies*, eds. S. Aalto, S. Hüttemeister, & A. Pedlar, *ASP Conference Series* 320, p. 253
- Schleicher D. R. G., Spaans M., & Klessen R. S. 2010, *A&A*, 513, 7
- Seta M., Hasegawa T., Dame T M. et al. 1998, *ApJ*, 505, 286
- Shetty R., Glover S. C., Dullemond C. P. & Klessen R. S. 2011a, *MNRAS*, 412, 1686
- Shetty R., Glover S. C., Dullemond C. P., Ostriker E. C., Harris A. I., & Klessen R. S. 2011b, *MNRAS*, 415, 3253
- Shirley Y. L., Evans N. J. II., Young K. E., Knez C., & Jaffe D. T. 2003, *ApJS*, 149, 375
- Smith D. A., Herter T., Haynes M. P., Beichman C. A., & Gautier T. N. III. 1995, *ApJ*, 439, 623
- Soifer B. T., Sanders D. B., Madore B. F., et al. 1987, *ApJ*, 320, 238
- Soifer B. T., Boehmer L., Neugebauer G., & Sanders D. B. 1989, *AJ*, 98, 766
- Soifer B. T., & Neugebauer G. 1991, *AJ*, 101, 354
- Solomon P. M., Radford S.J.E., & Downes D. 1990, *ApJ*, 348, L53
- Solomon P. M., Downes D., & Radford S.J.E. 1992, *ApJ*, 387, L55
- Solomon P. M., Downes D., Radford S.J.E., & Barrett J. W. 1997, *ApJ*, 478, 144
- Solomon P. M., & Vanden Bout P. A., 2005, *ARA&A*, 43, 677
- Staguhn J. G., Schinnerer E., Eckart A., & Scharwächter J. 2004, *ApJ*, 609, 85
- Surace J. A., Sanders D. B., Vacca W. D., Veilleux S., & Mazzarella J. M. 1998, *ApJ*, 492, 116
- Surace J. A., Sanders D. B., & Evans A. S. 2000, *ApJ*, 529, 179

- Tacconi L. J., & Genzel R. 1996 in *Science with Large Millimetre Arrays* Proceedings of the ESO-IRAM-NFRA-Onsala Workshop, Garching, Germany, Peter A. Shaver (Ed.) Springer-Verlag, p.125
- Tacconi L. J., Genzel R. Tecza M., Gallimore J. F. Downes D., & Scoville N. Z 1999, ApJ, 524, 732
- Tacconi L. J., Genzel R., Lutz D., et al. 2002, ApJ, 580, 73
- Tacconi L. J., Neri R., Chapman S. C., et al. 2006, ApJ, 640, 228
- Tacconi L. J., Genzel R., Smail I., et al. 2008, ApJ, 680, 246
- Thomas H. C., Alexander P., Clemens M. S., Green D. A., Dunne L., & Eales S. 2004, MNRAS, 351, 362
- Thompson T. A., Quataert E., & Murray N. 2005, ApJ, 630, 167
- Thompson T. A. 2009, Astronomical Society of the Pacific Conference Series, 408, 128
- Tinney C. G., Scoville N. Z., Sanders D. B., & Soifer B. T. 1990, ApJ, 362, 473
- Veilleux S., Kim D.-C., Sanders D. B., Mazzarella J. M., & Soifer B. T. 1995, ApJS, 98, 171
- Veilleux S., Kim D.-C., & Sanders D. B. 2002, ApJS, 143, 315
- Wall, W. F. 2007, MNRAS, 379, 674
- Wang Z., Scoville N. Z., & Sanders D. B. 1991, ApJ, 368, 112
- Weiss A., Neininger N., Hüttemeister S., & Klein U. 2001, A&A, 365, 571
- Weiss A., Walter F., & Scoville N. Z. 2005, A&A, 438, 533
- White G. J., Ellison B., Claude S., Dent W. R. F., Matheson D. N. 1994, A&A, 284, L23
- Wilson C. D., Petitpas G. R., Iono D. et al. 2008, ApJS, 178, 189
- Wu J., Evans N. J. II., Gao Yu., Solomon P. M., Shirley Y. L., & Vanden Bout P. A. 2005, 635, L173
- Xia X. Y., Xue S. J., Mao S., Boller Th., Deng Z. G., & Wu H. 2002, ApJ, 564, 196
- Yao L., Seaquist E. R., Kuno N., & Dunne L. 2003, ApJ, 588, 771
- Young J. S. & Scoville N. Z. 1991, ARA&A, 29, 581

Zhu M., Seaquist E. R., & Kuno N. 2003, ApJ, 588, 243

Zhu M., Papadopoulos P. P., Xilouris E. M., Kuno N., & Lisenfeld U. 2009, ApJ, 706, 941

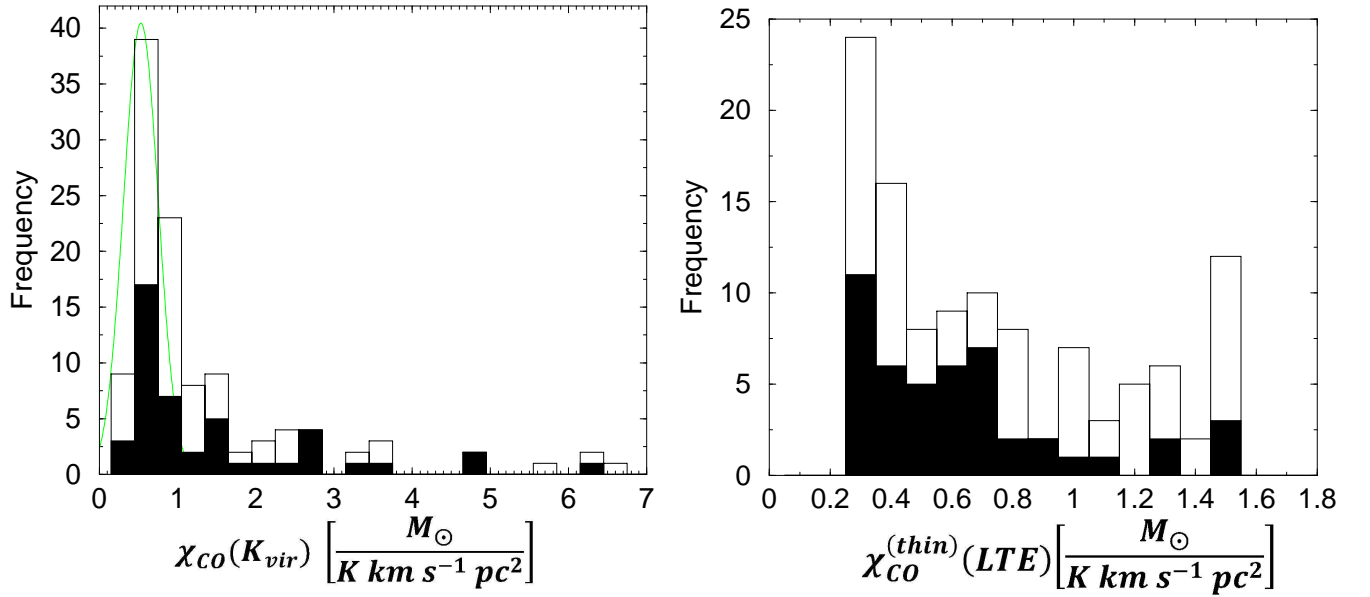


Fig. 1.— The X_{CO} factors, estimated from Equations 3 and 5, using the results from one-phase LVG radiative transfer models. The black-bar histogram corresponds to the best and least degenerate solutions obtained from these models.

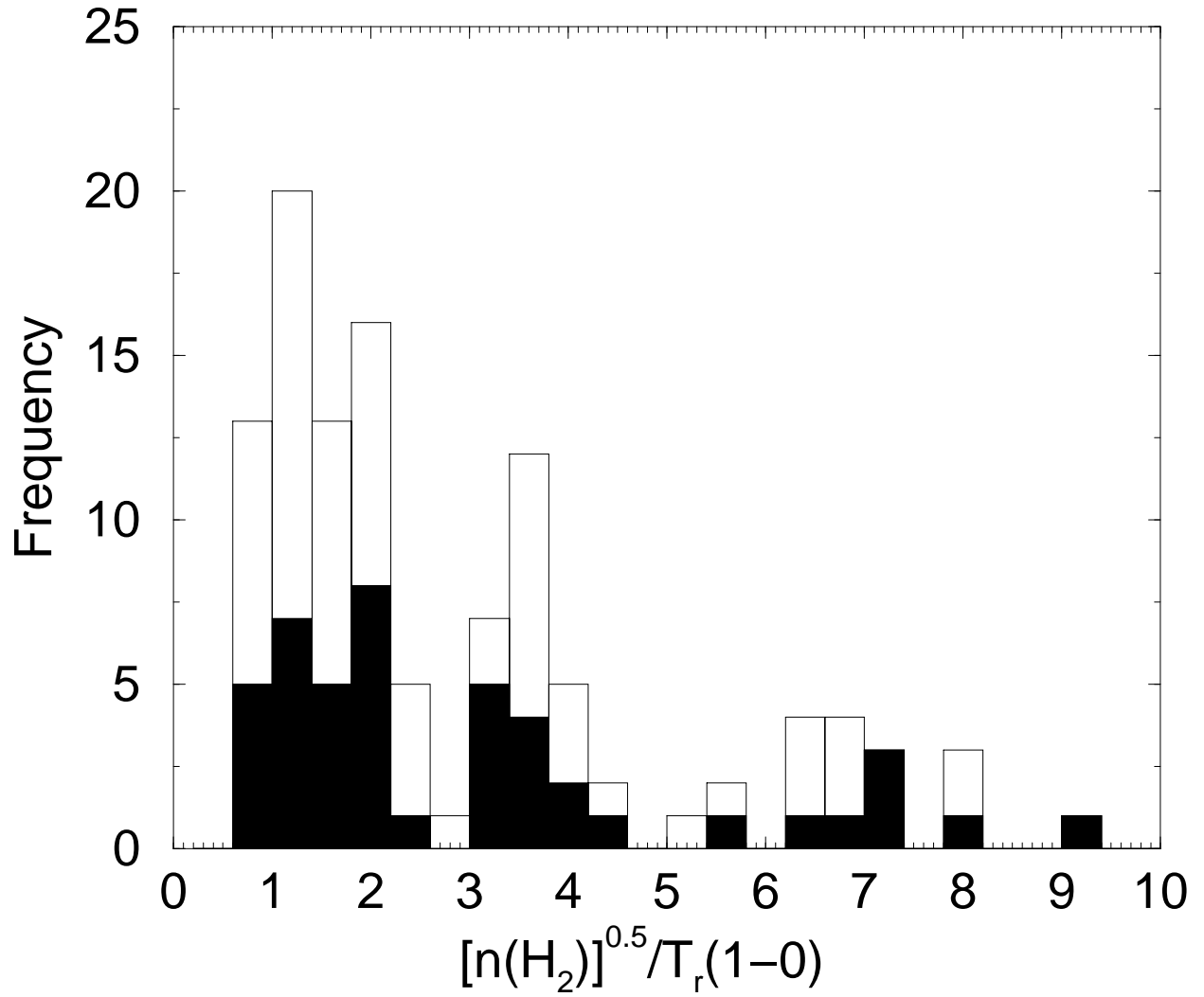


Fig. 2.— The distribution of the $\sqrt{n(\text{H}_2)}/T_{r,1-0}$ factor for the LVG solutions obtained for the sample (black bars as in Figure 1).

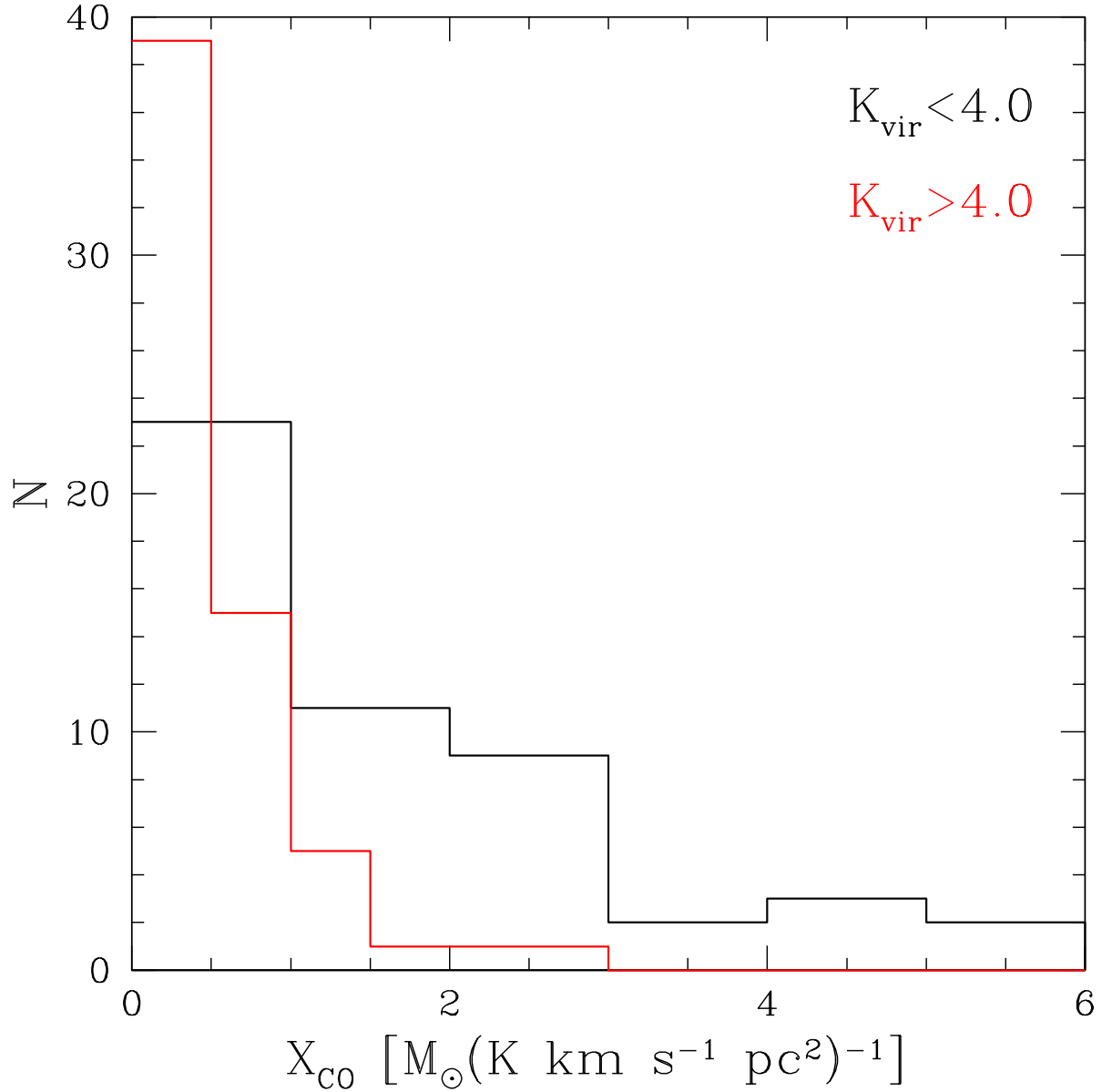


Fig. 3.— The X_{CO} factors, computed from Equation 3 and the 1-phase LVG solutions obtained for the CO line ratios measured in LIRGs (see Paper I) for two different dynamical regimes of average gas motions: self-gravitating ($1 \lesssim K_{\text{vir}} \lesssim 4$), and unbound ($K_{\text{vir}} > 4$).

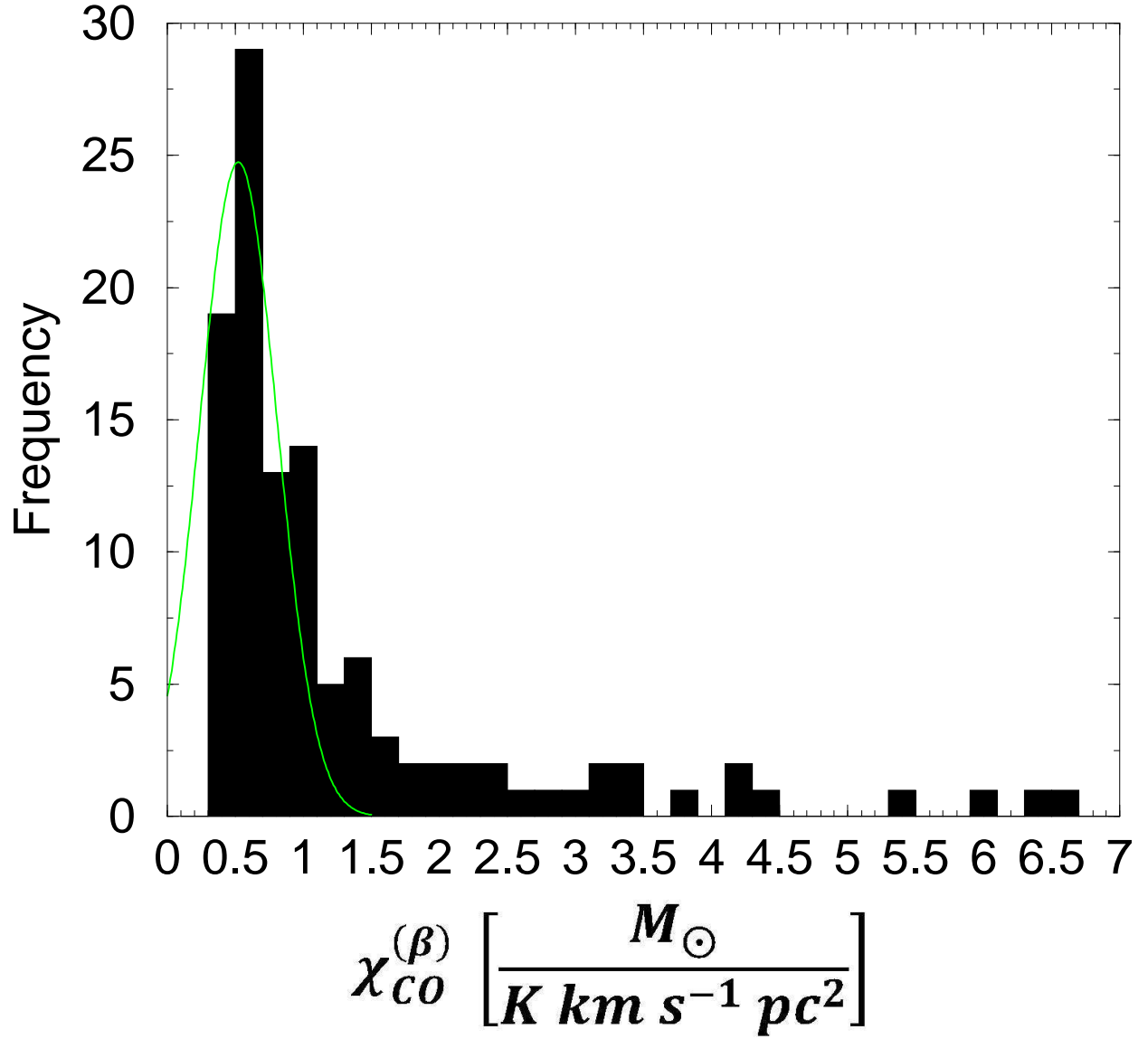


Fig. 4.— The X_{CO} factor, estimated from Equation 6 using the β_{J+1J} values computed from one-phase radiative transfer models.

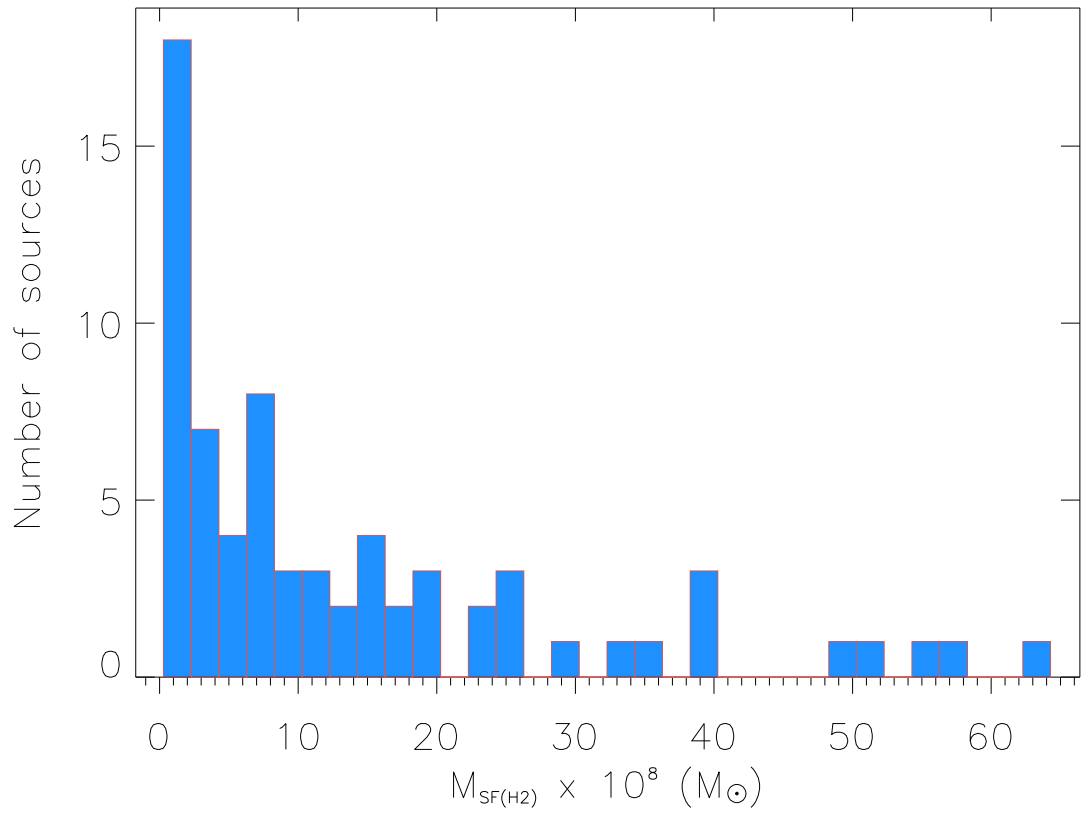


Fig. 5.— The minimum molecular gas masses necessary for fueling and Eddington-limited star formation in the LIRGs of our sample (see section 2.3).

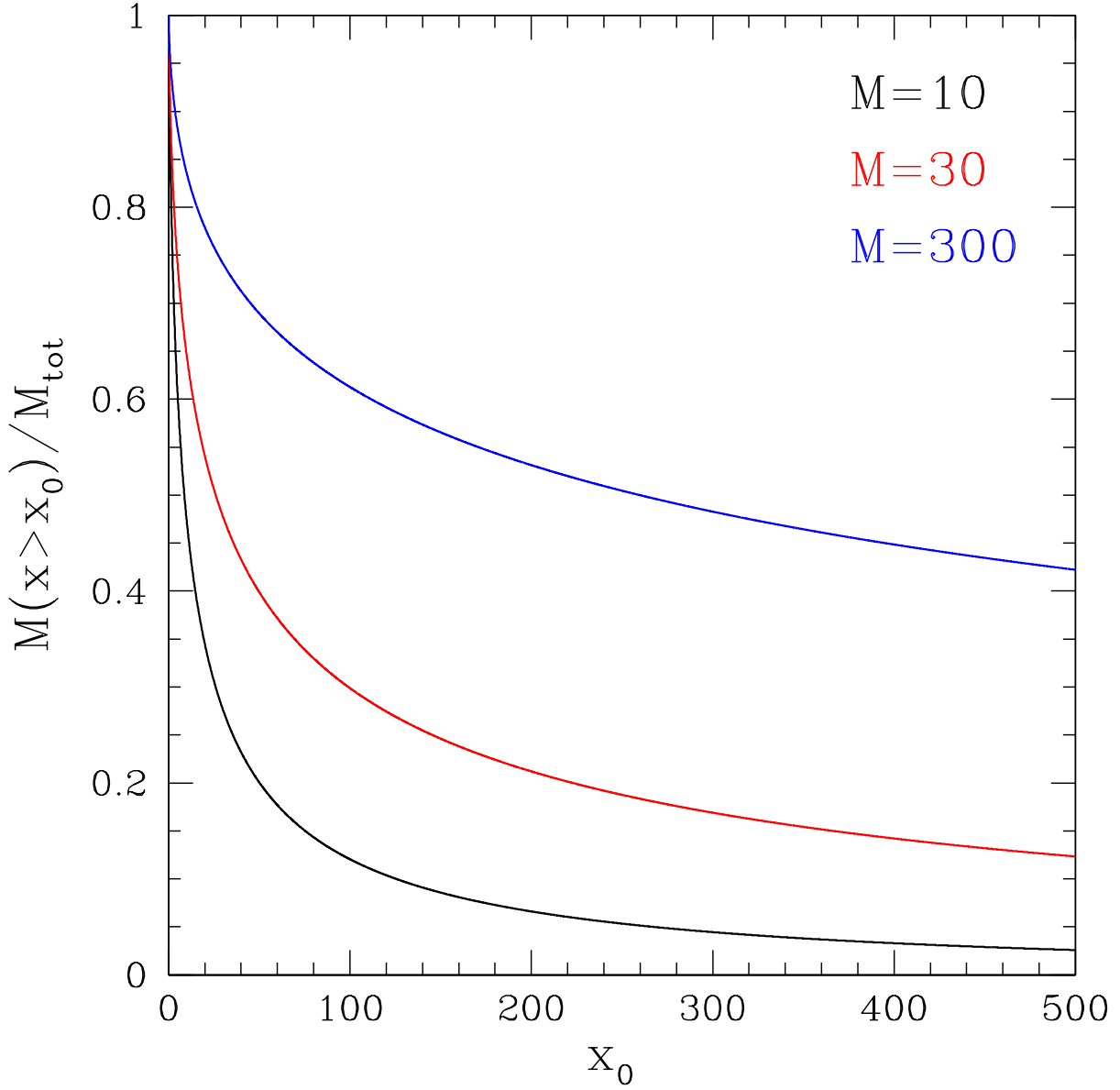


Fig. 6.— The gas mass fraction expected at overdensities $x \geq x_0$ where $x = n / \langle n \rangle$ (see Equation 13) in supersonic turbulent gas, from spiral disks ($M=10$) up to ULIRGs ($M=300$).

Table 1. Molecular gas masses and X_{co} factors

Name	$M_{\text{tot}}(X_{\text{co}})^{\text{a}}$ ($10^9 M_{\odot}$)	$M_{\text{tot}}^{(2\text{-ph})}(X_{\text{co}}^{(2\text{-ph})})^{\text{b}}$ ($10^9 M_{\odot}$)	M_{SF}^{c} ($10^9 M_{\odot}$)	$M_{\text{h-ex}}^{\text{d}}$ ($10^9 M_{\odot}$)	Remarks
IRAS 00057+4021	4.5 (1.1)	3.4-8.2(0.83-2.0)	1.2	1.6	degenerate $X_{\text{co}}^{(1)}$ values
IZw 1	8.6 (1.5)	9.5 (1.65)	0.4	2.8	Galactic $X_{\text{co}}^{(1)}$ adopted
NGC 828	4.6-6.3 (0.8-1.1)	4-14 (0.7-2.5)	0.3	0.3	degenerate $X_{\text{co}}^{(1)}$
IRAS 02483+4302	1.6 (0.45)	4.3-8.6 (1.2-2.4)	1.4	3.3	degenerate $X_{\text{co}}^{(1)}$ values
IRAS 03359+1523	22 (2.5)	...	0.8	...	SF-quiescent ISM
VII Zw 031	14.5 (1.25)	39 (3.4)	2.0	3.1	Cold extended disk?
IRAS 05189-2524	13.7 (3.5)	9.4 (2.4)	3.6	3.6	(h)-phase SLED assumed
IRAS 08030+5243	14.3-42.9 (1.5-4.5)	...	2.4	...	degenerate 1-phase solutions
IRAS 08572+3915	4.8-9.6 (3-6)	...	3.9	...	Highly excited CO J=6-5 line
Arp 55	2.9-9.2 (0.25-0.8)	...	0.9	...	degenerate 1-phase solutions
UGC 05101	1.9-2.9 (0.4-0.6)	...	1.6	...	
NGC 3310	0.03-0.15 (0.4-2.2)	...	0.1	...	degenerate X_{co} values
IRAS 10565+2448	3.8-4.8 (0.6-0.75)	4.8 (0.75)	2.6	2.6	(h)-phase SLED assumed
Arp 299	1.2 (0.42)	...	1.9	...	
IRAS 12112+0305	15.2-53.5 (1.5-5.3)	7.1-34.3 (0.7-3.4)	4.8	4	Unconstrained $X_{\text{co}}^{(1)}$
Mrk 231	1.8-3.2 (0.25-0.45)	21-49 (3-7)	5.5	8-25	CO 6-5, HCN lines used in 2-phase model
Arp 193	1.6-3.5 (0.35-0.75)	3.3-8.1 (0.7-1.8)	0.9	1.7-7.1	CO 3-2, HCN lines used in 2-phase model
NGC 5135	1.1-1.4 (0.35-0.45)	...	0.3	...	
Mrk 273	10.4 (2.0)	13 (2.5)	3.3	6	Cold extended disk?
3C 293	2.3-7.4 (0.5-1.6)	13.4-18 (2.9-3.9)	0.05	1.1-3.5	Galactic $X_{\text{co}}^{(1)}$ adopted
IRAS 14348-1447	11-17 (0.65-1)	24-30 (1.4-1.7)	5.6	5.6	degenerate (l)-phase
Zw 049.057	0.30-0.52 (0.35-0.6)	...	0.47	...	

Table 1—Continued

Name	$M_{\text{tot}}(X_{\text{co}})^{\text{a}}$ ($10^9 M_{\odot}$)	$M_{\text{tot}}^{(2\text{-ph})}(X_{\text{co}}^{(2\text{-ph})})^{\text{b}}$ ($10^9 M_{\odot}$)	M_{SF}^{c} ($10^9 M_{\odot}$)	$M_{\text{h-ex}}^{\text{d}}$ ($10^9 M_{\odot}$)	Remarks
Arp 220	1.85 (0.30)	14.7-27.5 (2.4-4.5)	4	12.6-25.2	HCN lines used in 2-phase model
NGC 6240	2.5 (0.30)	8.4-27.8 (1-3.3)	1.5	4.9-24.5	HCN lines used in 2-phase model
IRAS 17208–0014	5.2 (0.40)	9.8-33 (0.75-2.5)	6.2	3.5-6	degenerate $X_{\text{co}}^{(1)}$ values
“ “	“	34-77 (2.6-5.9)	“	27-70	HCN lines used in 2-phase model ^e
IRAS 22491–1808	6.3-22 (0.70-2.4)	...	5.2	...	degenerate X_{co} values
NGC 7469	2.5 (0.72)	6.5 (1.88)	0.65	1.65	Cold extended disk present
IRAS 23365+3604	7.3-9.5 (1-1.3)	3.7-22 (0.5-3)	2.5	1.4	Unconstrained $X_{\text{co}}^{(1)}$

^aTotal molecular gas mass from Equation 3 and the best one-phase LVG model parameters (the corresponding X_{co} value in X_1 units), with average values adopted in cases of significant LVG solution range degeneracy.

^bTotal molecular gas mass from Equation 10 and a 2-phase fit (the corresponding X_{co} value in X_1 units).

^cThe minimum molecular gas mass necessary for an Eddington-limited star formation rate (see 2.3).

^dThe gas mass of the (h)-phase in a 2-phase model when this is used. If a standard (h)-phase SLED and mass normalization is used (see 2.4) then $M_{\text{h-ex}}=M_{\text{SF}}$.

^eFor LVG solutions with $K_{\text{vir}}(\text{HCN})\sim 1-6$ (see B.24).